Universidad Autónoma de Madrid

Facultad de Ciencias
Departamento de Biología Molecular

Characterisation of the RAM pathway in *Ustilago maydis*

PhD
Elodie Sartorel
Madrid, 2009

Summary

Morphological changes that occur during cells life cycle are generally indispensable for their viability. Understand the signaling process that leads to the morphological adaptation appears to be essential to determine how the morphological control is established in eukaryotic cells. Different signaling pathways as the cAMP and MAPK pathways, are known to control cell morphological adaptation in response to external stimuli. Recently, a new protein network was identified involved in morphology, polarity, cell separation and virulence control. This pathway is the RAM protein network (Regulation of Ace2p activity and cellular morphology) known to be conserved from yeast to human. The RAM pathway has been shown to be indispensable for regulation of polarity in *S. cerevisiae*, *C. albicans* and also in high eukaryotes as *C. elegans* in which it controls neuronal differentiation.

To study more in detail the function of the RAM pathway in the regulation of morphology and pathogenicity, we used the dimorphic fungi *Ustilago maydis*, the causative agent of corn smut disease. This phytopathogenic fungi is able to switch from a yeast like form, in which cells divide by budding, to a filamentous form. In addition, because of its simple but conserved signal transduction pathways, *U. maydis* appeared to be an excellent model system to study the pathogenicity and the morphology at the molecular level. In *U. maydis*, the central kinase of this pathway, Ukc1 was identified by Dürrenberger *et al.*, (1999). In this work, we identified the regulator proteins of Ukc1 and showed that the RAM pathway regulated morphology, cell separation, polarity and pathogenicity. We showed that Δ*RAM* avirulence was a consequence of pheromone response defect due to a *pfr1* deregulation, and also a consequence of cell-cell fusion inability. Our study suggested that the RAM pathway could negatively regulate polar growth through *crk1* transcription regulation, in parallel to the cAMP pathway. We observed that Δ*slt2* mutant, could restore partialy of the severe Δ*ukc1* phenotype. Slt2 is the MAPK protein of the Cell Wall Integrity pathway, which has been shown in this work, to regulate polar growth in relation with RAM.

Abbreviations

aa: amino acid

DNA: Desoxirybo Nucleotid Acid

cAMP: cycle adenosil3´, 5´monophosphat

Cbx: Carboxin

CF: Calcofluor

CFP: Cyen Fluorescent Protein

DAPI: 4´, 6´-diamino-2-phenilindole

dCTP: 2´-desocitidine-5´-triophosphate

dNTP: 2´-desoxyribonucleoside-5´-triphosphate

OD: Optical Density

EDTA: Ethylene Diamine Tetra Acetic Acide

Fig: Figure

GFP: Green Fluorescent Protein

h: hour

Hyg: Hygromycin

Kb: Kilobase

MOPS: 3-(N-morpholino)propanesulfonic acid

PBS: Phosphate-buffered-saline

PCR: Polymerase Chain Reaction

PMSF: Phenyl Methane Sulphonyl Fluoride

RFP: Red Fluorescent Protein

RNA: Ribonucleic Acid

r.p.m: revolution per minute

rRNA: ribosomal Ribonucleic Acid

SDS: Sodium Dodecyl Sulfate

TAE: Tris-Acetate-EDTA

YFP: Yellow Fluorescent Protein

Introduction

1. Topic and model study

Regulation of morphogenesis is a central feature of eukaryotic life. Organisms require the coordination of numerous signaling pathways to control many cellular processes as cell division, cytoskeletal organisation, and vesicle transport. This morphological regulation is particularly important in dimorphic fungi which have to develop more than one structure during their life cycle. Indeed, in most of the case, fungi have to switch from a budding like form to a filamentous form, to develop hyphae or spores. All these changes are necessary for viability, adaptation and full virulence, and the study of the proteins involved in the morphological regulation that occurred in these organisms has become a very interesting challenge.

Some conserved protein networks as the cyclic-AMP (cAMP) or the mitogen-activated protein kinase (MAPK) pathways, responding to environmental stimuli, are known to play a function in this regulation (Lengeler *et al.*, 2000; Borges-Walmsley and Walmsley, 2000). More recently, a new pathway has been described as a principal player in the control of morphology, involved in cell separation and cell polarity regulation. This protein network is the RAM pathway (Regulation of Ace2p activity and cellular Morphogenesis). This pathway has been described in few organisms in which its functions in morphology regulation have been shown to be conserved (Bidlingmaier *et al.*, 2001; Walton *et al.*, 2006; Seiler *et al.*, 2006; Song *et al.*, 2008).

Ustilago maydis, is a model organism extensively used in addressing fundamental questions of pathogenic development in fungi (Pérez-Martín *et al.*, 2006; Klosterman *et al.*, 2007). This filamentous fungus provides an ideal experimental system due to its easiness to grow under laboratory conditions and the availability of molecular genetic tools. In addition, it has the ability to adopt different cell structures during its life cycle, and appears to be an ideal model to study the molecular events regulating

morphogenesis adaptation. So, the characterisation of the RAM pathway in *U. maydis* seems to be a solution to understand the function at the molecular level of this central protein network as well as its integration into a cellular signaling context. This work will also permit to better understand the indispensable process of cell morphology regulation in filamentous fungi.

2. Principal pathways involved in morphology regulation in fungi

A fundamental property of living cells is the ability to sense and to adapt their morphology responding appropriately to changing environmental conditions. Two frequently utilized molecular devices for eliciting these responses are the cyclic AMP-signaling pathway and the three-tiered cascade of protein kinase known as the MAPK module (Lengeler *et al.*, 2000).

2.1. The nutrient-sensing cAMP pathway

cAMP-signaling pathway has been reported to regulate a variety of processes in filamentous fungi, including morphogenesis, sexual development and virulence (Kronstad *et al.,* 1998, Lengeler *et al.,* 2000; Borges-Walmsley and Wallmsley. 2000; Lee *et al.,* 2003). This pathway is a nutrient-sensing network involving a G protein-couple receptor and a Ras protein to transmit the signal (Fig.1). cAMP is produced as a second messenger from ATP by adenylate cyclase after activation by Ras. cAMP-dependent protein kinase (PKA) has been found in all eukaryotes, and is the major downstream effector of cAMP. PKA is a tetrameric protein that is composed of a regulatory and a catalytic subunit. In most of the cases, this enzyme is inactive and

unable to phosphorylate substrate proteins (Lengeler *et al.*, 2000). Binding the cAMP to the regulatory subunits results in the release of the catalytic subunit, which is then able to phosphorylate target proteins (Fig.1). This cAMP pathway has been shown to play a central role in regulating morphological changes and filamentous growth in parallel to others protein networks as the MAPK pathway.

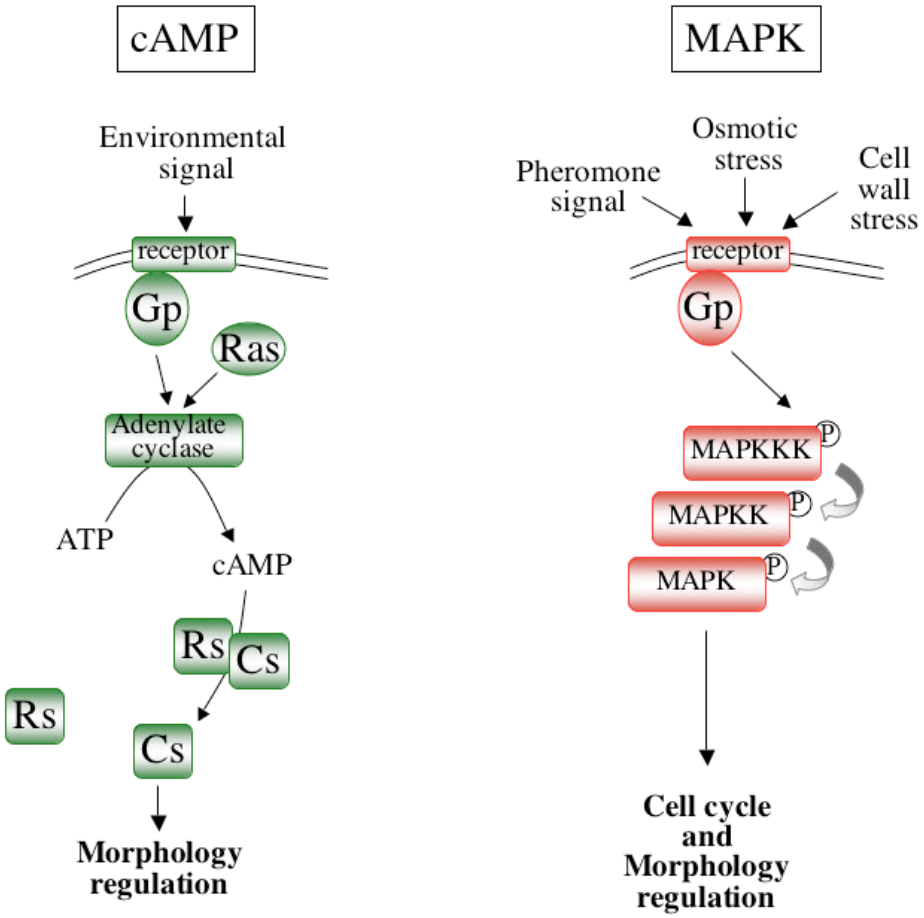

Figure 1: Schematic representation of cAMP and MAPK pathway.
The cAMP pathway (in green) regulates PKA protein composed of Rs (Regulatory subunit) and Cs (Catalytic subunit). The MAPK network (in red) regulates cell cycle and morphology transition through the activation of pheromone, osmotic stress or cell wall stress signal.

2.2. The MAPK cascade

The MAPK pathway contains three components signal relay in which an activated MAPK kinase kinase (MAPKKK) activates a MAPK kinase (MAPKK), which then actives a MAPK (or ERK, for Extracellular signal Regulated Kinase) (Fig.1) (Robinson and Cobb, 1997).

Upon activation, a MAPKKK phosphorylates two serine or threonine residues at conserved positions in the activation loops of its target MAPKK. The activated MAPKK then proceeds to phosphorylate both the threonine and tyrosine residues of a conserved -Thr-X-Tyr- motif in the activation loops of its target MAPK. These phosphorylations activate the MAPK by causing substantial conformational changes (Errede *et al*., 1993; Gartner *et al*., 1992).

To initiate a MAPK cascade, the MAPKKK must be activated. Upstream events that can lead to this activation include a variety of extracellular stresses and molecular signals. The binding of appropriate ligands to the receptor stimulates production of activated G-protein, which then transmits the signal through the MAPK cascade (Fig.1). MAPK protein kinases phosphorylate diverse set of well-characterised substrates, including transcription factors, translational regulators, phosphatases and other kinds of proteins, thereby regulating metabolism, cellular morphology and cell cycle progression (Chen and Thorner, 2007).

Five MAPK signaling pathways are described in *Saccharomyces cerevisiae* but, three MAPK cascades have been well studied also in other fungi and their functions in morphology regulation has been shown conserved in eukaryotic cells. One is involved in pheromone sensing (Kss1), another one in cell wall integrity (Mpk1/Slt2) and the third one in osmotic stress sensing (Hog1) (Fig.1) (Butty *et al.,* 1998; Lamson *et al.,* 2002; N. Carbó, PhD thesis 2009).

3. The RAM pathway: new signaling network

The RAM pathway has been studied intensively during the last teen years in different organisms where it has been shown to be involved in the regulation of important processes in cell development. This pathway has been well described in *S. cerevisiae* and later in other organisms where it appears conserved and plays a key role in parallel to other signaling networks.

3.1. The RAM pathway in *Saccharomyces cerevisiae*

The RAM protein network was first described by Bidlingmaier and colleagues in 2001. It is composed of six proteins: Cbk1p, Mob2p, Kic1p, Hym1p, Tao3p and Sog2p (Fig.2) (Nelson *et al.,* 2003). Cbk1p (Cell wall biosynthesis Kinase) is an NDR (Nuclear Dbf2 related) kinase, member of the super family of AGC serine/threonine protein kinase (Hergovich *et al.,* 2006). Mob2p is a Cbk1-binding protein required for full Cbk1p kinase activity. Kic1p is the yeast sterile 20 (STE20)-like kinase that functions genetically upstream of Cbk1p kinase, probably activating the Cbk1p-Mob2p complex (Nelson *et al.,* 2003). Hym1p, an orthologous protein of *Aspergillus nidulans* HymA, interacts with Cbk1p and Kic1p and is important for the catalytic activity and proper localization of the Cbk1p-Mob2p complex (Karos and Fisher, 1996; Nelson *et al.,* 2003). Tao3p belongs to a group of large, conserved scaffolding proteins and may facilitate Cbk1p-Mob2p kinase activation by Kic1p (Du and Novick, 2002; Hergovich *et al.,* 2006). Sog2p, a leucine-rich-repeat-containing protein, binds Hym1p, Kic1p and Cbk1p (Nelson *et al.,* 2003) (Fig.2). It has been also demonstrated that Mob2p binds Cbk1p throughout the cell cycle, and the formation of this complex is critical for all known RAM functions (Weiss *et al.,* 2002).

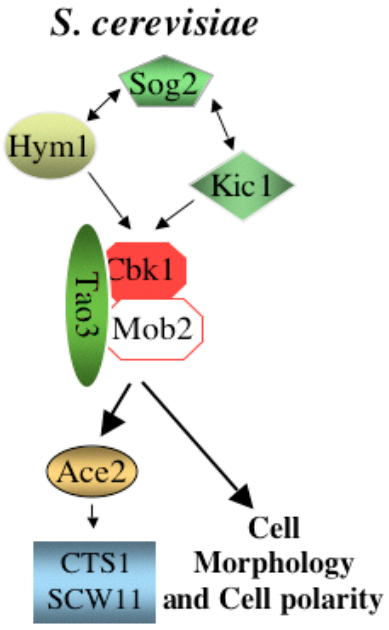

Figure 2: RAM pathway in *S. cerevisiae*. The central complex Cbk1p-Mob2p is regulated by the Kic1p kinase, Hym1p, Sog2p and the scaffold protein Tao3p. This pathway controls cell separation by the regulation of Ace2p localisation. Translocated in the daughter nucleus, Ace2p regulates the transcription of CTS1 and SCW11. The RAM network is also involved in cell morphology and cell polarity regulation but the targets have not been identified yet.

Consistent with a role for the RAM pathway in morphogenetic transitions, loss-of-function mutation of one of the RAM components lead to defects in cell separation after mitosis, bud site selection, polarized growth and cell integrity. In *S. cerevisiae*, mutant cells are rounder than wild-type and organized in chains (Racki *et al.*, 2000; Bidlingmaier *et al.*, 2001; Colman-Lerner *et al.*, 2001; Jorgensen *et al.*, 2002; Weiss *et al.*, 2002; Kurischko *et al.*, 2005; Voth *et al.*, 2005). The cell separation defect in RAM mutants, can be explained by the role of the RAM network in the daughter-specific localization of the transcriptional factor Ace2p (Colman-Lerner *et al.*, 2000; Nelson *et al.*, 2003). Ace2p remains in the cytosol until late mitosis, at this point it translocates to the daughter nucleus, where it is responsible for activating a set of daughter-specific genes necessary for cell separation, as *CTS1* or *SCW11* (Fig.2) (Dohrmann *et al.*, 1992; Bidlingmaier *et al.*, 2001, Colman-Lerner *et al.*, 2001; Weiss *et al.*, 2002). Cells deleted for *ACE2* gene are organised in chains but do not present defects in cell polarity. This result suggests that the Cbk1p-Mob2p complex acts on other targets that have not been found yet. In addition, it has been shown that in *S. cerevisiae* cells lacking a functional

CBK1 gene, the expression of more than 50 genes was altered by more than 2.2 fold (Bidlingmaier *et al.,* 2001) suggesting that the deregulation of the RAM network affects a lot of process, and that many of its targets remain to be discovered.

3.2. The RAM pathway is conserved from yeast to human

Knowing the implication of the RAM pathway in polarity regulation, this network has been also studied in diverse fungi. In *Aspergillus nidulans*, the CotA-MobB complex is required for the site selection of germ tube emergence and is involved in the process of hyphal polarity. Furthermore, HymA, appears to be indispensable for conidiospore development (Table 1) (Karos and Fisher, 1996; Johns *et al.,* 2006; Shi *et al.,* 2008). In *Candida albicans*, all RAM mutants exhibited cell separation defects, a multinucleate phenotype and loss of cell polarity (Song *et al.*, 2008). These genes are critically required for normal hyphal growth and to polarize cortical actin patch at the growing tip (Table 1) (McNemar and Fonzi, 2002; Song *et al.,* 2008). The RAM pathway also appears to control cell separation in *C. albicans* and, as in *S. cerevisiae*, through the CaAce2 protein regulation (Mulhern *et al.,* 2006). Interestingly, Ace2p homologues are infrequent, suggesting that the RAM pathway is conserved but can have diverse targets or functions. In the basidiomycete *Cryptococcus neoformans*, it has been demonstrated that besides not having Ace2p homolog, the RAM pathway was involved in a negative control of polarity, contrary to the positive polarity regulation that was demonstrated in other organisms. In this fungus, disruption of this pathway resulted in hyperpolarized cells with a defect in cell separation (Table 1) (Walton *et al.,* 2006). The RAM pathway has also been intensively studied in *Neurospora crassa* where colonial temperature sensitive-1 (Cot-1) and Pod6 respectively, have been shown to be essential for normal tip extension, coordinated branch formation as well as cell-wall organization

(Table 1). *cot-1* mutant cells cannot elongate normally and tip inhibition causes an abnormal increase in hyphal branching (Yarden, 1992; Gorovits and Yarden, 2003; Seiler *et al.*, 2006).

	NDR kinase	Mob	Ste20-like	Scaffold	Regulator	functions
S. cerevisiae	Cbk1	Mob2	Kic1	Tao3	Hym1/ Sog2	Cell separation and cell polarity regulation
Higher eukaryotes						
C. elegans	Sax-1			Sax-2		Neurite outgrowth and dendritic tiling control
D. melanogaster	Trc	Dmob		Fry		Integrity of epidermal outgrowths maintenance. Dendritic tiling and branching control
H. sapiens	Ndr1/2	Mob1A	Mst3			Neuronal growth and differentiation control
Filamentous fungi						
A. nidulans	CotA	MobB			HymA	Polarity growth and morphology control
C. albicans	CaCbk1	CaMob2	CaKic1	CaPag1	CaSog2	Morphology maintenance and regulation
N. crassa	Cot-1		Pod6			Hyphal elongation and branching regulation
C. neoformans	Cbk1	Mob2	Kic1	Tao3	Sog2	Cell morphogenesis regulation
U. maydis	Ukc1					Morphogenesis, pathogenicity and pigment formation regulation

Table 1: Characterized RAM pathway homologues. Cbk1p is a Ser/Thr kinase in the AGC family of kinases. Kic1p is also a Ser/Thr protein kinase that is related to the PAK/Ste20 family of protein (Sullivan *et al.*, 1998). Mob2p, Sog2p, Hym1p and Tao3p interact with at least one of these kinases to mediate their functions in *S. cerevisiae* (Nelson *et al.*, 2003).

In higher eukaryotes, the RAM pathway has been also shown to play an important role in polarity and morphology regulation (Table1). In *Drosophila melanogaster*, Tricornered (Trc) and Furry (Fry) are required for the correct morphogenesis of cell extensions and the control of dendritic tiling and branching of sensory neurons (He *et al.*, 2005; Cong *et al.*, 2001; Emoto, *et al.*, 2004). Equally, Stork and colleagues (2004), proposed that NDR2 has a role in coupling morphological changes of neurons and are

most important in neurite outgrowth (Table 1). Similarly, in *Caenorhabditis elegans*, the RAM pathway is also important for neurite tiling. But interestingly, the neuronal cells of *sax-1* mutants are irregularly expanded and extended instead of displaying a normal compact and spherical phenotype suggesting that Sax-1 is a negative regulator of polarity (Zallen *et al.*, 2000; Gallegos *et al.*, 2004).

Through the study of the RAM pathway in different organisms, we can observe that this protein network is conserved and plays an important function in cell morphology regulation. But some differences as the negative control of polarity in some cases (*C. elegans* or *C. neoformans*) or the absence of conserved target (Ace2p homolog), suggest that the functions of this pathway can diverge from one organism to another.

3.3. Interplay between the RAM pathway and other signaling networks in morphology regulation

Different protein networks are known to be involved in extracellular sensing responding to different stresses or pheromones stimuli to adapte the morphology. Interestingly, some of them, as the cAMP and the MAPK pathways, have been shown to play a function in parallel in numerous organisms, allowing a quick and complete cell adaptation (Lengeler *et al.,* 2000). An interconnection between the RAM pathway and other signaling networks has also been observed in different organisms. Indeed, in *Aspergillus nidulans* and *Cryptococcus neoformans*, the calcineurin pathway (Ca_2^+-calmodulin-activated protein phosphatase) has been shown to play an important function acting directly or in parallel to the RAM pathway. In *C. neoformans*, simultaneous inhibition of both pathways is lethal (Walton *et al.,* 2006), whereas in *A. nidulans*, release of Ca_2^+ is involved in osmotic suppression of *mobB* and *cotA* mutant

phenotypes (Shi *et al.,* 2008), suggesting a potential function for the calcineurin pathway in parallel to the RAM pathway.

Much more is known about the link between the RAM pathway and other signaling networks in *N. crassa*, where it has been recently suggested a relationship between the RAM, the PKA and two MAPK pathways. In this fungus, different studies have shown that inhibition of PKA activity can suppress the *cot-1 thermo sensitive (ts)* mutant phenotype rescuing the hyphal tip extension defect (Gorovits and Yarden, 2003; Seiler *et al.*, 2006). It has also been demonstrated a link between Cot-1 and MAPK signaling. In this case, the loss of *mak2,* encoding a kinase acting in cell fusion and female fertility pathway, can rescue the *cot-1(ts)* phenotype, the double mutant presenting normal growing tip. Furthermore, the phospho-MAK1 kinase activity, kinase acting in cell integrity pathway, has been shown to increase in *cot-1(ts)* mutant cells (Maerz *et al.*, 2008) suggesting that Cot-1/Pod6 pathway regulates negatively MAK1 activity.

In mammals, Ndr1 has been shown to be regulated by the Kic1 protein kinase but also by the calcineurin phosphatase, suggesting that NDR1/2 along with its partners may form part of novel calcium dependent signaling pathway (Millward *et al.,* 1998, Tamaskovic *et al.,* 2003). Furthermore, neurite initiation in *C. elegans* has been shown to be regulated in parallel by both the Sax-1 RAM pathway and a calcium/calmodulin dependent protein kinase Unc-43 (Zallen *et al.,* 2000).

In all these organisms a relationship between the RAM signaling network and other well characterised pathways has been demonstrated, showing that the RAM pathway could play a key role controlling morphology adaptation depending on divers signal outputs or metabolites concentration (Ca^{2+} or cAMP).

4. The fungal model *Ustilago maydis*

4.1. *U. maydis* life cycle

In *U. maydis*, virulence and sexual development are intricately interconnected (Kahmann and Kämper, 2004). Haploid cells are non-pathogenic and grow in a yeast-like unicellular form (so-called sporidia) that divides by budding (Fig.3, a). The pathogenic form, the filamentous dikaryon, is established after mating of two compatible sporidia that have to harbour different mating type allele (Fig.3, b). Cell recognition and cell fusion require the transduction of the pheromones signal, controlled by the *a* mating type locus, which results in the formation of conjugation tubes that can fuse and develop the filamentous dikaryon (Fig.4) (Mayorga and Gold, 1999; Müller *et al.*, 1999; Andrews *et al.*, 2000). This change from budding to filamentous growth coincides with a change of lifestyle from saprophytic to pathogenic development. The filamentous dikaryon forms appressoria-like structures to allow penetration (Fig.3, c) (Snetselaar and Mims, 1992, 1993). The fungal hyphae proliferate and accumulate intercellularly (Snetselaar and Mims, 1992), followed by a switch to sporogeneous hyphae that differentiate into the highly melanized diploid spores (Snetselaar and Mims, 1994). Characteristic symptoms of the disease are tumors in which the spore mature (Banuett and Herskowitz, 1996), and the stress reaction response of the host: the antocyanin production. The masses of black spores accumulate in the tumors and tissue burst to be disperse for subsequent inoculation of other maize plants (Fig.3, d). Under appropriate conditions, the spores germinate and undergo meiosis to generate new haploid sporidia.

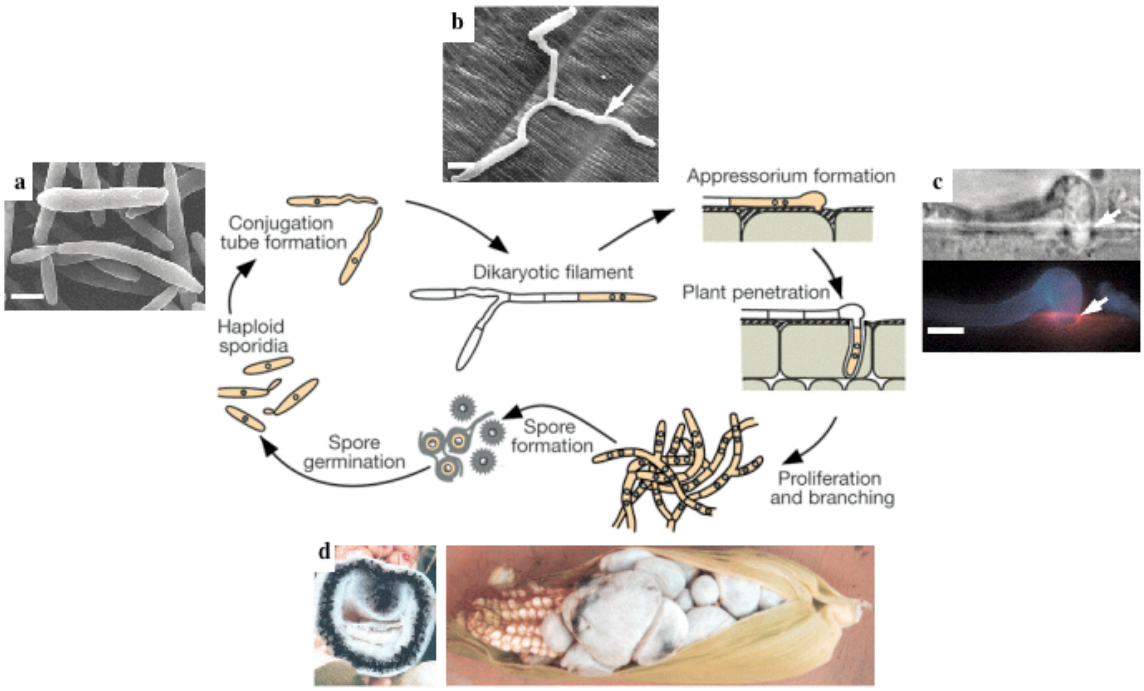

Figure 3: Developmental stages during the *U. maydis* life cycle.
a: scanning electron microscopy (SEM) image of haploid sporidia. **b**: SEM image of mated sporidia on plant epidermis; arrow denotes dikaryotic filament. **c**: Top: differential interference image of apprasorium, bottom: epilurescence image of fungal cell wall stained with calcofluor (blue) and endocytotic vesicles stained with FM4-64 (red). The bright ring indicates active secretion and endocytosis at the fungus-plant interface; arrows indicate the penetration point. **d**: black teliospores visible in tumour section of plant maize infection. Scale bars, 5μm. Figure adapted from Kämper *et al*., 2006.

4.2. The mating type loci

In order to find a mate, *U. maydis* must be able to distinguish between self and non-self partners. In consequence, *U. maydis* has a tetra-polar mating-type (MAT) system composed of two MAT loci with at least two alleles at each locus. In this case, a distinct *a* locus governs cell fusion between haploid partners and a *b* locus controls sexual development after fusion and pathogenicity. Together with *a*, the *b* locus controls the transition from yeast-like growth of haploid cells to hyphal growth of the dikaryon as well as maintenance of the dikaryon (Fig.4) (Banuett, 1992).

The *a* locus in *U. maydis* has two different alleles, *a1* and *a2*. The *a1* locus encodes a pheromone precursor (from the *mfa1* gene) and the corresponding receptor for the *a2* pheromone (from the *pra1* gene). The *a2* locus contains the *mfa2* gene encoding

lipoprotein pheromone precursor, and the receptor Pra2, for the *a1*-encoded pheromone. The secreted pheromone from one mating type is recognized by the corresponding receptor of the opposite mating-type (Fig.4). This "recognition" starts a cascade of signaling events that regulates gene expression in the *a* and *b* loci.

After cells have fused, subsequent development depends on the *b* locus. The *b* locus consists of two divergently transcribed genes encoding the homeodomain protein bW and bE (Gillissen *et al.*, 1992). The bE and bW products originated from different alleles interact to form a heterodimer that acts as functional transcription factor (Fig.4) (Gillisen *et al.*, 1992; Brachmann *et al.*, 2001). This bE/bW heterodimer controls the expression of a large number of genes (at least 246) involve in the transition to the filamentous dikaryotic stage as well as pathogenicity (Kamann and Kamper 2004).

At the transcriptional level, the *a* and *b* loci are regulated through the two major signaling pathways described in *U. maydis*, the cAMP pathway and the pheromone response MAPK cascade (Hartmann *et al.*, 1996; 1999).

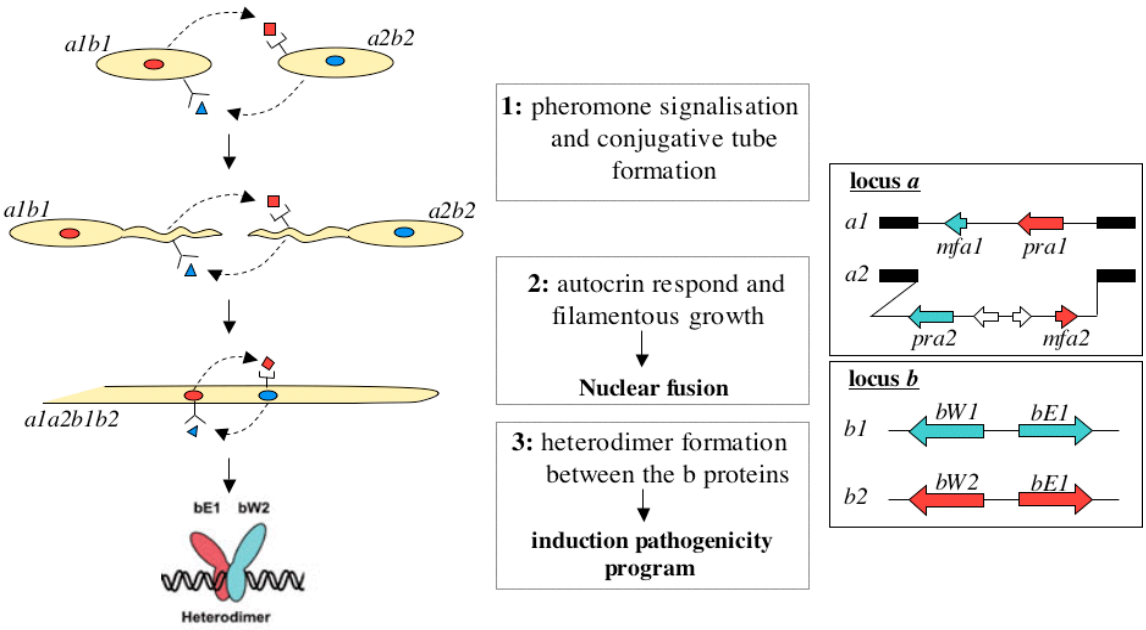

Figure 4: Schematic illustration of the pheromone recognition model. *a* and *b* loci organisation involved in pheromones recognition and morphological adaptation. The *a* locus encodes a pheromone precursor *mfa* and the corresponding receptor *pra*. The *b* locus contains two divergently transcribed genes encoding the homeodomain proteins bW and bE able to form an heterodimeric transcriptional factor.

5. Signaling pathways in *U. maydis*

The cAMP, the pheromone MAPK and, recently the Cell Wall Integrity (CWI) signaling MAPK pathways have been characterised in *U. maydis*. These pathways regulate important processes, integrating input signals and regulating fungal dimorphism and pathogenicity. The cAMP and the pheromone MAPK appears to be the key element to set off the mating process, but in addition of the CWI pathway, they are indispensable for the morphological adaptation.

5.1. The cAMP/PKA pathway

The phytophathogenic fungus *U. maydis* adopts a yeast-like, non-pathogenic form and a pathogenic filamentous form. These morphological transitions are controlled partially by the cAMP signaling pathway. In *U. maydis*, this pathway consists of the heterotrimeric G protein α subunit Gpa3 (Kruger *et al.,* 1998), a β subunit Bpp1 (Müller *et al.,* 2004) and a possible Ras1 protein, that transmit the signal to the cyclic AMP-dependent PKA via the adenylate cyclase Uac1 (Fig.5 pathway in green) (Gold *et al.,* 1997; Durrenberger *et al.,* 1998).

Activation of Uac1, which produces the second messanger cAMP (Barrett *et al.*, 1993), allows the activation of the PKA composed of the regulatory subunit Ubc1 and the catalytic subunit Adr1 (Durrenberger *et al.;* 1998, Gold *et al.;* 1997). Binding of the Ubc1 to the catalytic subunit Adr1 prevents PKA activity. cAMP binds to cAMP-binding sites present in the Ubc1 subunit and consequently induces a conformational change that causes the release of the active catalytic Adr1 subunit (Taylor *et al.,* 1990; Gold *et al.,* 1994; Durrenberger *et al.,* 1998). Strains disrupted in *uac1*, *adr1*, *gpa3* or *bpp1* grow filamentously and exhibit reduced pheromone gene expression (*a* and *b* loci), whereas a strain exhibiting constitutively active PKA caused by the deletion of

ubc1 displays a multiple budding mutant phenotype, which results from a defect in bud site selection and cytokinesis (Barrett *et al.,* 1993; Durrenberger *et al.,* 1998; Gold *et al.*, 1997). These results indicate that elevated PKA activity inhibits filamentation, whereas disruption of the PKA activity promotes filamentous cells.

Like in other organisms, the cAMP pathway regulates pathogenicity and morphology in *U. maydis*. But strikingly, in contrast with what it has been shown in *S. cerevisiae*, *C. albicans* or *N. crassa* cells, where an increase of cAMP level stimulates the transition from yeast-like cells to the filamentous forms, in *U. maydis* the activation of the PKA protein inhibits filamentation (Cruz *et al.,* 1988; Gold *et al.,* 1994).

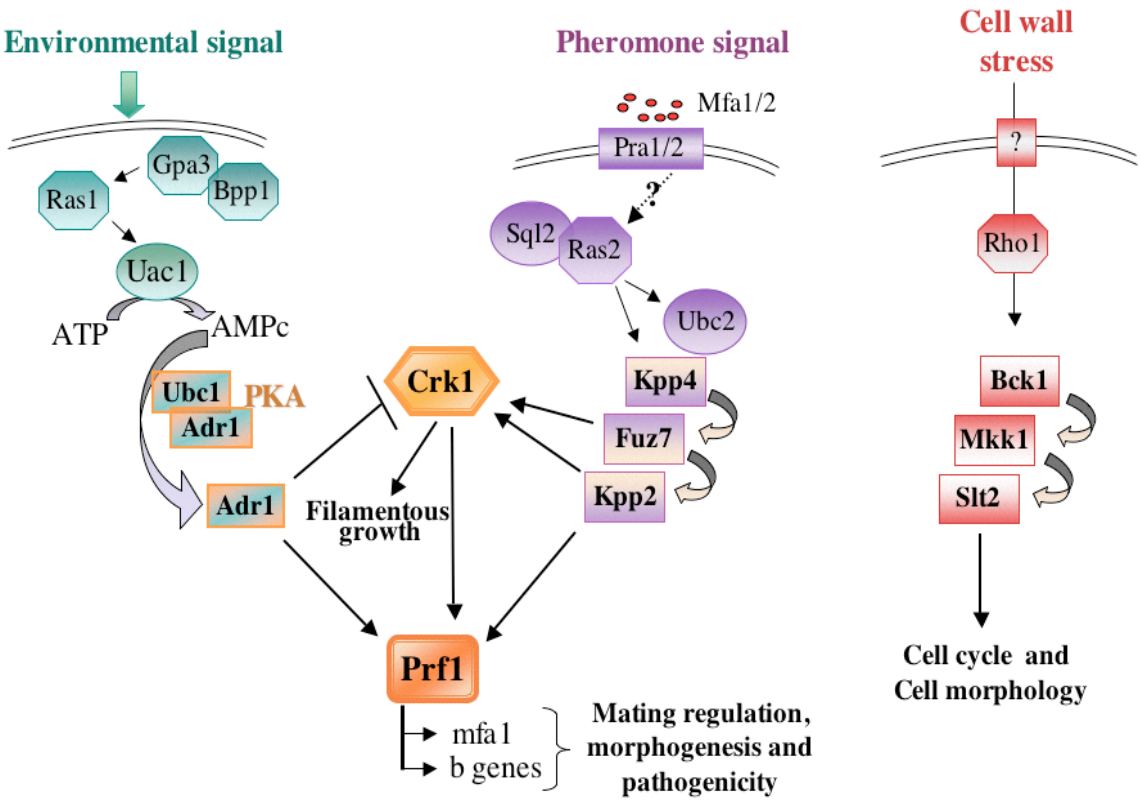

Figure 5: Signaling pathways in *U. maydis*.
Interplay between the cAMP (green) and MAPK (violet) pathways in *U. maydis*. Both pathways are involved in the regulation of the transcriptional factor Prf1 and the Crk1 kinase, to modulate mating, morphogenesis and pathogenicity. The cell wall integrity pathway components are shown in red.

5.2. The pheromone signaling MAPK pathway

The other pathway involved in the control of environmental-induced outcomes in *U. maydis* is the pheromone MAPK pathway. It is organised around a central MAPK cascade composing of a MAPKKK (Kpp4/Ubc4) (Andrew *et al.,* 2000), a MAPKK (Fuz7/Ubc5) (Banuett and Herskowitz, 1994) and a MAPK (Ubc3/Kpp2) (Fig.5 pathway in violet) (Mayorga and Gold, 1999; Müller *et al.,* 1999). Mutations in the *ubc* genes, encoding components of this cascade, have been obtained as specific suppressors of the filamentous phenotype of strains defective in the adenylate cyclase (Uac1) activity (ubc stands for Ustilago bypass of cyclase) (Mayora and Gold, 1998).

Upstream this cascade, the Ubc2 protein has been recently shown to interact physically with the Kpp4 protein kinase (Fig.5) (Klosterman *et al.,* 2008). Interestingly, both proteins (Ubc2 and Kpp4) contain a Ras-association domain (Mayorga and Gold, 2001), suggesting an interaction with the Ras2 protein. More recently, it has been shown that Ras2 is activated via the Sql2 protein, a Cdc25-like Ras guanine nucleotide exchange factor (Ras GEF) (Müller *et al.,* 2003) (Fig.5). So, the activation of the MAP kinase cascade seems to occur through a Ras-mediated signaling mechanism but the connection to the upstream Pra1/2 receptor remains unclear.

The function of the MAPK cascade in morphology and pathogenic regulation has been shown by the deletion of *kpp2*, which abolishes pheromone-dependent expression of the *a* locus as well as conjugative tube formation (Müller *et al.,* 1999). Furthermore, deletion of *fuz7* also results defective in conjugative tube formation (Banuett *et al.,* 1994). In addition, the constitutive expression of Ras2 increases pheromone gene expression and promotes filamentation (Lee and Kronstad, 2002).

5.3. Cell wall integrity MAPK pathway in *U. maydis*

The CWI pathway in *U. maydis* has been recently characterised in our laboratory (N. Carbó, PhD thesis). It is organised around a central MAPK cascade composed of a MAPKKK (Bck1), a MAPKK (Mkk1) and a MAPK (Slt2) (Fig.5 pathway in red). Upstream this cascade, Rho1 could be the central GTPase transmiting the signal through receptors involved in drugs and cell wall stress sensing. N. Carbó´s work showed that the CWI MAPK pathway in *U. maydis* was not involved in virulence regulation but played an important function in cell cycle regulation. A constitutive activation of this cascade led to an accelerated G2/M transition which resulted in a defective morphology. In this condition, cells were rounder, and organised in chains due to a defect in cell separation.

5.4. Interplay between cAMP and MAPK pathways in *U. maydis*

It is well known that during the sexual development both nutritional and pheromone signals have to be integrated (Kahmann *et al.,* 1999). In *U. maydis*, a cross talk between the pheromone signaling MAPK and the cAMP pathways regulates fungal mating and dimorphism (Lengeler *et al.*, 2000). Integration of both pathways depends on the activation of the transcription factor Prf1, as well as of the regulation of the Crk1 protein kinase.

5.4.1. Integration of both signals by Prf1

Prf1 is a key element in the pheromone response pathway. It is highly regulated at the transcriptional as well as post-transcriptional level by different proteins and by the

cAMP and pheromone MAPK pathways, allowing to the cell a very sensitive adaptation to different environmental conditions (Fig.6 A and B).

Prf1 is a high mobility group (HMG)-domain transcription factor that recognizes pheromone-response elements (PREs) localised in the regulatory region of pheromone-induced genes (Urban *et al.*, 1996). These PREs elements are found in the promoter region of the genes composing the *a* and *b* mating type loci (Fig.6 B) and also in the regulatory region of *prf1* itself, where two PREs have been identified (Fig.6 A) (Hartmann *et al.,* 1996, 1999). In addition to PREs domains, other motives have been found to be involved in the *prf1* transcription control. These domains are: one UAS domain integrating the sensing of carbon source and kinase signaling (PKA and Crk1 regulation) (Hartmann *et al.,* 1999; Garrido *et al.,* 2004), three RRS elements (Rop1 Recognition Sequences) allowing the regulation of the transcriptional factor Rop1 (Bredfort *et al.,* 2005) and one or more CCAAT boxes binding by the Hap2 protein (Fig.6 A) (Mendoza-Mendoza *et al.*, 2009).

At the post-transcriptional level, regulation of Prf1 activity occurs by phosphorylation. Prf1 contains six putative MAPK sites and five putative PKA sites (Fig.6 B). The level of phosphorylation by the PKA or the MAPK pathway permits to adjust the *prf1* transcription function. It has been demonstrated that the induction of *a* genes transcription required the phosphorylation of the PKA sites, whereas the induction of *b* genes transcription is dependent on the integration of both pathways (Fig.6 B). A yeast two hybrid analysis allowed the identification of Adr1 and Kpp2 as the direct kinases involved in Prf1 regulation (Fig.6 B) (Kaffarnik *et al.,* 2003).

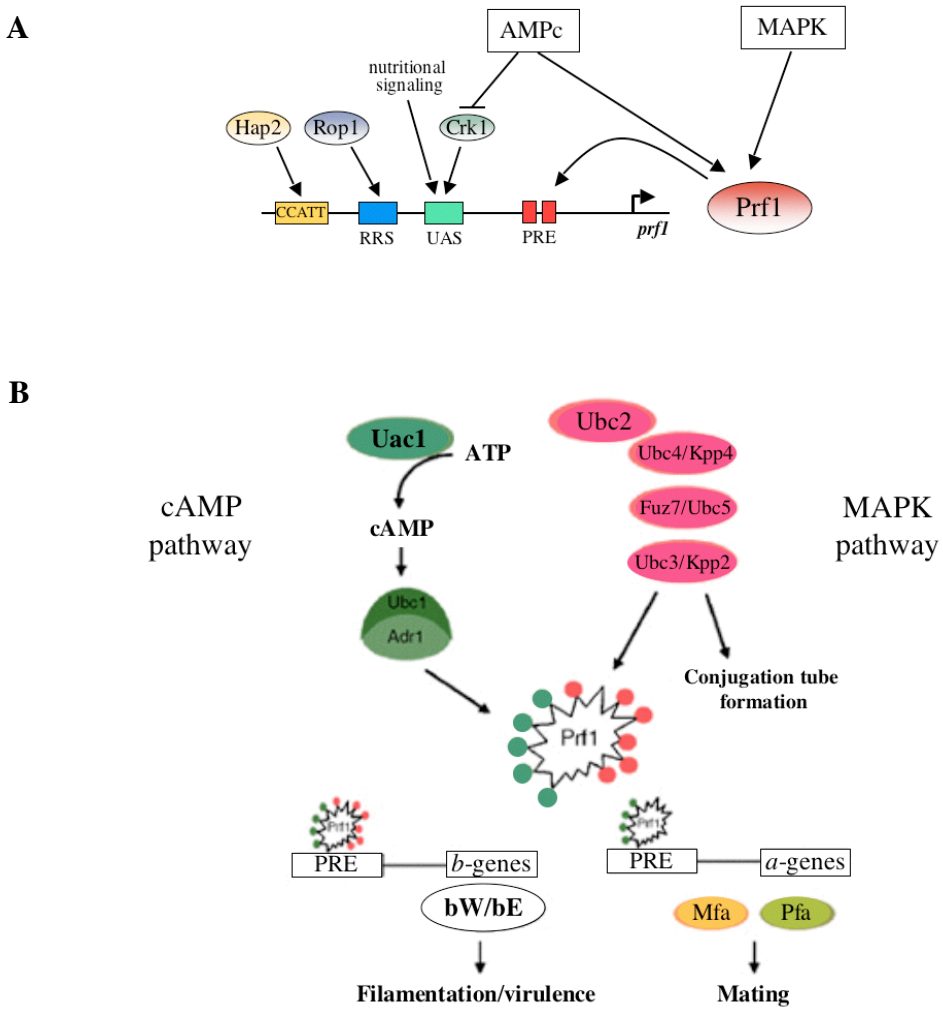

Figure 6: Regulation of the Prf1 transcription factor.
A. Integration of the multiple signals regulating Prf1 at the transcriptional and post-transcriptional level.
B. In *U. maydis* Prf1 regulates the *a* and *b* loci by the PRE elements localized in their promoters. Furthermore, Prf1 is post-transcriptionally co-regulated by the MAPK (pink) and PKA (green) pathways controlling mating and filamentous development in *U. maydis* (Adapted from Nadal *et al.*, 2008).

5.4.2. Integration of both signals by Crk1

The integration of the cAMP and MAPK signaling also has been demonstrated, through the study of Crk1, to be required for an appropriate mating and development. The Crk1 kinase was described as a new class of MAPK. This gene encodes a putative Ser/Thr kinase in which the catalytic domain shows a high sequence similarity to those present in cyclin dependent kinase, and that is conserved from yeast to human (Garrido and Pérez-Martín, 2003).

A major role of Crk1 in morphogenesis is evident because the over-expression of this gene prompts filamentous growth while deletion of *crk1* supresses the filamentous phenotype of a mutant defective in the cAMP pathway (Garrido and Pérez-Martín, 2003). Additionally, strains deficient in PKA activity produce highly elevated levels of the *crk1* messanger, suggesting that the cAMP pathway negatively regulates *crk1* expression (Fig.5). In contrast, the MAPK pathway counteracts this negative regulation of Crk1. Immunoprecipitation experiments revealed that both Kpp2 and Fuz7 interact physically with Crk1p (Garrido and Perez-Martin, 2003; Garrido *et al.,* 2004). In addition to regulate filamentous growth, this protein kinase has also been involved in pathogenicity, regulating *prf1* expression through the UAS domain contained in the *prf1* promoter (Fig. 6 A). Taken together, these findings indicate that, as well as Prf1, Crk1 is a key integration point of the cAMP and pheromone signaling MAPK pathways in *U. maydis*.

6. The RAM pathway in *U. maydis*

At the moment, three signaling pathways (cAMP, pheromone and CWI MAPK pathways) have been characterised and shown to be involved in morphology regulation in *U. maydis*.

Knowing the importance of PKA in morphological and pathology, Dürrenberger and colleagues (1999), decided to search for additional protein kinases playing important roles in morphogenesis and pathogenicity, and identified the Ukc1 protein kinase. This protein belongs to the NDR protein kinase family as Cot-1 of *N. crassa* or Cbk1p of *S. cerevisiae*, which are central components of the RAM signaling network. Strikingly, the RAM pathway, has been shown to be a very important player in polarity and cell separation regulation in many organisms (Nelson *et al.*, 2003; Seiler *et al.*, 2006;

Walton *et al.*, 2006; Song *et al.*, 2006). Disruption of the *ukc1* gene in an haploid background resulted in cells highly distorted in their morphology, organised in clusters composed of round cells with hyphal extensions or elongated buds. In addition, mutant cells were highly pigmented, incapable of generating aerial filaments during mating and defective in their ability to cause disease on corn plants (Dürrenberger *et al.*, 1999). These results demonstrated an important role for the *ukc1*-encoding protein kinase in the control of morphogenesis, pathogenesis and pigmentation of *U. maydis*.

So, the characterisation of the RAM pathway in this organism appears to be an exiting project to understand how the morphological changes indispensable for the adaptation and the pathogenicity of many fungi occur and are regulated.

Objectives

1. To identify the RAM pathway components and to analyse whether RAM pathway organisation is conserved in *U. maydis*.

2. To describe the morphological problems presented by cells defective for *ukc1* gene.

3. To determine which aspects of the pathogenicity are defectives in cells deleted for one of the RAM pathway components.

4. To analyse whether the RAM pathway could have a relationship with cAMP and MAPK pathways in *U. maydis*.

Materials and Methods

1. Strain, media and growth conditions

1.1. Strains and plasmids

U. maydis strains used in this work are listed in the Table 2, in which the genotype and the origin of each one is indicated. Plasmids used in different constructions are listed in Table 3. For cloning purposes, the *Escherichia coli* K-12 derivative DH5α (Bethesda Research Laboratories) was used.

Table 2: *U. maydis* strains used in this work

Strain	*Relevant genotype*	*References*
FB1	*a1b1*	Banuett and Herskowitz, 1989
FB2	*a2b2*	Banuett and Herskowitz, 1989
AB31	*a2P$_{crg1}$:bW2 P$_{crg1}$:bE1*	Brachmann *et al.*, 2001
UMN4	*a1b1 fuz7DD^{crg1}*	Müller *et al.*, 2003 (B)
UMC33	*a1b1 P$_{crg1}$:wee1-myc*	Sgarlata and Pérez-Martín, 2005
UMP71	*a1 b1 fim1-GFP*	Castillo-Lluva *et al.*, 2007
UMP61	*a1 b1 tub1-GFP*	Carbó and Pérez Martín, 2008
FB1 PRF1 CON	*a1b1 prf1^{con}*	Hartmann *et al.*, 1999
FB2 PRF1 CON	*a2b2 prf1^{con}*	Hartmann *et al.*, 1999
UMP12	*a1 b1 Δ crk1::hyg*	Garrido *et al.*, 2003
FB1Δfuz	*a1 b1 Δ fuz7::hyg*	Banuett and Herskowitz, 1994
UMA3	*a1 b1 Δ slt2::nat*	Carbó, doctoral thesis
UMA20	*a1b1 mkk1DD^{crg1}*	Carbó, doctoral thesis
ELO1	*a1 b1 Δ ukc1::cbx*	This work
ELO2	*a2 b2 Δ ukc1::cbx*	This work
ELO3	*a1 b1 Δ mob2::cbx*	This work
ELO8	*a2 b2 Δmob2::cbx*	This work
ELO35	*a1 b1 Δhym1::cbx*	This work

ELO40	*a2 b2 Δhym1::cbx*	This work
ELO45	*a1 b1 Δtao3::cbx*	This work
ELO52	*a1 b1 Δsog2::cbx*	This work
ELO41	*a1 b1 Δnak1::hyg*	This work
ELO21	*a1 b1 Δace2::cbx*	This work
ELO32	*a1 b1 ukc1-myc*	This work
ELO31	*a1 b1* P_{crg1} *:T7-mob2*	This work
ELO33	*a1 b1 ukc1-myc* P_{crg1} *:T7-mob2*	This work
ELO27	*a1 b1 ukc1-GFP*	This work
ELO6	*a1 b1* $ukc1^{nar1}$	This work
ELO17	$a2P_{crg1}$*:bW2* P_{crg1}*:bE1* $ukc1^{nar1}$	This work
ELO16	*a1b1* $ukc1^{nar1}$ $fuz7DD^{crg}$	This work
ELO26	*a1b1* $ukc1^{nar1}$ $wee1^{crg}$	This work
ELO22	*a1 b1* $ukc1^{nar1}$ *sep1-GFP*	This work
ELO23	*a1 b1* $ukc1^{nar1}$ *sep2-GFP*	This work
ELO24	*a1 b1* $ukc1^{nar1}$ *sep3-GFP*	This work
ELO25	*a1 b1* $ukc1^{nar1}$ *sep4-GFP*	This work
ELO29	*a1b1 ukc1-GFP mlc1-RFP*	This work
ELO43	*a1 b1* $ukc1^{nar1}$ *fim1-GFP*	This work
ELO28	*a1 b1* $ukc1^{nar1}$ *myoV-GFP*	This work
FB1-YFP	*a1b1* P_{otef}*:YFP*	This work
FB2-CFP	*a2b2* P_{otef}*:CFP*	This work
ELO47	*a1b1* $ukc1^{nar1}$ P_{otef}*:YFP*	This work
ELO50	*a2b2* $ukc1^{nar1}$ P_{otef}*:CFP*	This work
ELO64	*a1b1* $prf1^{con}$ *Δ ukc1::cbx*	This work
ELO65	*a2b2* $prf1^{con}$ *Δ ukc1::cbx*	This work
ELO58	*a1 b1 Δ crk1::hyg Δ ukc1::cbx*	This work
ELO61	*a1 b1 Δ fuz7::hyg Δ ukc1::cbx*	This work
ELO61	*a1 b1* $ukc1^{nar1}$ *Δ slt2::nat*	This work
ELO80	*a1 b1 Δ slt2::nat Δ ukc1::cbx*	This work
ELO78	*a1b1* $ukc1^{nar1}$ $mkk1DD^{crg1}$	This work

Table 3: List of plasmids

Plasmids	*References*
PUMa260	Brachmann *et al.*, 2001
PUMa261	Brachmann *et al.*, 2001
pRU2-CBX	Brachmann *et al.*, 2001
pRU2-HYG	Brachmann *et al.*, 2001
pRU11	Brachmann *et al.*, 2001
pRU11-T7	Laboratory collection
pBS-Myc	Laboratory collection
p123	Spellig *et al.,* 1996
p123-YFP	Laboratory collection
p123-CFP	Laboratory collection
p123-GFP	Laboratory collection
pukc1^{nar}	This work
p123-ukc1-GFP	This work
pBS ukc1-myc	This work
pRU11-t7-mob2	This work
pRU11-Mkk1DD	Laboratory collection
pFim-GFP-CbxA	Laboratory collection
p3GFPmyoV	Laboratory collection
pGEM-T Easy	PROMEGA

1.2. Growth media and conditions

1.2.1. General conditions and mediums

U. maydis strains were grown at 28°C in yeast peptone (YP), complete medium (CM), or minimal medium (MM). YP and CM were used as described by Holliday (1974) and Kaiser *et al.* (1994). MM with nitrate (MM+NO_3) or ammonium (MM+NH_4) were prepared as described by Alfa *et al.* (1993). In all media carbon source (glucose (D) or arabinose (A)) was adjusted at 1% final concentration. In liquid medium, *U. maydis* strains were grown at 28ºC with agitation (250 r.p.m).

To visualise dikaryotic filaments or *b*-induced genes, compatible strains were grown (or spotted) on CM-charcoal plates containing CM medium, 2% agar and 1% activated charcoal.

E. coli strain was grown in LB (Luria-Bertoni) medium (Sambrook and Gething, 1989) at 37ºC with ampicilin (100 μg/ml).

All chemicals used were of analytical grade and were obtained from Sigma or Merck. All media were prepared with Milli-Rho water.

1.2.2. Regeneration and transformants selection

To obtain protoplast regeneration, regeneration agar (Schult *et al*., 1990) was used with sacarose as carbon source. To select transformant cells, antibiotics as carboxin (2 μg/ml) and hygromycin (200 μg/ml) were used. In regeneration agar, double concentration of antibiotics was added.

1.2.3. Inducible and constitutive promoters in U. maydis

Controlled expression of genes under the *crg1* and *nar1* promoters were first grown in non-inductor media until an OD_{600} = 0.6. After 3 washes with sterile water, cells were transferred to inductive media. P_{crg1} is induced with arabinose and repressed with glucose (Bottin *et al*., 1996) whereas P_{nar1} is induced with nitrate (NO_3) and repressed with ammonium (NH_4) found in CM or YP media (Brachmann *et al*., 2001).

In constitutive expression experiments, the P_{otef1} promoter (Spellig *et al*., 1996) was used. Cells were grown in media until an OD_{600} = 0.6 to then perform the adequate experiment.

2. Molecular methodology

2.1. Restriction mapping and subcloning

Restriction mapping, subcloning and plasmid DNA extraction from *E. coli* were carried out according to the methods described by Ausubel *et al.*, (1997), and always using the reagents according to manufacture´s instructions. Restriction enzymes were provided by New England Biolabs. Ligations were carried out using T4 DNA Ligase from Roche. DNA fragment were isolated from TAE electrophoresis gels using the QIAGEN QIAquick Gel Extraction Kit. *E. coli* competent cells have been transformed with purified plasmids by the heat shock method described by Hanahan (1983).

2.2. PCR reaction

PCR amplification was performed in a termocycler machine. Mix and PCR programme were adjusted in function of the DNA length and the DNA polymerase enzyme used. Two polymerase enzymes were used in this study: Taq (own production), and Expand Long Template (Roche, 1681 834). One PCR reaction of 50 µl for the Taq enzyme contained 5 µl of Taq buffer10X, 500 nM of each oligonucleotide, 10 ng DNA, 200 µM of each dNTP and one unit of polymerase. The Long Expend Template mix contained for one PCR reaction of 50 µl, 5 µl of enzyme buffer, 1 µg of each oligonucleotide, 15 ng DNA, 500 µM of each dNTP and one unit of Long Expand Template enzyme. Taq polymerase was used to amplify fragments from 300 bp to 1800 bp whereas Long Expand Template was used to amplify fragments longer than 1800 bp.

2.3. *U. maydis* transformation

All procedures were performed at 4ºC unless otherwise noted. Log-phase cells (50 ml at 10^7 cells/ml) were washed once in SCS buffer (20 mM sodium citrate [pH 5.8] –1 M sorbitol buffer) and resuspended in 1 ml of the same buffer containing Novozyme 328 (6mg/ml). After obtaining round cells (14 min incubation with gentle mixing), the resulting protoplasts were centrifuged at 2500 r.p.m for 5 min, washed twice with SCS buffer and once with STC buffer (10 mM Tris-HCl [pH 7.5] –1 M $CaCl_2$ – 1 M sorbitol buffer). Approximately 70% of the protoplasts could be regenerated to viable cells.

For transformation, protoplasts were resuspended in 50μl ice cold STC buffer. Transforming DNA (5 μl), 1 μl of heparin and 50 μl of protoplast suspension were mixed and incubated on ice. After 25 min, 0.5 ml of STC containing 40% polyethylene glycol was added, and the sample was incubated for an additional 15 min on ice.

The entire mixture was spread on 3 plates of regeneration agar (YP or MM, 1 M sorbitol, 1.5% agar). These plates were composed of two regeneration agar layers; the first one containing the selective antibiotic or fungicid at double concentration, whereas the second one was free of selective agent. After one night at 28ºC, plates were turn down and keep at 28ºC until colonies formed.

3. Biochemical techniques

3.1. Genomic DNA extraction

U. maydis DNA extraction was carried out according to the method described by Hoffman and Winston (1987). According to this protocol, cells were mechanically lysated. To this end, cells were grown in liquid culture to an OD_{600} = 0.6 and 1.5 ml of culture was spun down at 14000 r.p.m at RT for 5 minutes. The supernatant was

discarded and 500μl of lysis buffer (10 mM tris-HCl pH 8, 1mM EDTA, 100mM NaCl, 1% SDS, 2% Triton) were added with glass beads (Sigma). Cells were smashed in a Hybaid ribolyser set at speed 6 for 20 s at RT. After lysis, DNA was extracted with a phenol:chlorophorm solution. Finally, DNA was resuspended in 50 μl of distil water, incubated for 5 min at 70ºC and kept at -20ºC.

3.2. Biological methods involving RNA

3.2.2. RNA extraction from U. maydis cells grown in liquid medium

RNA total extraction was carried out according to the method described by Schmitt *et al.* (1990) in which cells were lysated mechanically with TES Tampon (10 mM Tris-HCl pH 7.5, 10 mM EDTA, 0.5 % SDS). RNA was extracted with a phenol acid solution and chloroform:IAA (24:1) solution. After precipitation with AcNa 3M, RNA was air dried and dissolved in 50-100μl H_2O DEPC (0.1% Dietyl pirocarbonate). RNA concentration was measured by absorbance (A_{260}) and the RNA conserved at –80ºC.

3.2.3. RNA extraction from tissue powder

In the case of strains grown in solid medium, cells were harvested and grounded with a mortar and pestled in liquid nitrogen. The powder obtained was transferred into a 1.5 ml eppendorf tube containing TES tampon with glass beads and processed as described above for cells grown in liquid medium.

3.2.4. Northern blot analysis

RNA samples were separated on gel [100ml: 1% agarose, 10 ml 10X Mops Buffer (20 mM Mops, 5 mM AcNa, 10 mM EDTA), 6 ml Formaldehyde and 84 ml

distil water]. 10 μg RNA plus 16 μl Loading Buffer (43,5 mM Mops, 11 mM AcNa, 2,2 mM EDTA, 9,6% Formaldehyde and 51% Formamide) were incubated at 65ºC for 15 min and loaded on gel. The gel was run in 1% Mops Buffer at 65 V.

RNAs from the gel were transferred to a Zeta-Probe® Blotting Membrane (Bio-Rad), using capillary action with 10X SSC buffer overnight (20X SSC: 3M NaCl, 0,3M sodium citrate $2H_2O$). RNAs were crosslinked to the membrane by UV crosslinking (1200 J/m^2). To control the RNA good transfer and quality, the membrane was stained with methylene blue (40 mg/100ml methylene blue, 0,5 M AcNa pH 5,2).

Subsequently, the membrane was prehybridated at 65ºC for 2 hours with 20 ml of prehybridation Buffer (0,2M Phosphate Tampon pH 7,2, 1mM EDTA, 7% SDS). Then the 32 P- Labelled probe was add in the same buffer for incubation overnight.

Finally, the membrane was rinsed 3 times: 1) just a rinse with wash Buffer (0,1% SDS-2X SSC) 2) a 30 min wash at 65 ºC with the same buffer and 3) a 30 min wash at 65ºC with a solution containing 0,1 % SDS and 0,2 % SSC. The washed membrane was exposed to a phosphoimager Screen (Storage phosphor Screen, Amersham-pharmacy Biotech). A phosphoimager (Molecular image FX, Bio-Rad) and the suitable program (Quantity One, Bio-Rad) were used for visualization and quantification of radioactive signal.

Radioactive labelling was performed with the Ready –To-Go DNA Labelling kit (-dCTP) (Amersham), [α-$_{32}$P] dCTP (PerkinElmer) and 50-100 ng RNA according to the commercial home protocol. After labelling, the probe was purified with the ProbeQuant$_{TM}$ G-50 column (Amersham-Pharmacia).

To wash radioactivity and reuse the membrane, a 10 min wash with 1% SDS at 100ºC was carried out before the prehybridation.

3.3. Biological methods involving Protein

3.3.1. Protein extraction

U. maydis protein extraction was carried out from cell grown liquid culture to an OD_{600} = 0.6. Cells were mechanically lysated with lysis buffer (125 mM Tris-ClH pH 6.8, 1% ß-mercaptoethanol, 4% SDS, 0.005% bromophenol blue, 20% glycerol, 5 mM EDTA pH 8, 1 mM PMSF and 1/10 of Protease Inhibitor Cocktail Tablets from Roche). These lysates were incubated 5 min at 100ºC and loaded on the gel or stored at – 80ºC.
To perform immunoprecipitation, cells from a liquid culture to an OD_{600} of 0.8 were washed 3 times with 1X PBS at 4ºC. Then, cells were mechanically lysated (3 times maximal speed and 2 min on ice between them) with a lysis buffer BF (50 mM Tris-ClH pH 7.5, 250 mM NaCl, 0.1% Triton X100, 50 mM NaF, 1 mM ß-glycerolphosphate, 1 mM EGTA, 12.5 mM sodium pyrophosphate, 0.1 mM $NaVO_3$, 5 mM EDTA pH 8, 1 mM PMSF and 1/10 of Protease Inhibitor Cocktail Tablets from Roche). These lysates were incubated 5 min at 100ºC and loaded on the gel or stored at – 80ºC.

3.3.2. Immunoprecipitation

Immunoprecipitation was carried out with the commercial system Dynabeads® (Invitrogen) according to the manufacture´s recommendations. Briefly, the protein extract was incubated with BF Buffer (500 μl) for 2 hours. Then magnetic beads were added (300 μl of resin with G protein bound to magnetic beads). This mix was incubated 1 hour at 4ºC with slow agitation. Then 3 washes were realised with BF buffer before to dilute the proteins in lysis tampon. These lysated samples were incubated 5 min at 100ºC and localised directly in ice before being used or conserved at –80ºC.

3.3.3. Western blotting

Cell extracts obtained as described above were separated by polyacrylamide gel electrophoresis using an 8-10% polyacrylamide gel prepared as per (Laemmli, 1970). The proteins were transferred to an Immobilon-P membrane (Millipore), pre-wetted with transfer buffer (48 mM Tris-ClH pH 7.5, 39 mM glycine, 0.13 mM SDS, 20% methanol), using a Bio-rad Mini Trans-blot® cell at 0.15 mA for 25 min. Blocking of non-specific sites on the membrane was performed for 1 h using 5% milk in PBS. Then, the membrane was incubated with the antibody diluted in milk. This incubation was done for 1 hour at RT. The membrane was washed at least three times with 0.05% Tween in PBS. Proteins were detected using the Western Lightning plus Chemiluminiscence Reagent Kit (PerkinElmer), according to the manufacture´s instructions. In this study, the following conjugated antibodies were used: α-[MYC-peroxidase] (1:10 000 Roche) and α-[T7-peroxidase] (1:10 000 Novogen).

4. Microscopy

Samples were mounted on microscope slides and visualized in a Nikon eclipse 90*i* microscope equipped with a Hamamatsu ORCA-ER CCD camera. Images were taken using the appropriate filter sets, a Nikon Plan Apo *VC* x100 NA 1.40 lens and Nikon Immersion oil Type A nd=1.515. The software used with the microscope was MetaMorph 6.1 (Universal Imaging, Downingtown, PA). Images were further processed with Adobe Photoshop 7.0.

GFP and DAPI filter was used for the analysis of nuclear staining with DAPI (4', 6'-diamidino-2-phenylindole) (García-Muse *et al.*, 2003), wheat germ agglutinin (WGA), and Calcofluor. YFP (Yellow-hifted fluorescent protein; Clontech, Palo Alto, CA), CFP (Cyan-shifted fluorescent protein; Clontech) and RFP (Red-hifted fluorescent protein; Clontech, Palo Alto, CA), were analysed with specific filters.

4.1. Nucleus staining

To prepare cells for staining, 1 ml of each culture was washed twice with 1 ml of PBS and concentrated 10 times in PBS. 2 μl of sample were applied to a coverslip and air-dried at room temperature. 2 μl of mounting medium (10 μl of DAPI plus 90 μl of PBS 1X) were added to a glass microscope slide, and the coverslip carrying the cells was inverted onto the small drop.

4.2. Septum staining

Septum observation was performed with two different stainings: WGA-FITC or calcofluor staining. To prepare cells for WGA-FITC staining, 1 ml of culture was washed twice with 1 ml of PBS and concentrated 10 times in WGA-FITC solution (8 μg/ml in PBS). Cells were incubated in the dark at 28ºC with agitation for 10 min. Finally, cells were washed 3 times with PBS and mounted onto coverslip for microscopic observation. For the calcofluor staining, cells were mixed with calcofluor (0,2 mg/ml in H_2O) directly on a coverslip and observed.

5. Mating on water agar assay

Cell fusion after mating was assayed on 2% water agar. 50 µl of water agar were placed on a coverslip and kept in a wet chamber until use. Strains expressing YFP or CFP cytoplasmic, were grown to an OD_{600} = 0.8. Cells were grown in YPD medium to repress the *ukc1* expression in *ukc1*^{nar1} strain. WT FB1 and WT FB2 were also grown in YPD as control. These pre-inoculum were washed 3 times in CMD medium (3000 r.p.m. for 3 min) and concentrated to a final OD_{600} = 5.0. 2 ml of each suspension were combined and incubated for 1 h at room temperature at 150 r.p.m. Subsequently, 3 µl of the cell mixture were placed on top of the water agar droplet and slides were incubated in a moist chamber overnight. Cell fusion was analysed by detecting CFP and YFP signals. Structures that contained both fluorescent proteins were counted as products derived from fusion of two cells, whereas cells with only CFP or YFP signals were considered to be single.

6. Mating and pheromone stimulation

Mating was performed according to Müller *et al.*, (2003, B). Briefly, compatible strains were co-spotted on a CM-charcoal plate, and this plate was sealed with Parafilm and incubated at 25ºC for 48 h. For pheromone stimulation, strains were grown in CM-glucose to an OD_{600} = 0.6. The incubation with synthetic pheromone (Bachem AG, Switzerland) (dissolved in DMSO and used at a final concentration indicated in each experiment) was performed at 28ºC in 2 ml eppendorf tubes with slow agitation (100 r.p.m.) for periods of time indicated in each experiment.

7. Pathogenicity assays

Pathogenicity was tested by syringe inoculation of 14-days-old maize plant of the variety Gaspar Flint. We injected approximately 0.5 ml of a suspension of cells grown in YPD medium overnight to an OD_{600} = 0.8 and concentrated in H_2O to a final OD_{600} = 2.5. The inoculated corn seedlings were grown in a greenhouse and disease symptoms were evaluated according to the disease-rating scheme reported by Kämper *et al.*, (2006). Pathogenicity test was repeated 3 times using more than 30 plants in total for each strain.

8. *In silico* analysis

The homology research for the Mob2, Nak1, Hym1, Sog2 and Ace2 proteins was performed with the BLAST program of the *U. maydis* database web page (http://mips.gsf.de/genre/proj/ustilago/) using the *S. cerevisiae* sequences as probes. Blast verification was performed with the NCBI BLAST program using the protein homolog sequences of *U. maydis* as probe.

Protein alignments were performed with the ClustalW program and domain analysis was performed using Pfam database (www.expasy.ch) and the conserved protein domain database (CDD) from NCBI website (www.ncbi.nlm.nih.gov/Structure/cdd/).

9. Strain and plasmid constructions

To generate the different strains, the constructs drawn and detailed below were used to transform protoplasts. The integration of the plasmids by homologous

recombination into the corresponding loci was verified by diagnostic PCR. On the different figures, oligonucleotides (oligos) used to performe the construction are indicated in black and those used to check positive insertion are in red (Oligos are detailed in Appendix 1).

Plasmid pGEM-T easy was used for cloning, subcloning and sequencing of genomic fragments and fragments generated by PCR.

9.1. Constructions realized for RAM pathway components deletions

Deletion of the *ukc1* gene was performed according to the method described by Kämper (2004) and Brachmann *et al*. (2004). A PCR fragment flanking the *ukc1* open reading frame (ORF) was digested by the restriction enzyme *Sfi*I to be subsequently ligated to the carboxine resistant gene, digested by the same enzyme (from the pUMa260 plasmid). This construct was introduced into the native locus by homologous recombination (Fig.7).

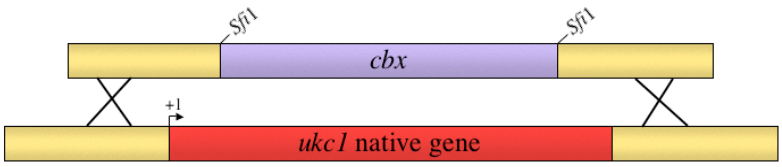

Figure 7: Schematic representation of the *ukc1* gene substitution by the ukc1 deletion cassette via homologous recombination.

PCR fragment flanking the 5´ homologue region was amplified with the ukc1-2 and ukc1-3 oligos. PCR fragment flanking the 3´ homologue region was amplified with the ukc1-6 and ukc1-7 oligos. Then, the ligated fragment was transformed in several strains.

Transformants were checked by PCR, using ukc1-1/cbx1 oligos for the 5´ side and cbx2/ukc1-8 oligos for the 3´ side (Fig.8).

The same protocol was followed to construct the deletion strain of *mob2*, *tao3*, *hym1*, *sog2*, *nak1* and *ace2* genes. Oligos used in each construction are described in figure 8. In the case of the *nak1* gene deletion construct, the *hygromycin* gene was ligated to the PCR fragments of the flanking regions instead of the *carboxin* gene. This *hygromycin* gene was obtained by digestion of the pUMa261 plasmid with *Sfi*I enzyme.

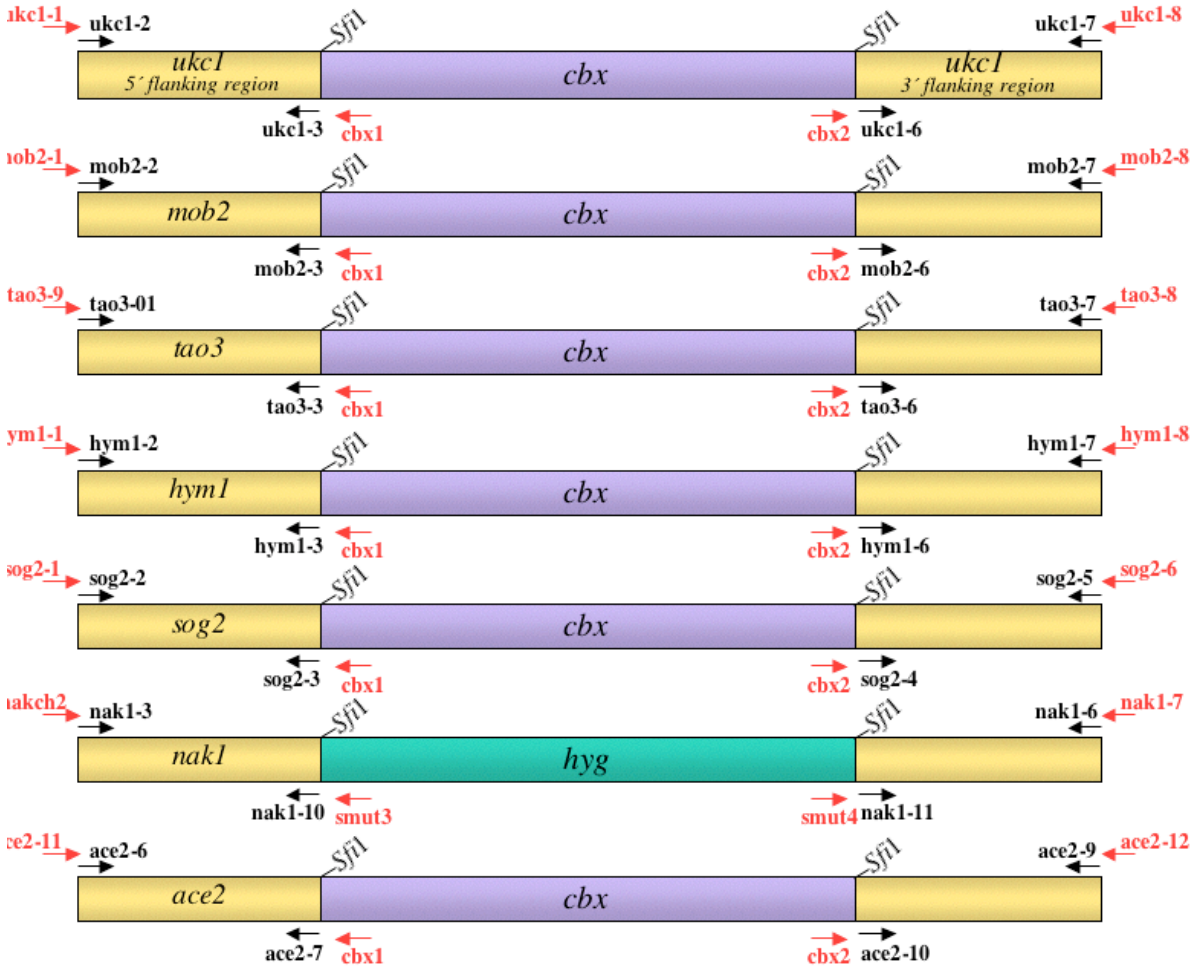

Figure 8: Schematic representation of the deletion cassettes of *ukc1*, *mob2*, *tao3*, *sog2*, *nak1* and *ace2* genes.

9.2. Constructions realized for the Ukc1 characterisation

9.2.1. Substitution of the native ukc1 promoter by the P_{nar1} conditional promoter

To produce a conditional *ukc1*^{nar1} allele, we constructed a plasmid by ligation of a pair of fragments into pRU2-HYG, digested with *Nde*I and *Eco*RI. The *ukc1* N-terminal region (flanked by *Eco*RI and *Kpn*I) was produced by PCR using the primers ukc1-2 and ukc1-3. The *ukc1* promoter region (flanked by *Nde*I and *Kpn*I) was obtained by PCR amplification with primers ukc1-1 and ukc1-4. The resulting plasmid pukc1^{nar1}-HYG was integrated, after digestion with *Kpn*I, by homologous recombination into the *ukc1* locus (Fig.9).

The same construction was done with the pRU2-CBX, which conferred the carboxine resistance. The plasmid obtained in this case was named pukc1^{nar1}-CBX.

To control the *pnar* promoter activity, it is necessary to play with the medium. In rich medium (YPD medium), nitrogen source are diversified (NH_4 or NO_3…) and the *pnar* promoter is inhibited by the presence of NH_4. In contrast, in minimal medium, *pnar* promoter is activated by the unique presence of NO_3 for nitrogen source.

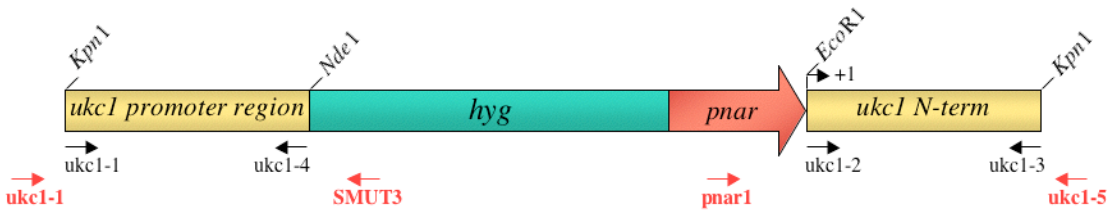

Figure 9: Schematic representation of the *ukc1*^{nar1} construct digested by *Kpn*I

9.2.2. Construction of Ukc1-GFP protein fusion

To construct the *ukc1-GFP* allele, the C-terminal part of the *ukc1* ORF without the stop codon was amplified with the ukc1-14 oligo, having the *Nco*I restriction site,

and the ukc1-17 oligo having the *Hind*III restriction site (+487bp to +2535bp). This ukc1 DNA fragment was digested with *Nco*I/*Hind*III and ligated to the p123 plasmid, also digested with *Nco*I/*Hind*III. The ukc1 fragment was placed in phase with the *gfp* gene. This plasmid (p123-ukc1) was digested by *Sac*I (in the middle of the ukc1 DNA fragment) and introduced by homologous recombination into the *ukc1* locus. Transformants were checked by their carboxine resistance and by PCR amplification with the ukc1-17 and the gfp-1 oligos (PCR product of 2110bp) (Fig.10).

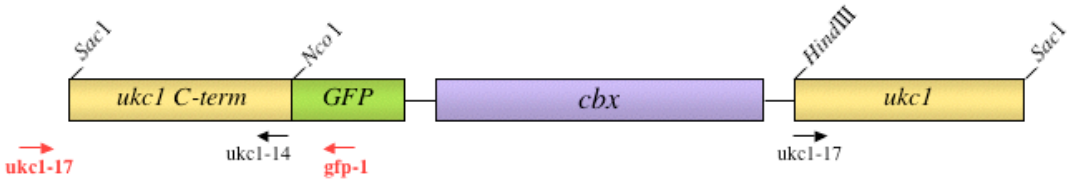

Figure 10: Schematic representation of p123-ukc1 construction already digested by *Sac*I.

9.3. Constructions realized to show the interaction between Ukc1 and Mob2

9.3.1. Construction of Ukc1-myc protein fusion

To construct the *ukc1-myc* allele, the C-terminal part of the *ukc1* ORF without the stop codon was amplified with the ukc1-11 oligo, having the *Bam*HI restriction site, and the ukc1-12 oligo having the *Mfe*I restriction site (+1721bp to +2535bp). This ukc1 DNA fragment digested by *Bam*HI/*Mfe*I, was ligated to the pBS-MYC plasmid (digested by *Bam*HI/*Eco*RI), in which it was cloned in phase with three copies of the *myc* epitope. This plasmid (pBS-ukc1-myc) was digested by *Eco*NI (in the middle of the ukc1 DNA fragment) and introduced by homologous recombination into the *ukc1* locus. Transformants were checked by their hygromycine resistance and by PCR amplification

with the ukc1-13 and the tag1 oligos (PCR product of 1208bp) (Fig.11). After insertion, the Ukc1-myc protein fusion was as functional as a wild-type untagged ukc1 protein.

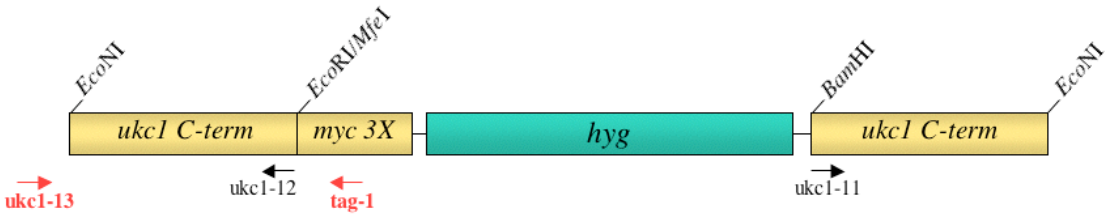

Figure 11: Schematic representation of pBS-ukc1-myc digested by *Eco*NI.

9.3.2. Construction of T7-Mob2 protein fusion

To construct the *t7-mob2* allele, we overexpressed *mob2* under the control of the P_{crg1} promoter. The *mob2* ORF was amplified by PCR from genomic DNA with mob2-15 (having a *Bam*HI site) and mob2-5 oligos. The ATG codon start was exchanged with a *Bam*HI site inserted in the same translational phase as a T7 epitope cloned under the control of P_{crg1} in the pRU11T7 plasmid. This plasmid (pRU11T7-mob2) was digested by *Ssp*I (in the middle of carboxine fragment) and introduced by homologous recombination into the *carboxine* locus. Transformants were checked by their carboxine resistance and by PCR amplification with pcrg1 and cbx2 oligos (PCR product of 1416bp) (Fig.12). The T7-Mob2 protein fusion was as functional as a wild-type untagged Mob2 protein.

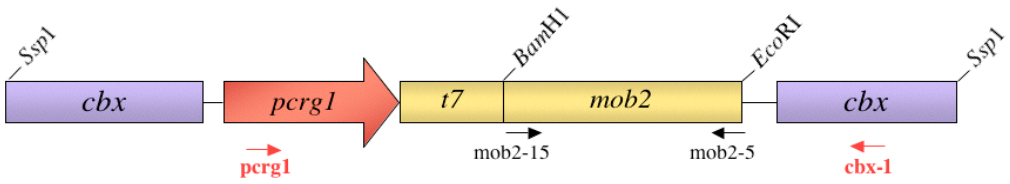

Figure 12: Schematic representation of pRU11-T7-mob2 digested by *Ssp*I.

Results

Section I: The RAM pathway organization in Ustilago maydis

1. The central NDR kinase Ukc1

1.1. Sequence analysis

In 1999, Dürrenberg and colleagues identified the putative Cbk1 homologue protein in *U. maydis*, which they called Ukc1. Ukc1 shows a high sequence similarity (60% similarity) with Cbk1p.

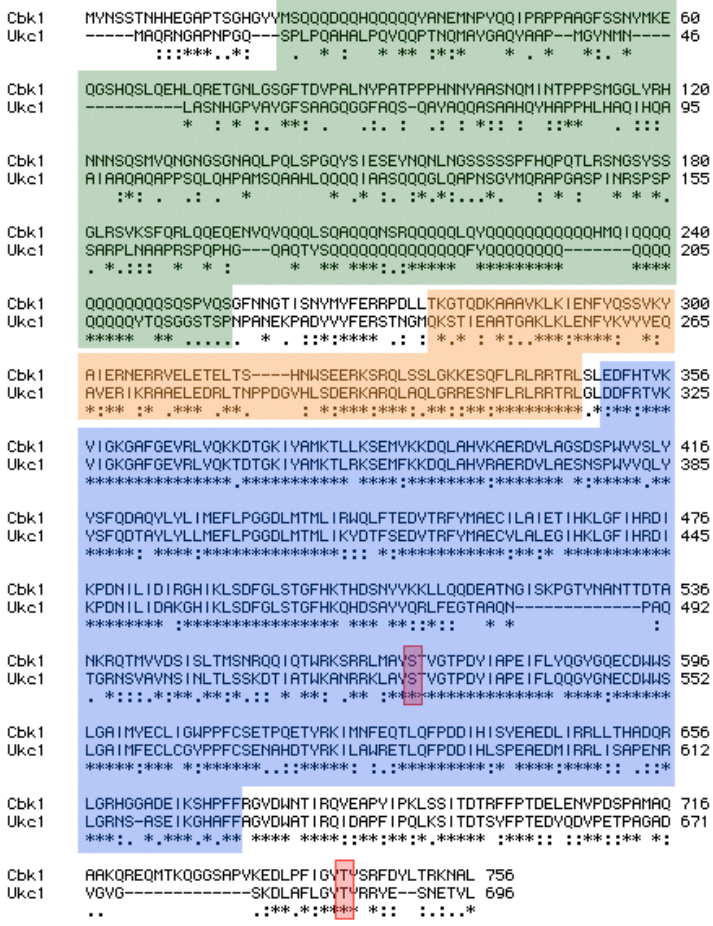

Figure 13: Cbk1p *vs* Ukc1 protein alignment.
Cbk1p is composed of a Q-rich domain (green), a SMA domain (orange) and a kinase domain (blue). Cbk1p activity is regulated through two major phosphorylation sites (red) S(570) and T(743). Alignment was obtained with the ClustalW software.

In order to know whether the function and the regulation of Ukc1 could be similar to the ones described in *S. cerevisiae*, we analysed the protein domains conservation performing an alignment of both proteins (Fig.13). This protein alignment allowed us to observe that the Q-rich domain (30% similarity) presented low similarity whereas the SMA domain (66,2% similarity) was highly conserved. In *S. cerevisiae*, this SMA domain is recognized by the Mob2 regulator, indispensable for Cbk1p kinase activity. We could also observe that the kinase domain of Ukc1 was highly similar to the Cbk1p kinase domain (80,9% similarity). Interestingly, the phosphorylation sites involved in Cbk1p regulation were also conserved in Ukc1. It has been demonstrated that the phosphorylated site (Serine 570) localised in the T-loop of the kinase domain of Cbk1p is an autophosphorylation site whereas the second site, localised in the C-terminal part (Threonine 743), is phosphorylated by the Kic1 protein kinase regulator (Jansen *et al.*, 2006).

This high sequence conservation between both proteins suggests a similar regulatory system, assuming the conservation of the same Cbk1p functions and regulation for Ukc1 in *U. maydis*.

1.2. Ukc1 is involved in morphology, cell separation and virulence regulation

In *S. cerevisiae* or in *C. albicans*, deletion of the central Ndr kinase of the RAM pathway leads to cells defective in cell growth polarity and cell separation. These cells are organised in chains and are rounder than Wild Type (WT) cells (Nelson *et al.*, 2003; Song *et al.*, 2008). In *U. maydis*, first study showed that deletion of *ukc1* resulted in cells with aberrant morphology (Dürrenberger *et al.*, 1999). Mutant cells form clusters composed of round cells with hyphal extensions or elongated bud. This phenotype

appeared to be more related to the phenotype described in *C. neoformans*, in which RAM mutant cells develop hyperpolarized cells in spite of having a polar growth defects as observed in *S. cerevisiae* (Walton *et al.*, 2006).

A strain deleted for *ukc1* was created in this study to carry out a further characterisation of the mutant phenotype. Mutant cells resulted in aggregates of round cells in the centre and hyperpolarized at the extremity, showing a strong defect in cell separation and morphology (Fig.14). Cells in the centre of the mutant were able to form more than one bud at both extremities, which appeared as branching cells suggesting a defect in bud site selection. The size of these cells appeared bigger than WT cells and the round phenotype suggest a defect in cytoskeleton organisation. The apical compartments of mutant cells were, in opposite, very elongated and appeared wavy. Nuclear staining with DAPI showed proper nuclear segregation and the presence of one nucleus in each compartment (Fig.14).

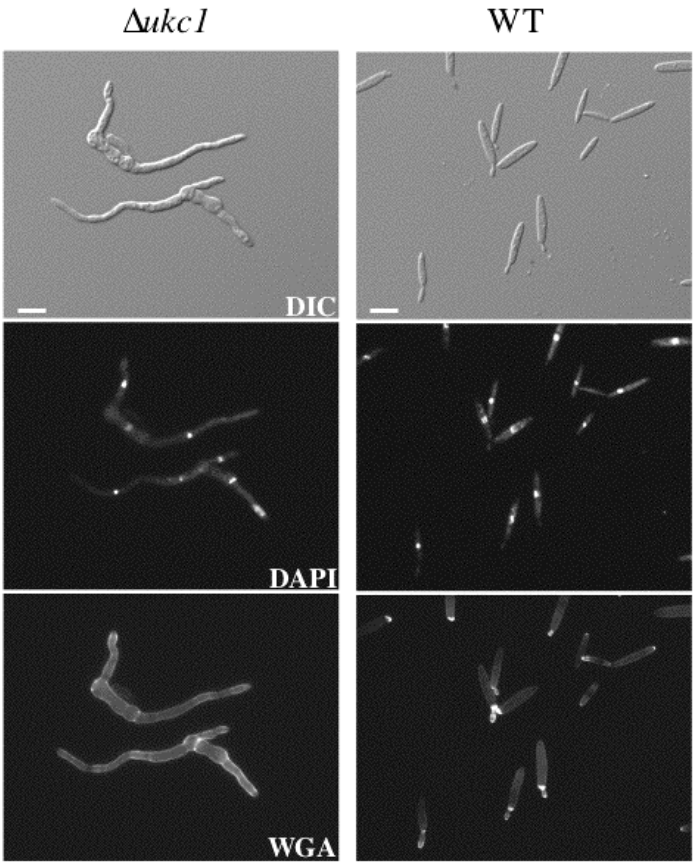

Figure 14: Deletion phenotype of *ukc1* in *U. maydis*. Mutant cells appeared organised in chains due to a defect in cells separation (more than one nucleus were visible in the DAPI panel). In addition, multiple septa were visible by WGA staining. Cells were round in the central region of the mutant and very elongated at the extremity, indicating an important defect in morphology. Bar, 10μm.

Due to the dramatic morphological defect of *ukc1* deleted cells, it was not possible to produce protoplasts of this mutant to carry out further genetic analysis. Therefore, we constructed a strain in which the expression of the *ukc1* gene could be conditionally regulated by an inducible promoter, the *ukc1*^{nar1} strain. In this conditional strain, *ukc1* is under the control of the P_{nar1} promoter, negatively regulated by ammonium (present in YPD) and in opposite, activated by nitrate (present in MM). In figure 15, we can observe that under repressive conditions (YPD), the conditional strain *ukc1*^{nar1} showed the same morphological defects as the deleted strain Δ*ukc1*, whereas in MM, when *ukc1* was normaly expressed, *ukc1*^{nar1} cells presented a WT phenotype.

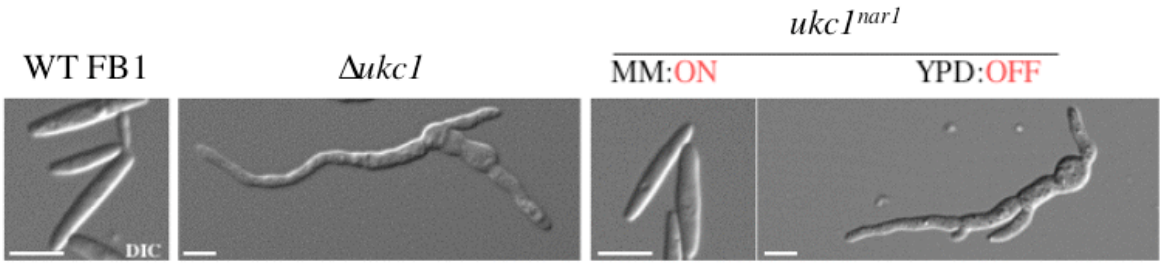

Figure 15: *ukc1*^{nar1} cells phenotype.
ukc1^{nar1} cells grown in MM (nitrate nitrogen source) showed a WT FB1 phenotype, whereas *ukc1*^{nar1} cells grown in YPD for 12 hours, showed the same mutant phenotype as the Δ*ukc1* cells. Bar, 10μm.

1.3. Ukc1 subcellular localisation

In *U. maydis*, we observed that the RAM deleted cells presented a distinct mutant phenotype than the one described in *S. cerevisiae*. *U. maydis* mutant cells were round in the centre and presented filamentous cells at the extremity whereas in *S. cerevisisae*, mutant cells are organised in chains of round cells without elongated cells. To test whether Ukc1 could play different or additional functions that the ones described for NDR kinases in other organisms, we decided to study the subcellular localisation of Ukc1. To this end, a C-terminal Ukc1-GFP fusion protein was created and inserted at the *ukc1* native locus of a WT strain. This fusion protein looked functional as cells had a

wild type appearance. Representative images of cells at different stages of the cell cycle were assembled to show the localisation of Ukc1-GFP fusion protein, which localised in different cell regions during the cell cycle progression (Fig.16). In unbudded cells (G1 phase), Ukc1-GFP was found within the nucleus. At the bud emergence stage, it localised to the bud extremity and in the mother nucleus. When the daughter cell was ready to separate it of the mother cell, Ukc1-GFP localised to the cell separation site. These results are in accordance with the defects observed in cells lacking *ukc1*, which showed alteration in polarity and cell separation. In addition, we could observe the Ukc1-GFP protein within the nucleus throughout the cell cycle, whereas Cbk1p localises within the nucleus only during the G1-M transition (Colman-Lerner *et al.*, 2001; Weiss *et al.*, 2002), suggesting possible additional or different functions for Ukc1 protein kinase in *U. maydis*.

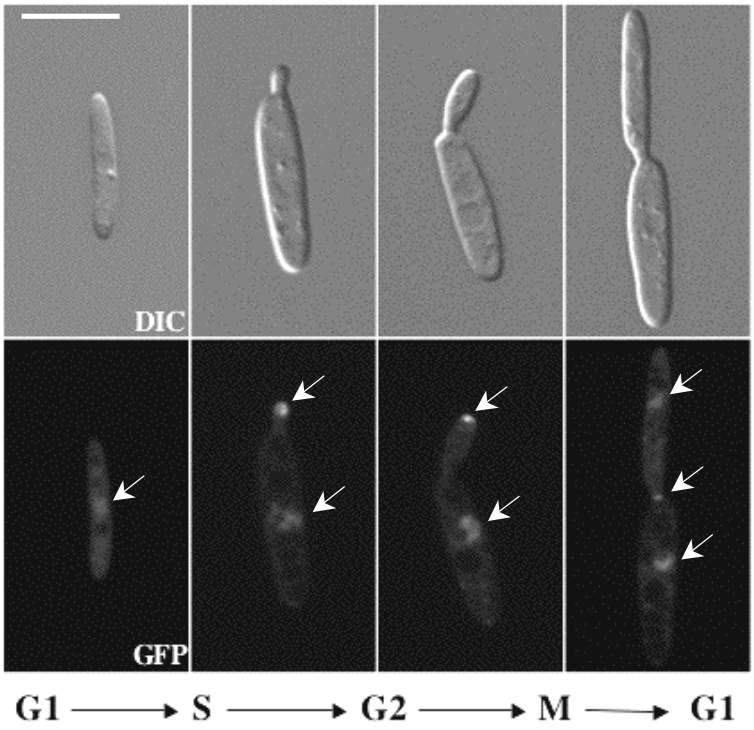

Figure 16: Localisation throughout the cell cycle of Ukc1-GFP.
Representative individual haploid cells expressing the Ukc1-GFP fusion, show the localisation of Ukc1 at different stages of the cell cycle. During G1 the protein is only found in the nucleus, then it is also concentrated at the emerging bud site and at the tip of the bud. Just before cell separation, the protein localised around the bud neck and within the nucleus. In the figure, Ukc1-GFP signal is marked by arrows. Bar, 10μm.

2. The Mob2 regulator

2.1. Identification of the Mob2 protein homologue in *U. maydis*

Because Mob2 is the conserved binding partner required for Cbk1 kinase activity characterized in *S. cerevisiae* (Weiss *et al.*, 2002), we next asked whether a Mob2 homologue could regulate the activity of Ukc1 protein in *U. maydis*. To identify a Mob2 homologue, a Blast-homology search in the *U. maydis* genome database (http://mips.gsf.de/genre/proj/ustilago/) using the sequence of *S. cerevisiae* Mob2p as probe was performed. This analysis enable us to identify two homologue proteins: UM04352 and UM12135. Actually, two Mob proteins were identified in numerous organisms, Mob1 and Mob2 proteins. The phylogenetic tree presented in figure 17 (A), show that Mob1 and Mob2 form two distinct clusters for the selected organisms. In this tree, UM04352 appeared in the Mob1 cluster whereas UM12135 appeared to have a sequence closer to Mob2 homologues. Therefore, we assumed that UM12135 was the Mob2 homologue protein in *U. maydis* and called it Mob2 over our study. Sequence analysis showed that the Mob1/phocein domain characterising the Mob family protein was conserved in Mob2 of *U. maydis*. Alignment showed that the total Mob2 protein sequence shared a high homology (53% identity) with the homologue of the basidiomycete *C. neoformans* but only shared 31% and 30% of similarity with the ascomycetes *A. nidulans* and *N. crassa* respectively. The identity between *U. maydis* and *C. albicans*, *S. cerevisisae* and *S. pombe* was of 50%, 47% and 43% respectively suggesting a higher conservation of Mob2 sequence between basidiomycete and single cell yeast that with ascomycete filamentous fungi.

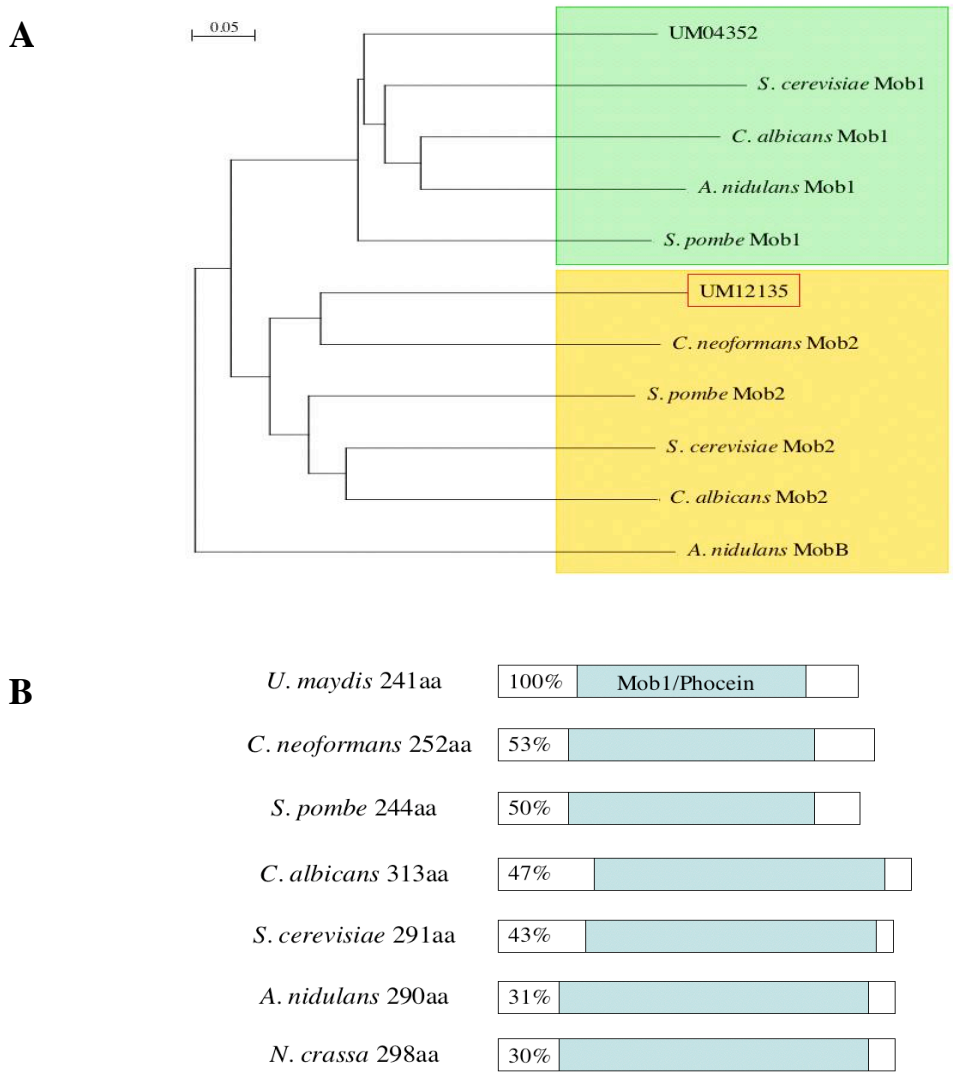

Figure 17: Mob2 protein identification in *U. maydis*.
A: Phylogenetic tree of Mob family protein in *S. cerevisiae*, *C. albicans*, *A. nidulans*, *S. pombe* *C. neoformans* and *U. maydis*. Mob proteins appeared to form two distinct clusters. In green the cluster of Mob1 homologue proteins and in yellow the cluster of Mob2 protein homologues for selected organisms. The tree was performed with the ClustalW program (http://www.ebi.ac.uk/clustalW)
B: Comparison of amino acid sequence identities between the total in sequence of Mob2 in *U. maydis* and Mob2-like family in selected fungi species. The blue box indicated that this area belongs to Mob1/phocein family by searching conserved domains in NCBI.

2.2. Deletion of *mob2* presented the same defects as Δ*ukc1* cells

To adress whether Mob2 protein could regulate the functionality of Ukc1 in *U. maydis*, we created a strain deleted for *mob2*, inserting the *mob2* deletion cassette in a FB1 background. Mutant cells presented the same phenotype as cells deleted for *ukc1*

(Fig.18). Cells appeared round in the centre of the cluster and elongated at the extremity. They were organised in chains due to a defect in cell separation and presented a defect in morphology with cells size bigger than WT. This mutant phenotype suggested that in *U. maydis* also, Mob2 protein played an essential function in the regulation of Ukc1 activity.

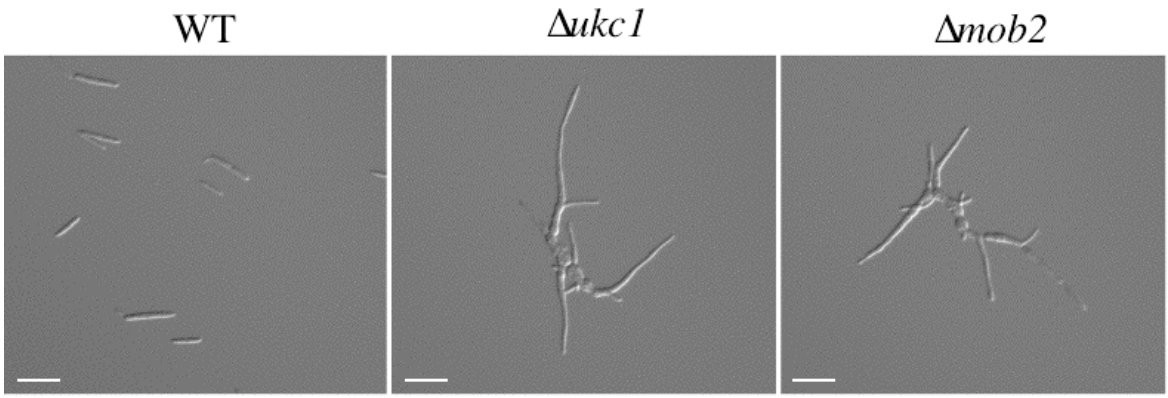

Figure18: Deletion phenotype of *mob2* in *U. maydis*.
Mutant cells appeared organised in chains due to a defect in cells separation. Cells appeared round in the centre region of the mutant and very elongated at the apical part showing an important defect in morphology as Δ*ukc1* strain. Bar, 10μm.

2.3. Mob2 forms a complex with Ukc1

The formation of the Cbk1-Mob2 complex is a prerequisite for Cbk1p full kinase activity and many NDR kinases have been shown to be regulated by a direct interaction with proteins of the Mob family (Devroe *et al.*, 2005). In *U. maydis*, we observed that the interaction domain between Cbk1p and Mob2p (SMA domain) was conserved in Ukc1 protein sequence. In order to study whether there was a physical interaction between Ukc1 and Mob2 in *U. maydis*, we constructed a strain containing both fusion proteins Ukc1-*myc* and *t7*-Mob2, and carried out a co-immunoprecipitation assay (Fig.19).

Mob2 and Ukc1 were co-immunoprecipitated together with both epitopes Myc and t7 (Fig.19, lane 3 and 4) confirming an interaction between Ukc1 and Mob2, and suggesting the conservation of the central complex Ukc1-Mob2 in the RAM pathway organisation of *U. maydis*.

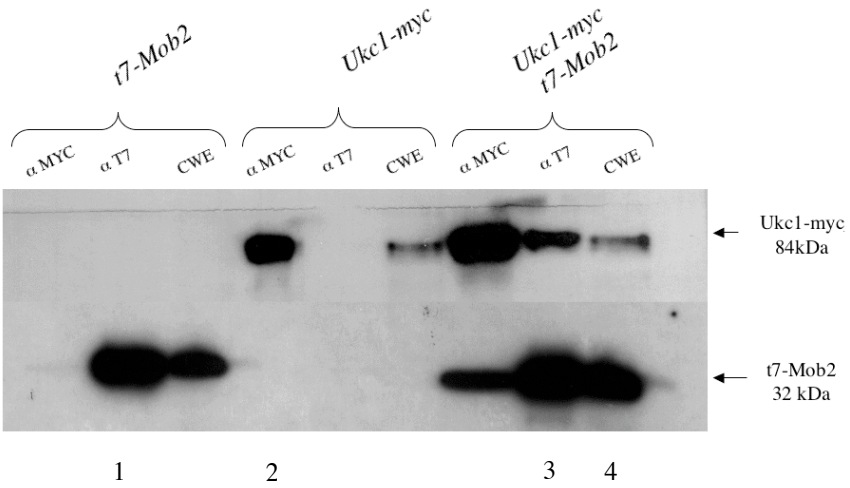

Figure 19: Co-immunoprecipitation assay between Ukc1-*myc* and *t7*-Mob2.
Extract were prepared from FB1 Ukc1-*myc* and FB1 P_{crg1}:*t7*-Mob2, grown in inducing condition (YPA) at an OD_{600} = 0.5. Anti-Myc peroxidase and Anti-T7 peroxidase were used to detect the fusion proteins. Ukc1-*myc* and *T7*-Mob2 have an estimated molecular mass of 84 kDa and 32 kDa respectively. In control strain, both polypeptides appear at their expected size (lane 1 and 2). In the strain having both protein fusions, the immunoprecipitation by the anti-Myc antibody precipitated Ukc1-*myc* and *T7*-Mob2 (lane 3) as well as the anti-T7 antibody precipitation (lane 4), demonstrating an interaction between Ukc1-*myc* and *t7*-Mob2 proteins.

3. Conservation of the regulatory proteins

In order to analyse the phenotypic consequence of an over-expression of Ukc1 in *U. maydis*, the *ukc1* ORF was expressed under the control of a constitutive promoter. Strikingly, cells over-expressing *ukc1* did not present any phenotype suggesting that the over-expression of *ukc1* alone was not sufficient to increase its activity. Knowing that Mob2 was necessary for Ukc1 activity, we suggested that *ukc1* over-expression was not effective due to a low level of its regulator Mob2. To bypass this problem, we created a

strain in which cells over-expressed at the same time *ukc1* and *mob2*. Unfortunately, the strain over-expressing both proteins did not present any mutant phenotype, suggesting that in addition to Mob2, other protein regulators were involved in the Ukc1 activity regulation.

3.1. Sequences identification of Tao3, Hym1, Kic1 and Sog2 homologues

In *S. cerevisiae*, in addition to Mob2p, the proteins Tao3p, Hym1p, Kic1p, and Sog2p are involved in the regulation of Cbk1p. In order to know whether these regulator proteins were also conserved in *U. maydis*, a Blast-homology search in the *U. maydis* genome database (http://mips.gsf.de/genre/proj/ustilago/) using the sequence of *S. cerevisiae* RAM pathway components as probe was performed.

This analysis allowed us to identify the Hym1 homologue (UM10613), the Tao3 homologue (UM10098), the Kic1 homologue (UM11396) and the Sog2 homologue (UM0256).

Hym1 homologue contained the Mo25-like protein domain characterising the HYM protein family (Fig.20 A). The Tao3 homologue shared 30% identity with its *S. cerevisiae* homologue. The Kic1p homologue UM11396 is known as Nak1 protein in *U. maydis*, because of its Nak1 domain conservation. The Nak1-subfamily domain contains a Serine Threonine domain kinase (STK domain). Whereas Nak1 total protein shared only 20% identity with the total protein Kic1 homologue, the Nak1-subfamily domain of *U. maydis* shared 71% identity with the Nak1-subfamily domain of *S. cerevisiae* (Fig.20 B). Finally, the Sog2 homologue presented in its sequence the conserved LRR domain (Leucine Rich Repeat) or protein-protein interaction domain, and a Sog2 family sequence (Fig.20 C).

This *in silico* analysis suggested that the RAM regulatory proteins were conserved in *U. maydis*. The conservation of the functional and characteristic domains of each of these proteins suggested that they could be involved in Ukc1 protein regulation, as their homologues in *S. cerevisiae*.

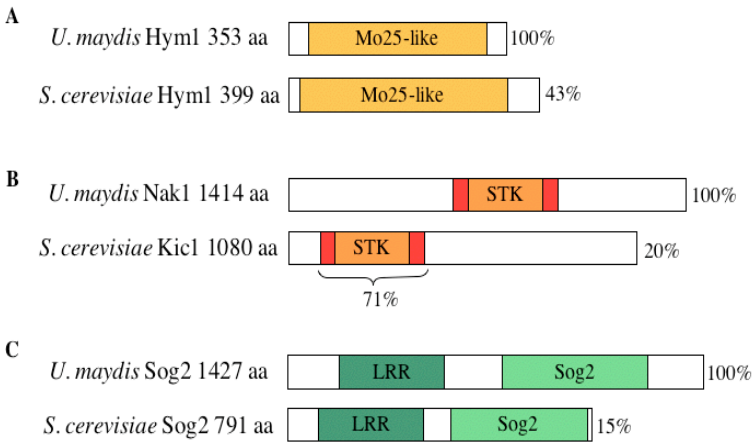

Figure 20: Comparison of the amino acid sequence identity between *U. maydis* and *S. cerevisiae* for the proteins:
A: Hym1. Proteins shared 43% identity and presented the same Mo25-like domain.
B: Nak1. Proteins shared 20% identity but had a high homology (71% identity) for the Nak1-domain containing the STK domain.
C: Sog2. Proteins shared 15% identity but presented the same LRR domain (Leucine Rich Repeat) and a Sog2 sequence domain specific from Sog2 protein.

3.2. Sog2, Hym1, Tao3 and Nak1 proteins seemed to act in the same protein network as Mob2 and Ukc1.

All proteins composing the RAM pathway present the same deleted mutant phenotype in *S. cerevisiae* or in *C. albicans* (Song *et al.*, 2008; Nelson *et al.*, 2003). In order to know whether the protein homologues identified *in silico* could play a function on Ukc1 regulation, we created deletion strains for *nak1*, *hym1, tao3 and sog2*. All these mutants presented the same phenotype as cells deleted for *ukc1* (Fig.21). We could observe, as in the Δ*ukc1* strain, a defect in cell separation and cell morphology (cell bigger than WT and the last one of the chain was very elongated). These results suggested that these proteins could act in the same pathway that Ukc1 and could affect

its function. These results could also explain why the over-expression of Mob2 was not sufficient to regulate the over-expressed Ukc1 protein.

4. Search of an Ace2p RAM target homologue in *U. maydis*

Ace2p is one of the known rare Ndr targets. The localisation of this transcriptional factor is regulated by the Cbk1p-Mob2p complex in *S. cerevisiae* and is necessary to complete cell separation. Mutant cells deleted for *ace2* are organised in chains of unseparated cells that present normal morphology.

In order to identify whether Ace2p could have an homologue in *U. maydis*, we first performed a blast research (ScAce2p *vs U. maydis* database). In this *in silico* study we identified the possible homologue Um10181, but the homology between both proteins appeared very low (19% identity). In order to study whether Um10181 protein could be involved in cell separation regulation as Ace2p, we constructed a deletion strain for the *ace2* homologue gene. In contrast with the result observed in *S. cerevisiae*, Δ*ace2* cells in *U. maydis* did not present any defect in cell separation, and actually showed a WT phenotype (Fig.21). This result was in accordance with the low similarity between ScAce2 and UmAce2 found performing the blast research, and suggested that Ace2p did not have an homologue in *U. maydis,* as it is the case in numerous organisms.

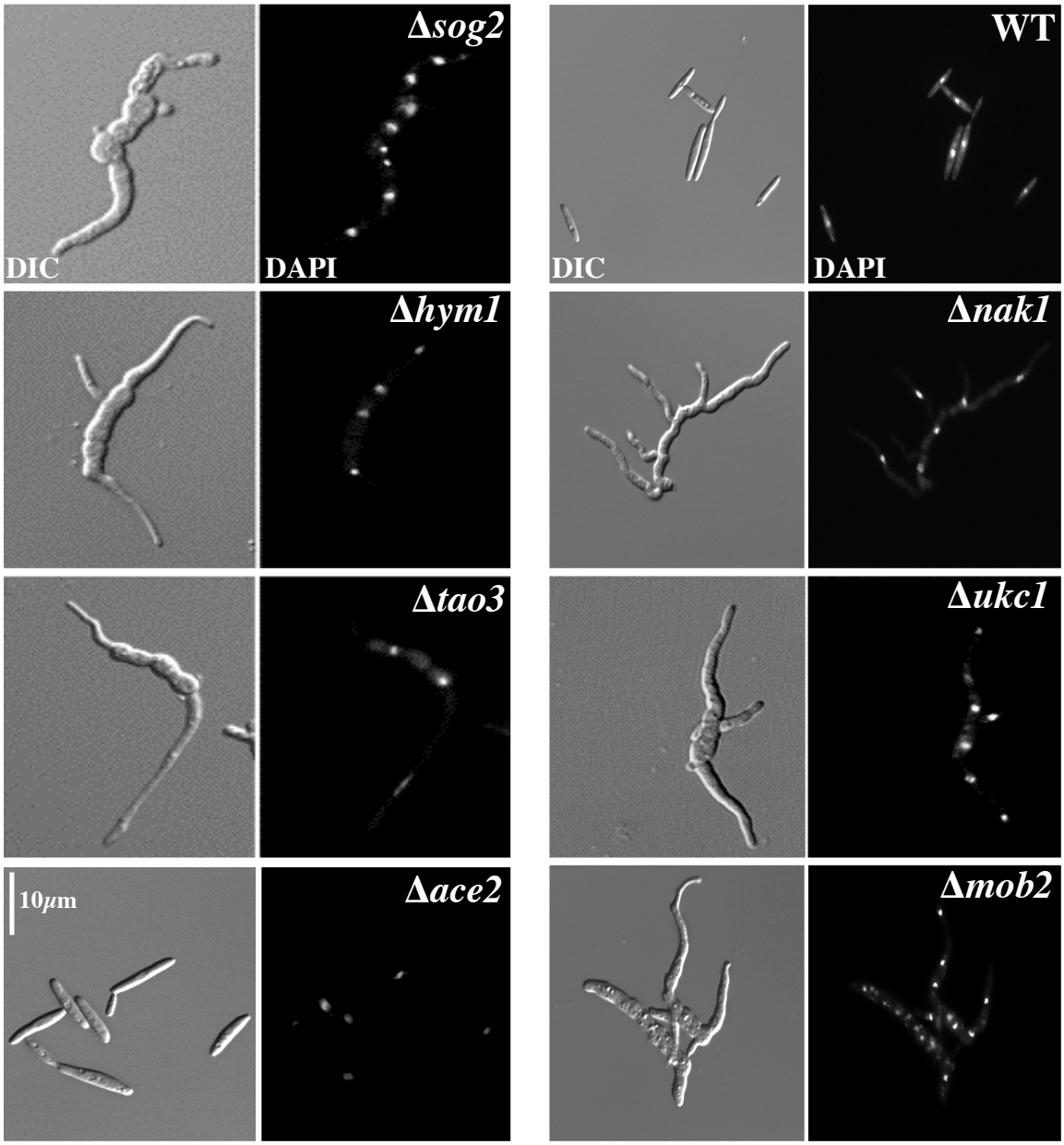

Figure 21: Deletion phenotype of the RAM pathway homologues in *U. maydis*.
Cells deleted for *ukc1* presented defects in cell separation (more than one nucleus is visible in the DAPI panel) and in cell morphology. These mutants presented chains of cells in the central region and at both extremities, very elongated cells. Deletion of *mob2*, *hym1*, *nak1*, *tao3* and *sog2* showed the same phenotype as Δ*ukc1* cells, whereas Δ*ace2* cells presented a WT phenotype.

Section II: The RAM pathway is involved in morphogenesis regulation

1. Cytoskeleton organization in Δ*ukc1* cells

1.1. F-actin organisation in Δ*ukc1* mutant cells

Cells deleted for RAM components presented strong defects in cell morphology. Cells were bigger than WT and the structural form of each cell was affected (Fig.21). In order to know whether the cell cytoskeleton organisation was affected by the deletion of *ukc1*, we analysed F-actin organisation, which participates in morphogenesis and polar growth in *U. maydis* (Banuett and Herskowitz, 2002).

The F-actin cytoskeleton is a complex structure composed of two types of polymerized actin forms: actin cables and cortical actin patches (Kilmartin and Adams, 1984; Amberg, 1998; Yang and Pon, 2002). Actin cables, which contain linear actin filaments, are involved in polarized secretion and organelle segregation (Bretscher, 2003). Cortical patches are seen as numerous punctuate structures and function in the internalization step of endocytosis (Kaksonen *et al.,* 2003). A classical manner to observe actin cytoskeleton is the use of fluorophore-associated phalloidin to stain actin structures. However, this staining technique does not work properly in *U. maydis*. To circumvent this caveat, we used a GFP tagged version of Fimbrin (Fim1-GFP), an actin-associated protein localises to cortical actin patches (Castillo-Lluva *et al.*, 2007), and a Myo5-GFP fusion to analyse functionality of actin cables (Schuchardt *et al.*, 2005).

Fim1-GFP protein fusion was integrated in an $ukc1^{nar1}$ strain to observe actin patches organisation. This experiment was easier to perform with the conditional strain $ukc1^{nar1}$, which permitted to observe the cytoskeleton components organisation in the presence or in the absence of *ukc1*, and this in the same strain. In permissive condition (MM) as in WT cells, actin patches were dispersed through the cell but concentrated at the cell

extremity (Fig.22). Interestingly, under repressive condition (YPD), actin patches were also found dispersed through the mutant cells but they were found highly accumulated at the bud tips in comparison of the organisation observed in non-repressive conditions (MM), suggesting that actin patches organisation was affected in cells repressing *ukc1*. This mislocalisation of actin patches could be a direct consequence of the *ukc1* repression, but could also be caused by the severe morphological defect induce in these mutant cells.

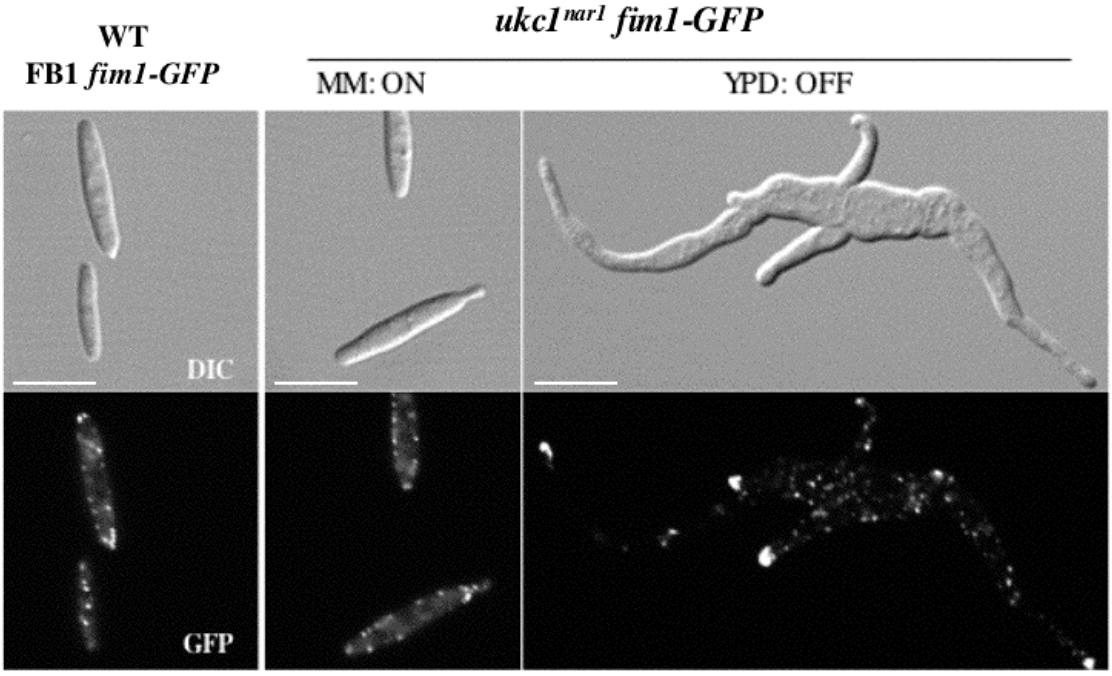

Figure 22: Fimbrin localisation in *ukc1*^{nar1} strain.
In WT FB1 cells, Fim1-GFP fusion protein was concentrated at the cell extremity, to the polarized growth site. In *ukc1*^{nar1} *fim1-GFP* cells grown at non-repressive conditions (MM), in which *ukc1* is expressed, Fim1-GFP was also localised at the cell extremity. However, in repressive conditions (YPD), Fim1-GFP appeared more concentrated at the cells ends than in MM. Bar, 10μm.

Myosin type V (MyoV) is a motor protein that uses actin cables to move from the cell separation site to the cell extremity. Weber and colleagues (2003) showed that in *U. maydis* MyoV-GFP fusion protein was concentrated at the cell extremity. The I

nsertion of MyoV-GFP protein fusion in *ukc1*^{nar1} cells showed that in cell repressing *ukc1* expression (YPD medium), MyoV-GFP localised correctly to the cell extremity (Fig.23) as in cells that were grown in MM. This result indicated that the localisation of MyoV was not affected in *ukc1*^{nar1} cells, suggesting the integrity of the actin cables in mutant cells.

These data suggested that the RAM mutant phenotype could be caused by a deregulation of actin patches localisation and that the RAM pathway might be conserved in regulating fundamental cellular processes including actin structure organisation.

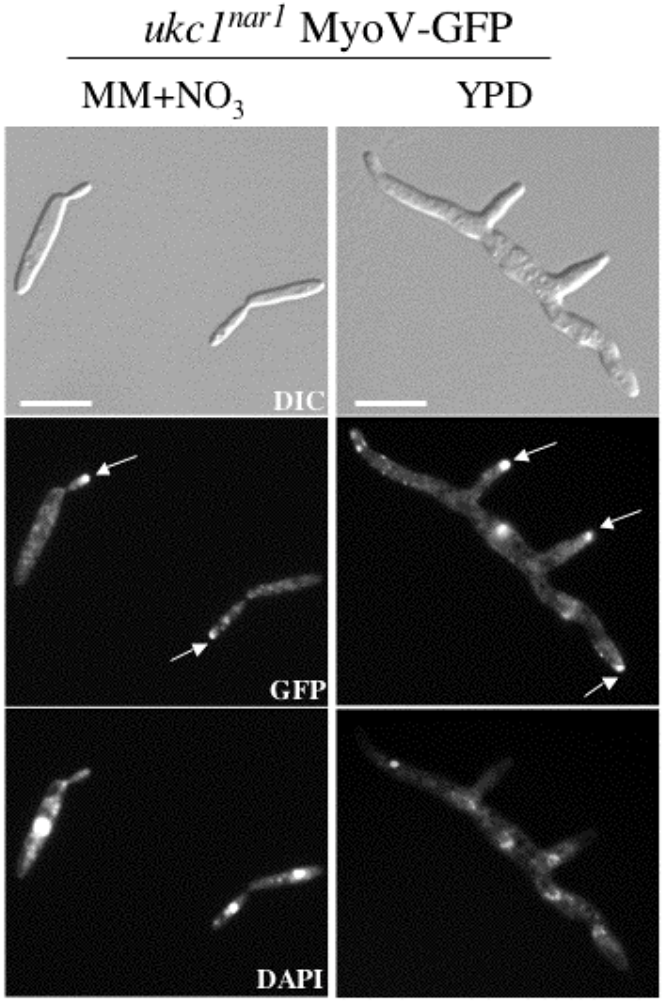

Figure 23: MyoV-GFP localisation in *ukc1*^{nar1} cells. In MM+NO_3, MyoV-GFP fusion protein localised to the cell extremity. In repressive medium (YPD), MyoV-GFP was also found concentrated in all extremities, as notified by several white arrows. Bar, 10μm.

1.2. Microtubules organisation in cells lacking *ukc1*

To determinate whether the cytoskeletal organisation was affected in cell lacking *ukc1*, we next studied the microtubule organisation of mutant cells. Microtubules are filaments consisting in numerous α/β dimers that are required for hyphal growth and mitosis in *U. maydis* (Steinberg *et al.*, 2000). In addition, disruption of microtubules organisation by Benomyl lead to an accumulation of large budded cells with bipolar growth and lateral budding, indicating that microtubules have a role in morphology and polarity (Fuchs *et al.*, 2005).

In this study, microtubules organisation was visualized using the α-tubulin tagging with RFP fluorescence protein (Steinberg *et al.*, 2000). The protein fusion was integrated in *ukc1*^{nar1} and WT cells and photos were captured (Fig.24).

In WT cells, long microtubules were visible into mother and daughter cells, as in *ukc1*^{nar1} cells that were grown in MM. In mutant cells (Fig.24 YPD panel), the resulting filament form at the apex of the cells contained long microtubules that reach into the hyperpolarized bud, as normaly observed in filamentous cells of *U. maydis* (Fuchs *et al.*, 2005). In round cells, microtubules were extended to all unseparated cells as long filaments fallowing the round form of the cells. These observations suggested that microtubules organisation was not affected by the *ukc1* repression in *U. maydis*.

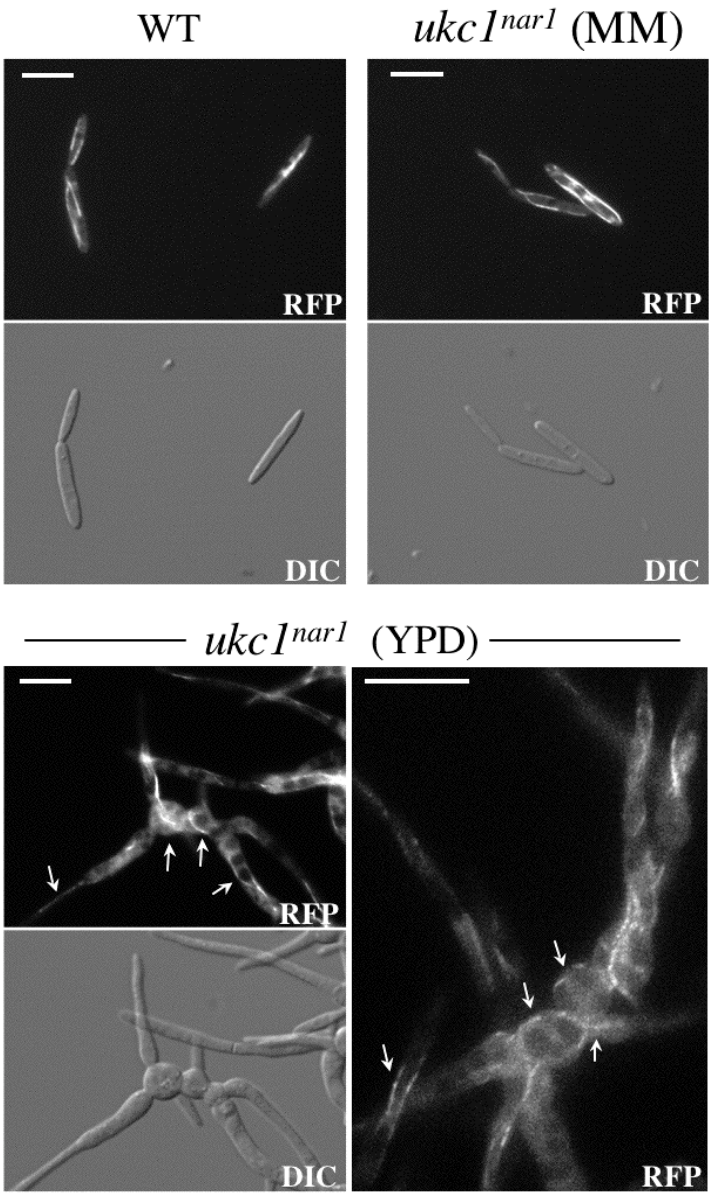

Figure 24: Microtubules organisation in cells lacking *ukc1*.
InWT cells or in *ukc1*^{nar1} cells grown in MM, microtubules were visible as long filaments extended in mother and daughter cells. In cells lacking *ukc1*, microtubules filaments were visible extended along the hyperpolarized bud. They were also visible in round cells in which they were found curved fallowing the form of the cells.

1.3. Septin organisation in Δ*ukc1* mutants

Septins are a conserved family of filament-forming, GTP binding proteins that have a conserved role during cellular division and morphology (Longtine *et al*., 2003). In *U. maydis*, *sep3* was identified as a septum homologue and has been shown to be required for normal morphology and division of haploid cells (Boyce *et al*., 2005). Recently, homologues of septin 1, 2 and 4 were identified in our laboratory and their characterisation suggested important functions in cell separation and morphology in *U*.

maydis. To study whether the severe defects observed in Δ*ukc1* mutant cells were due to septins mislocalisation, each protein fusion *sep1-GFP*, *sep2-GFP*, *sep3-GFP* and *sep4-GFP* was introduced in the conditional *ukc1*^{nar1} strain. Septins localised at the cell separation site and at the growth cell site during budding elongation. Microscopic observations of those strains showed a wild type localisation of each septin in the cells repressing *ukc1* (YPD medium, Fig.25). All septin-GFP proteins were found concentrated at the cell separation site and at the cell ends as in WT cells. These results demonstrated that the cell separation defect of cell lacking *ukc1* was not due to a mislocalisation of the septin proteins to the cell separation site.

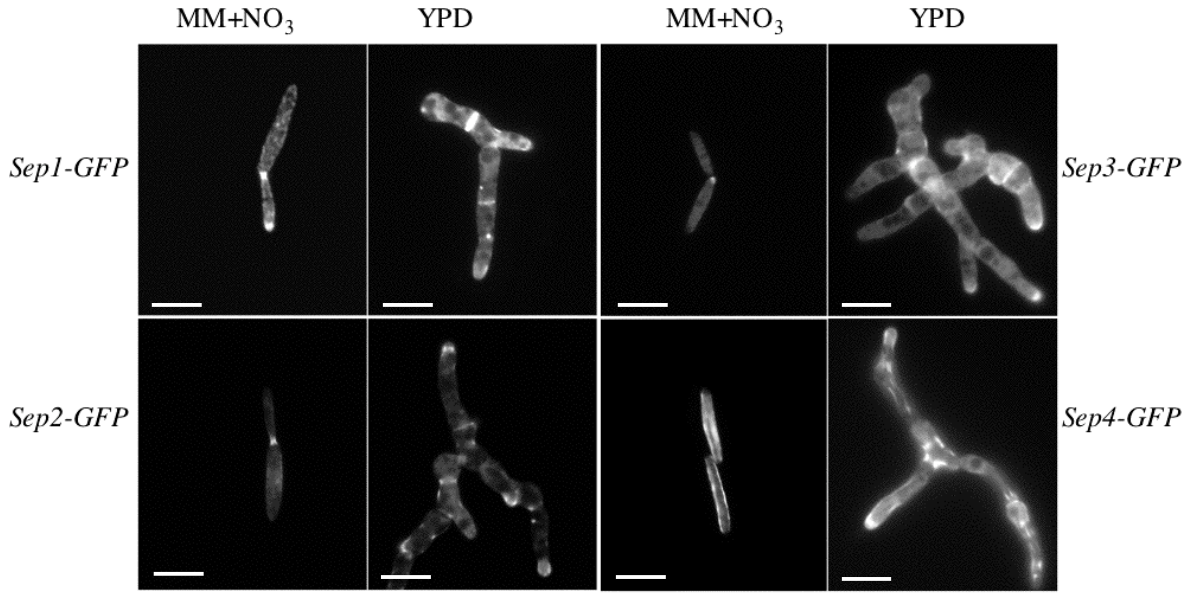

Figure 25: Septins localisation in *ukc1*^{nar1} strain.
Photos were captured 12 hours after repression of *ukc1* expression (YPD) or after induction (MM+NO_3). In MM+NO_3, *Sep1-GFP*, *Sep2-GFP* and *Sep3-GFP* fusion proteins was localised to the bud neck and *Sep1-GFP* was also visible at the cell extremity. *Sep4-GFP* was found localised along the filaments of the cell. The localisation of each septins was conserved in cells grown in YPD medium, presenting a mutant phenotype caused by the repression of the *ukc1* expression. *Sep1-GFP*, *Sep2-GFP* and *Sep3-GFP* was found localised at the cell separation site and cell ends, whereas *Sep4-GFP* was found localised along the filaments of the cell. Bar, 10μm.

2. RAM pathway and growth polarity

The RAM pathway has been involved in polar growth regulation in different organisms. Since *U. maydis* cells deleted for *ukc1* showed defects in bud site selection

as in cell size, we wanted to determine whether the morphological defects of this mutant were due to a problem in polar growth. To this end, we used the P_{crg1}*:wee1* strain in which the over-expression of *wee1* results in a cell cycle arrest in G2 phase. This cell cycle arrest results in the formation of a hyperpolarised bud (Fig.26 upper panel, YPA medium). Interestingly, *ukc1*^{nar1} cells over-expressing *wee1* and repressing *ukc1* at the same time (YPA medium), induced the formation of the hyperpolarised bud in each side of the mutant cell, presenting a defect in cell separation. The formation of this hyperpolarised bud in *ukc1*^{nar1} P_{crg1}*:wee1* cells, confirmed that polar growth was not affected by a deletion of *ukc1*.

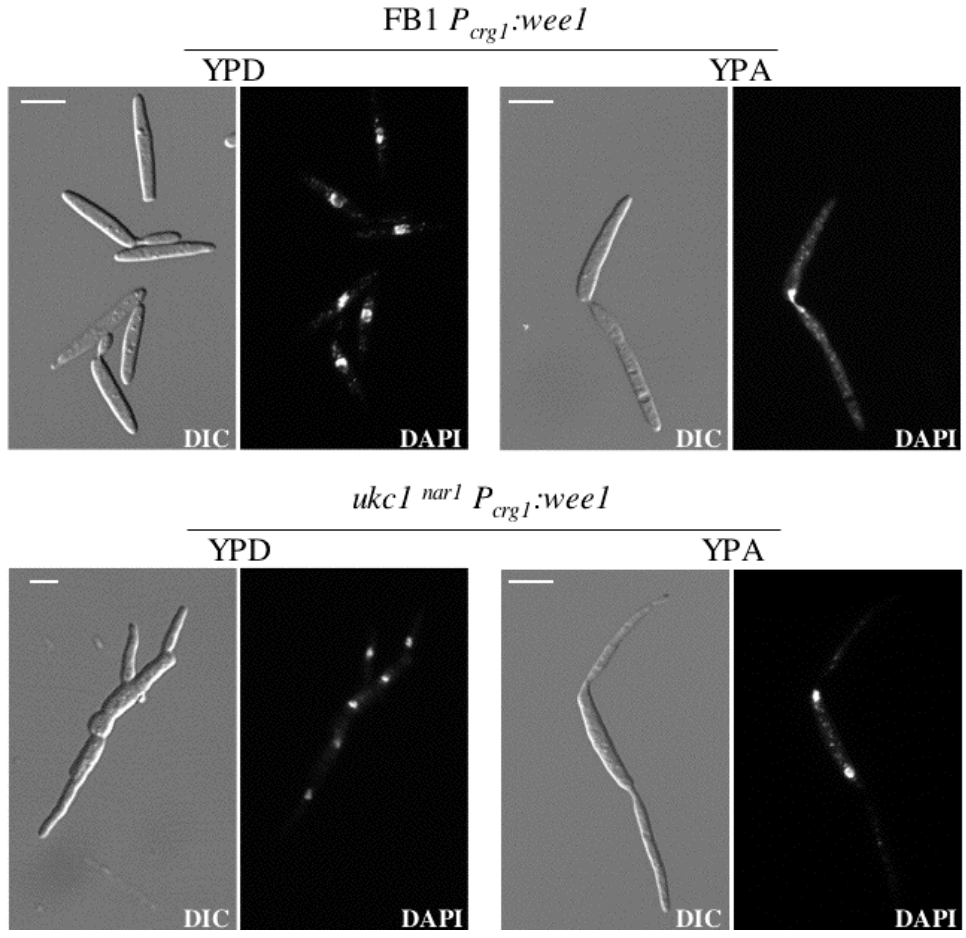

Figure 26: Induction of a hyperpolarised bud in *ukc1*^{nar1} P_{crg1}*:wee1* strain.
Photos were captured 7 hours after growth in YP+Glucose medium (YPD) or in YP+arabinose medium (YPA). FB1 P_{crg1}*:wee1* cells grown in inducible medium (YPA), formed a hyperelongated bud. *ukc1*^{nar1} P_{crg1}*:wee1* cells grown in YPD presented a mutant phenotype, caused by the repression of the *ukc1* expression. In YPA, *ukc1*^{nar1} P_{crg1}*:wee1* cells were also able to form a hyperelongated bud, on each side of the mutant cell, due to the defect in cell separation that present cells deleted for *ukc1*. In this mutant, two nuclei were found in the central compartment, showing that the mutant is composed of two unseparated cells. Bar, 10μm.

Section III: The RAM pathway is indispensable for Ustilago maydis virulence

1. Avirulence of RAM mutant cells

The first study realised by Dürrenberger and colleagues in 1999 showed that the strain deleted for *ukc1* was not able to infect plant maize. To study whether all RAM components were necessary for plant infection, a virulence test was carried out with Δ*hym1*FB1xΔ*hym1*FB2, Δ*mob2*FB1xΔ*mob2*FB2 and Δ*ukc1*FB1xΔ*ukc1*FB2. Figure 27 shows that after 17 days, plants infected by the control WTFB1xWTFB2 were dead. In contrast, plants infected by RAM mutant strains presented a normal growth without symptoms development (Fig.27).

Figure 27: Infective test of RAM components deleted strains.
Maize plants were infected by the different strains after 15 days of growth, at a concentration of 5.10^7 cells/ml. Photo shown plant damages 17 days post-infection. Plants infected with WT strains were dead whereas infection by *ukc1*, *mob2* and *hym1* deleted strains did not cause any infection symptoms. Plants grew normaly and did not produce the characteristic tumors induced by an *U. maydis* infection.

2. *ukc1* cells were able to induce infective structures

In response to pheromone, haploid cells formed a **conjugative tube**. Following the pheromone gradient, cells are able to find a mate and fuse. This fusion results in the formation of an **infective tube** able to penetrate and colonize the plant. The defect in morphology that we could observe for RAM mutant cells led us to asked whether these mutants were able to form infective structures necessary to carry out the plant host invasion. To this end, the fuz7^{DD} construct and the AB31 strain were used to observe whether the *ukc1* cells were able to form a conjugative or an infective tube.

2.1. Conjugative tube formation induced by *fuz7^{DD}* is not abolished by *ukc1* deletion

In response to pheromones, *U. maydis* form a hyperpolarise conjugative tube, resulting of the direct activation of the MAPK cascade. This hyperpolarised conjugative tube could also be induced without pheromones signal, using a constitutive form of the MAPK kinase Fuz7, the Fuz7^{DD} protein that mimics the active form of the MAPKK. In order to study whether cells defective in *ukc1* were able to form this hyperpolarised conjugative tube, a Fuz7^{DD} construct was introduced in an *ukc1^{nar1}* strain. The allele *fuz7^{DD}* was under the control of the P_{crg1} promoter. P_{crg1} promoter is induced by growing the cells in arabinose as carbon source, and strongly repressed in glucose containing medium. The induction of *fuz7^{DD}* expression in YPA medium, caused the formation of the conjugative tube in *ukc1^{nar1}* cells as in WT FB1 cells (Fig.28) showing that cells repressing *ukc1* were able to form the hyperpolarised conjugative tube.

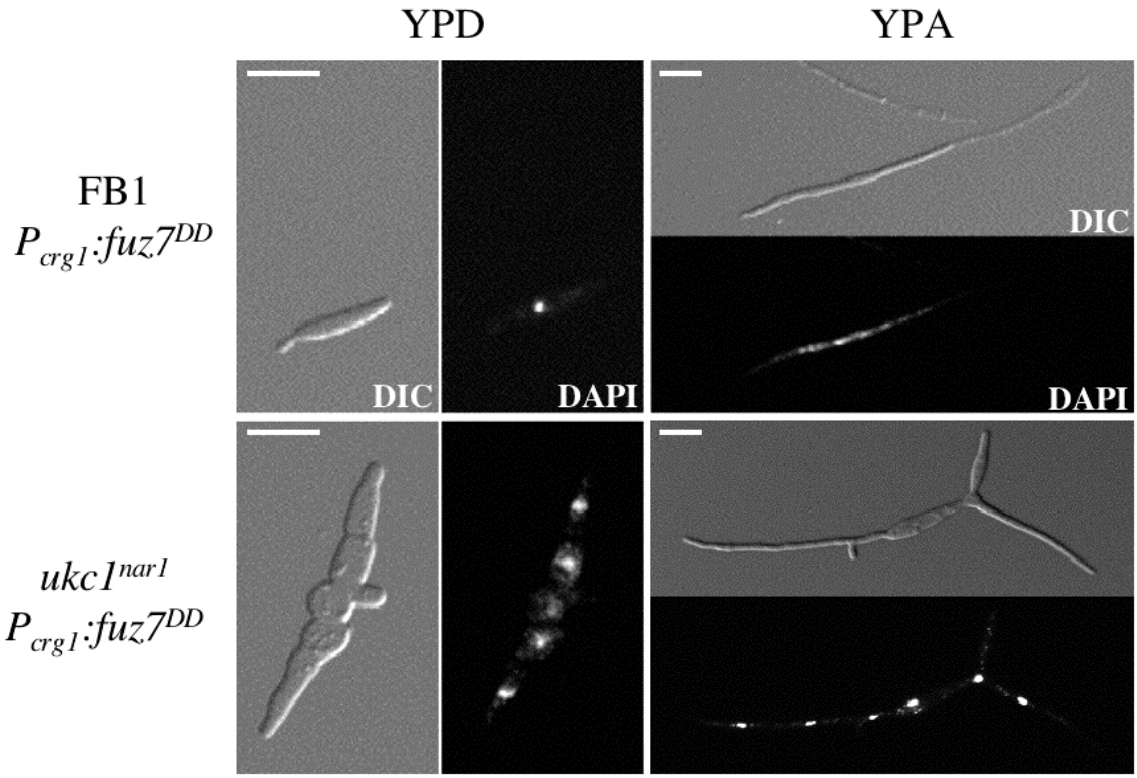

Figure 28: Induction of an hyperpolarised conjugative tube formation in $fuz7^{DD}$ $ukc1^{nar1}$ cells. Photos were captured 12 hours after incubation in YP+Glucose (YPD) or YP+arabinose medium (YPA) media. FB1 P_{crg1}:$fuz7^{DD}$ cells grown in inducible medium (YPA), formed a conjugative tube (hyperelongated cell). $ukc1^{nar1}$ P_{crg1}:$fuz7^{DD}$ cells grown in YPD presented a mutant phenotype, caused by the repression of the *ukc1*. In YPA, $ukc1^{nar1}$ P_{crg1}:$fuz7^{DD}$ cells were able to form a conjugative infective tube, in spite of the *ukc1* repression. Bar, 10μm.

2.2. *ukc1* mutant cells can form an infective tube

After cell fusion, *b* genes from both mating types form a heterodimer transcriptional factor that controls the induction of the infective tube. The AB31 strain genome contains both bE and bW genes under the control of a P_{crg1} promoter. Thus, after incubation in arabinose containing medium, *b* genes are expressed and the formation of the infective tube is induced, bypassing the cell fusion stage (Fig.29 YPA medium). As AB31, AB31$ukc1^{nar1}$ cell induced the formation of this hyperpolarised structure in arabinose containing medium even in the absence of *ukc1* expression (Fig.29). This result showed that the repression of *ukc1* expression did not abolish the formation of the infective tube produced in an AB31 background.

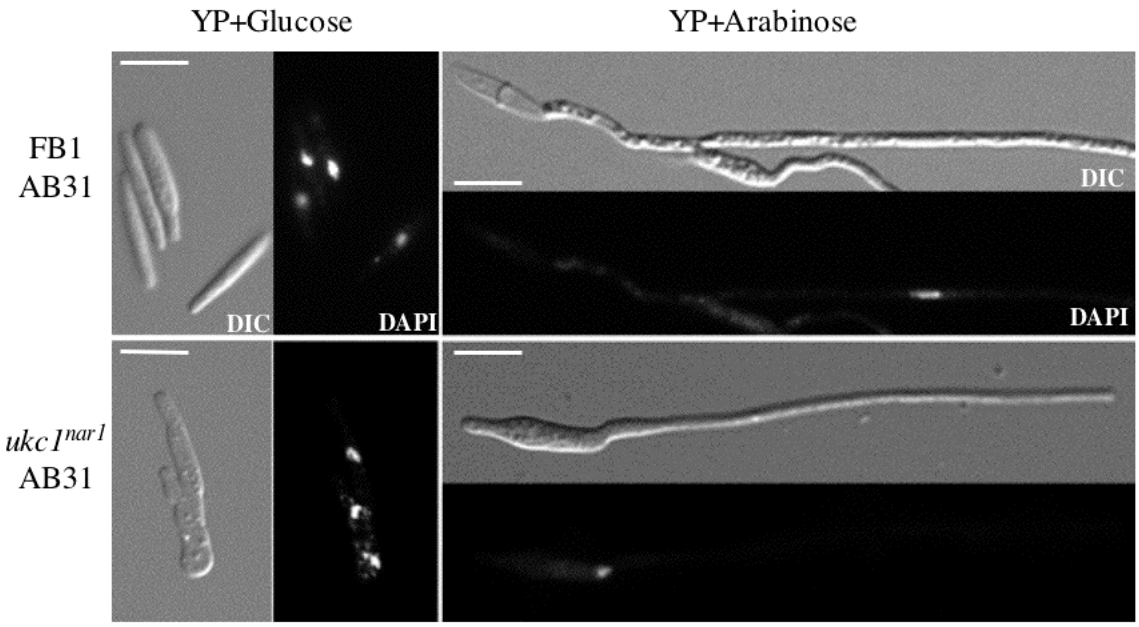

Figure 29: Induction of the formation of the infective tube in AB31*ukc1*^{nar1} strain.
Photos were captured 12 hours after incubation in YP+Glucose (YPD) or YP+arabinose (YPA) media. FB1 AB31 cells grown in inducible medium (YPA) formed an infective tube (hyperelongated cell). AB31*ukc1*^{nar1} cells grown in YPD presented a mutant phenotype, caused by the repression of *ukc1* expression. In YPA, AB31*ukc1*^{nar1} cells were still able to form a hyperpolarised infective tube, in spite of the *ukc1* repression. Bar, 10µm.

3. *Δukc1* cells are defective in cell-cell fusion

As mentioned above, cells deleted for*ukc1* gene were able to develop the conjugative or infective tubes. Accordingly with these data, we next wandered whether the lack of virulence could result from a problem in cell fusion. To test this, a cell-cell fusion assay was performed. To this end, we spotted a mix of compatible strains that expressed cytoplasmic CFP or YFP fluorescent proteins on water agar slides at 28ºC. In this fusion assay, control cells (WT FB1 and WT FB2) were able to fused and develop dikaryotic hyphae, which resulted in a faint yellow colour in the merge image (Fig.30). In contrast, in a mixture of compatible FB1*ukc1*^{nar1} and FB2*ukc1*^{nar1} cells, in which *ukc1* expression was first repressed, no cell-cell fusion was detected. Cells repressed for *ukc1*

expression were unable to develop dikaryotic hyphae (Fig.30), suggesting that Ukc1 was required for successful fusion with a compatible partner.

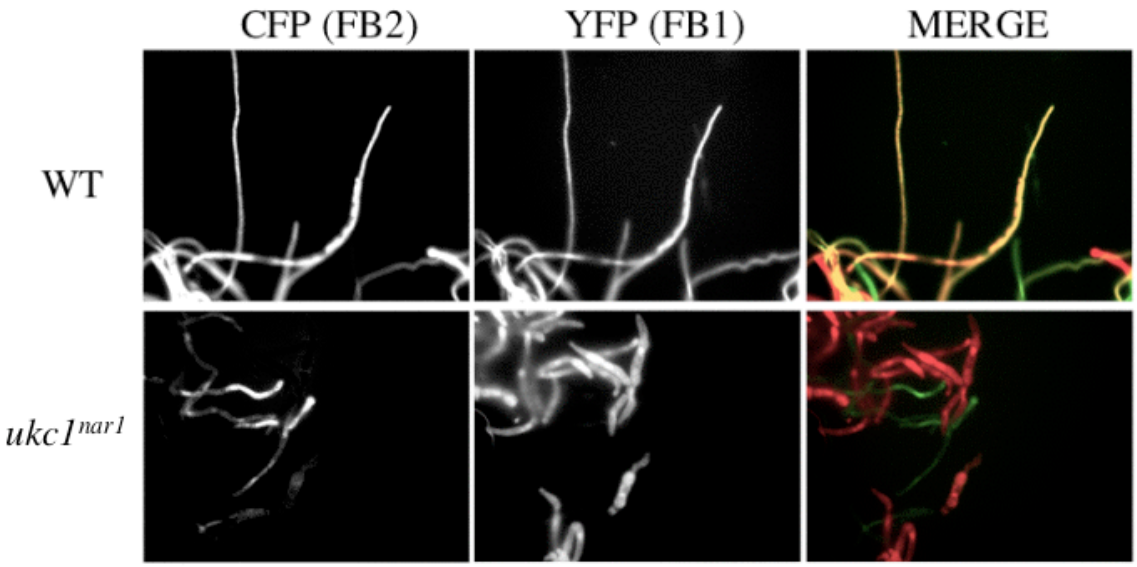

Figure 30: Fusion ability of cells repressing *ukc1*.
Fusion assay of CFP-YFP-labelled mating partners on water-agar 2% slides after incubation overnight. Cells expressing CFP were coloured in green whereas cells expressing YFP were coloured in red. Fused hyphae express both RFP and CFP, resulting in yellow.

4. Ukc1 localises at the extremity of the conjugative tube

Observing the indispensable activity of *ukc1* for mating, we next asked what was the localisation of Ukc1 during the mating process in *U. maydis*. To this end, using the Ukc1-GFP strain, conjugative tube formation was induced adding synthetic pheromone *a2* in the medium. Figure 31 shows that after 4h of induction, cells in presence of pheromone formed a conjugative structure, in which Ukc1-GFP was found at the extremity. This result suggested that Ukc1 activity kinase is required for mating, at the fusion cells site.

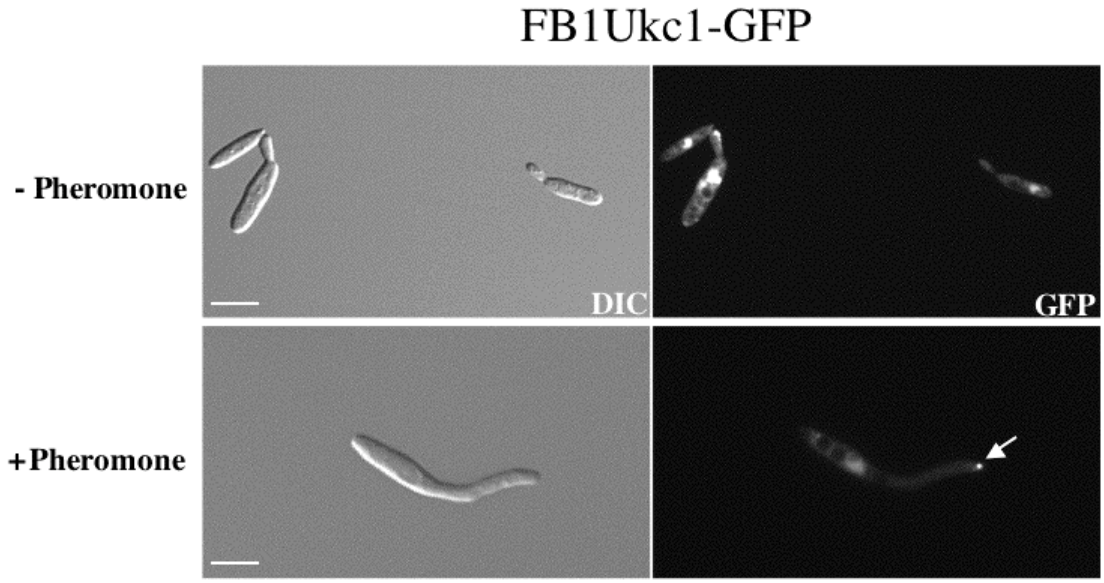

Figure 31: Ukc1-GFP localisation after pheromone induction.
Photos were captured after 4 h induction in pheromone diluted in DMSO (+ pheromone) or in DMSO without pheromone (- pheromone) as control. Ukc1-GFP localised in the nucleus and cells ends of control cells. When activated by pheromone, cells formed a conjugative tube. In this case, Ukc1-GFP was localised in the nucleus and interestingly at the extremity of the conjugative tube as indicated by the white arrow. Bar, 10μm.

5. Δ*ukc1* cells are defective in pheromone response

Cell fusion is the result of pheromone recognition between two compatible mating type cells. After pheromone recognition, cells respond by pheromone secretion, which at the molecular level is traduced by a strong expression of *mfa1* pheromone precursor. The activation of *mfa1* transcription induces the formation of a conjugative tube and cell fusion (Banuett, 1992). In other to find out whether a defect in pheromone response could be the cause of the cell-cell fusion defect observed in Δ*ukc1* cells, we analysed whether Δ*ukc1* cells were able to induce *mfa1* transcription after pheromone stimuli. To this end, a northern blot analysis with *mfa1* pheromone gene as probe was performed. Total RNA was isolated from a mix of WTFB1xWTFB2 and *Δukc1*FB1x*Δukc1*FB2. For pheromone induction, these mix of cells were grown in

charcoal plates, which stimulated mating and allowed the transcription of pheromone inducible genes as *mfa1*.

For the mix of WT strains, Northern blot analysis revealed the expected pattern of enhanced expression of *mfa1* gene (Fig.32). In contrast, the expression of *mfa1* was undetectable in the mix of *Δukc1* mutant cells (Fig.32). This experiment showed that cells deleted for *Δukc1* were defective in pheromone response, which could explain the defect in cell fusion mentioned above.

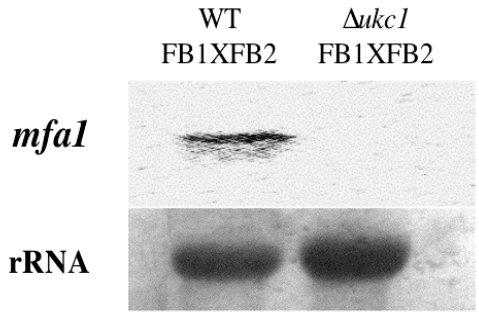

Figure 32: *mfa1* expression in response to pheromone. Both mating types (FB1 and FB2) of WT or *Δukc1* were mixed and inoculated in charcoal plates to stimulate the pheromone *mfa1* expression. RNA was prepared and 10μg of total RNA was loaded per lane. The filter was hybridized with *mfa1* (Top). rRNA served as loading control (Bottom).

6. *ukc1* deletion affects *prf1* transcription

Knowing that the expression of the *mfa* genes was under the control of the Prf1 transcriptional factor, we next wandered whether the expression of *prf1* was affected by *ukc1* deletion. To this end, we performed a northern blot analysis with *prf1* as probe.

To stimulate the mating between FB1 and FB2, which leads to the expression of pheromone-inducible genes as *prf1*, cells were grown in charcoal plates. For the WT strain FB1 (Fig.33 lane 2), Northern blot analysis showed a basal level of *prf1* expression and this level increased in a mix of FB1xFB2 WT cells (Fig.33 lane 1). In contrast, in *Δukc1* FB1 strains neither basal expression (Fig.33 lane 4) nor induced

expression in a FB1xFB2 mix could be detected (Fig.33 lane 3) suggesting that *prf1* expression was abolished in *Δukc1* cells.

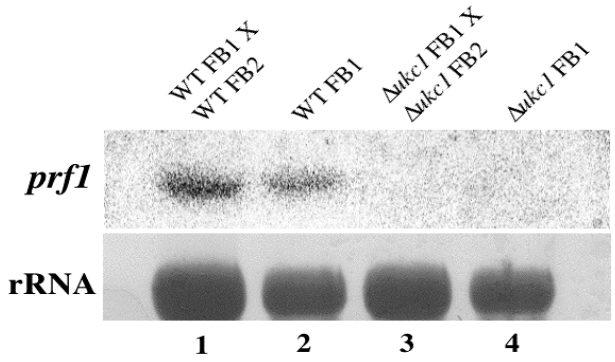

Figure 33: Ukc1 is essential for *prf1* expression. Both mating types (FB1 and FB2) of WT or *Δukc1* were mixed and inoculated in charcoal plates to stimulate the the *prf1* expression. RNA was prepared and 10μg of total RNA was loaded per lane. The filter was hybridized with *prf1* (Top). rRNA served as loading control (Bottom).

7. Constitutive expression of *prf1* rescue the pheromone response defect of *Δukc1 cells*

Since the *Δukc1* strain did not express *prf1*, we next asked whether the constitutive expression of *prf1* could bypass the *Δukc1* pheromone response defect. To this end, we inserted the *Δukc1* deletion cassette in a strain where the endogenous *prf1* gene was replaced by the $prf1^{CON}$ allele, whose expression of *prf1* was driven by the constitutive *otef1* promoter (Hartmann *et al.*, 1999). Subsequently, strains FB1, FB1*Δukc1*, FB1$prf1^{CON}$ and FB1*Δukc1*-$prf1^{CON}$ were monitored for *mfa1* gene expression.

For the WT strain FB1 (Fig.34 lane 1), Northern blot analysis showed a basal level of m*fa1* expression and this level increased in FB1$prf1^{CON}$ (Fig.34 lane 3). Interestingly, in the *Δukc1* strain no basal expression was detected (Fig.34 lane 2) but, in FB1*Δukc1*-

prf1^{CON} we could observe the rescue of the *mfa1* gene transcription (Fig.34 lane 4). This Northern blot analysis also shown that in FB1*Δukc1- prf1*^{CON} the *mfa1* transcription level appeared inferior to the level detected in FB1*prf1*^{CON} (Fig.34 lane 3 and 4).

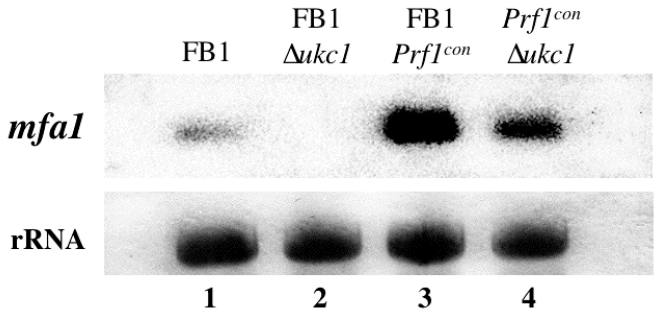

Figure 34: Constitutive expression of *prf1* rescued the pheromone response defect of the *Δukc1* mutant. Cells were grown in CMD medium. RNA was prepared and 10μg of total RNA was loaded per lane. The filter was hybridized with *prf1* (Top). rRNA served as loading control (Bottom).

As we observed the rescue of the pheromone response in *Δukc1- prf1*^{CON} cells, we decided to test whether the cell fusion defect detected in *Δukc1* was corrected in *Δukc1-prf1*^{CON} cells.

To test *Δukc1- prf1*^{CON} for mating, compatible deletion strains were co-spotted on CM-charcoal plates. On these plates, compatible WT or *prf1*^{CON} strains fused and formed dikaryotic hyphae, which appeared as white fuzziness (Fig.35 yellow arrow). When *Δukc1-prf1*^{CON} cells were co-spotted with a WT or a *prf1*^{CON} partner, a significant reduction in filament formation was observed (Fig.35 blue arrows). FB1*Δukc1-prf1*^{CON} co-spotted with its mating partner FB2*Δukc1-prf1*^{CON} (Fig.35 red arrow), appeared unable to mate and to form dikaryotic hyphae, despite the pheromone-response rescue due to *prf1*^{CON}. These data suggested that in addition to have a defect in pheromone response, *Δukc1* mutant cells could also be affected in another process during mating.

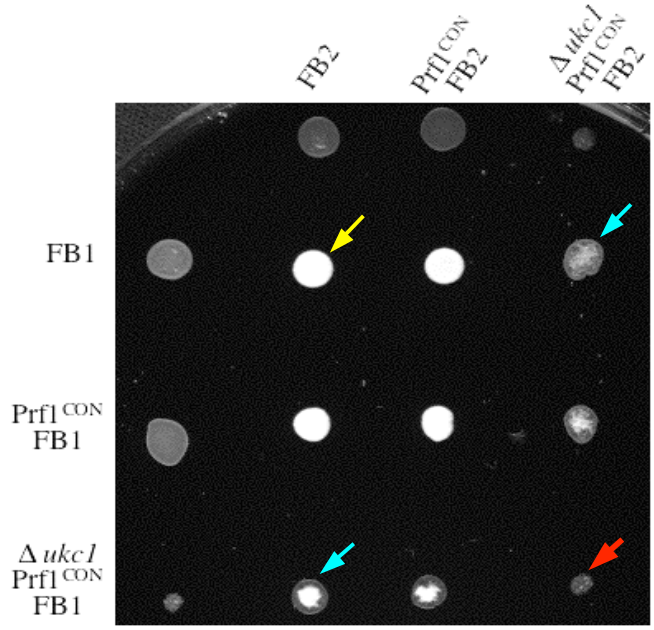

Figure 35: Mating and filament defects of *Δukc1-prf1*^{CON} strains.
Indicated WT and mutant strains were spotted alone or in combination on charcoal containing CM plate. The white fuzziness indicates the formation of aerial hyphae (or dikaryotic filaments) as indicated by the yellow arrow.

Section IV: Interplay between the RAM pathway and other protein networks

As saw in the section II and III, the RAM pathway appeared indispensable for morphology and pathogenicity regulation. Knowing that in *U. maydis* the cAMP and the pheromone inducible MAPK pathways are involved in pathogenesis regulation, and alongside the cell wall integrity pathway they control morphology, we decided to study whether in *U. maydis* also, the RAM pathway could act in relation with these signaling cascades.

1. Crosstalk between the cAMP and the RAM pathway

1.1. Inhibition of PKA activity induced stronger filamentation of Δ*ukc1* cells

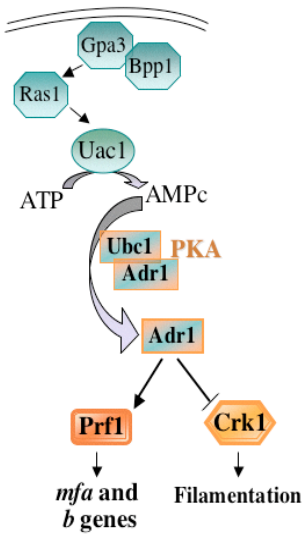

Figure 36: cAMP pathway in *U. maydis*

In order to examine a functional relationship between the cAMP and the RAM pathways, we first asked whether an inhibition of the cAMP pathway could rescue the Δ*ukc1* mutant phenotype. To this end, we tried to create the double mutant Δ*ukc1*Δ*adr1*, but it was not possible to obtain cells with both mutations, suggesting that the deletion of the PKA in parallel to the RAM pathway was synthetically lethal in *U. maydis*.

To bypass this problem we decided to use an inhibitor of PKA activity, the Rp-Adenosine 3´,5´-cyclic monophosphorothioate triethylammonium (Rp-cAMP)(Sigma). The Rp-cAMP is a

specific cAMP antagonist that blocks cAMP-mediated effects, as the activation of PKA (Fig.36). In order to know whether an inhibition of PKA activity could affect the Δ*ukc1* mutant phenotype, WT FB1 and Δ*ukc1* cells were incubated overnight with Rp-cAMP and a phenotypic analysis was carried out. Figure 37 shows that inhibition of PKA by Rp-cAMP provoked a strong filamentation of FB1 cells. For Δ*ukc1* strain, treatment with Rp-cAMP significantly increased the filamentation of mutant cells compared with untreated cells. This result suggested that the RAM pathway could act in relation with the PKA pathway regulating negatively polar growth.

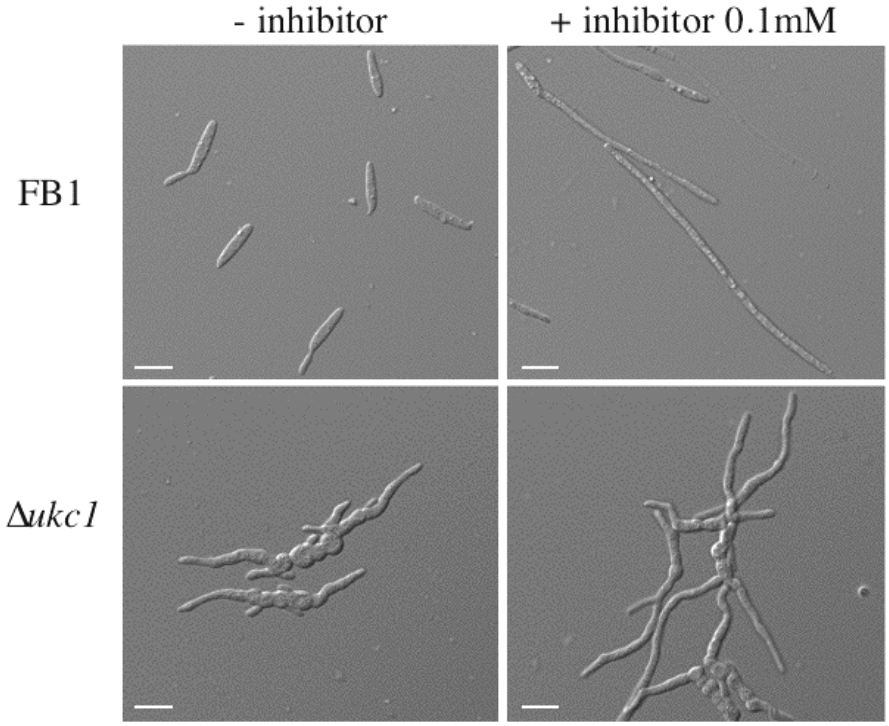

Figure 37: Influence of a PKA inhibitor on the morphology of FB1 and Δ*ukc1* strains. FB1 cells (upper panel) and Δ*ukc1* cells (lower panel) were grown overnight in CMD without PKA inhibitor (left panel) or in CMD containing 0.1mM inhibitor Rp-cAMP (right panel). Addition of 0.1mM PKA inhibitor induced strong filamentation of FB1 and Δ*ukc1* cells. Bar, 10μm.

1.2. PKA activation reduces filamentation of Δ*ukc1* cells

To examine more carefully a functional relationship between the cAMP and the RAM pathways, we hyper-activated the cAMP pathway in a Δ*ukc1* background and

performed phenotype analysis. The activation of the cAMP pathway was possible by the addition of exogenous cAMP into the liquid medium, which can activate the PKA subunit Adr1 kinase (Fig.36) (Krüger *et al.*, 1998).

In figure 38, we can observe that WT FB1 cells treated with 6mM of exogenous cAMP showed a multibudding phenotype and that addition of 15 mM severely affected cell morphology and cell separation. In Δ*ukc1* cells, addition of 15 mM of cAMP led to a worst phenotype, presenting cells more affected in morphology. Cells appeared rounder than untreated mutant cells (0mM cAMP) with more branching. We could observe that elongated cells normally present at the mutant cell extremity disappeared. These data suggested that hyper-activation of the cAMP pathway was able to reduce filamentation presented by Δ*ukc1* cells suggesting a link between the RAM pathway and the cAMP pathway in polar growth regulation, and the possibility that they act in parallel regulating polar growth in a negative manner.

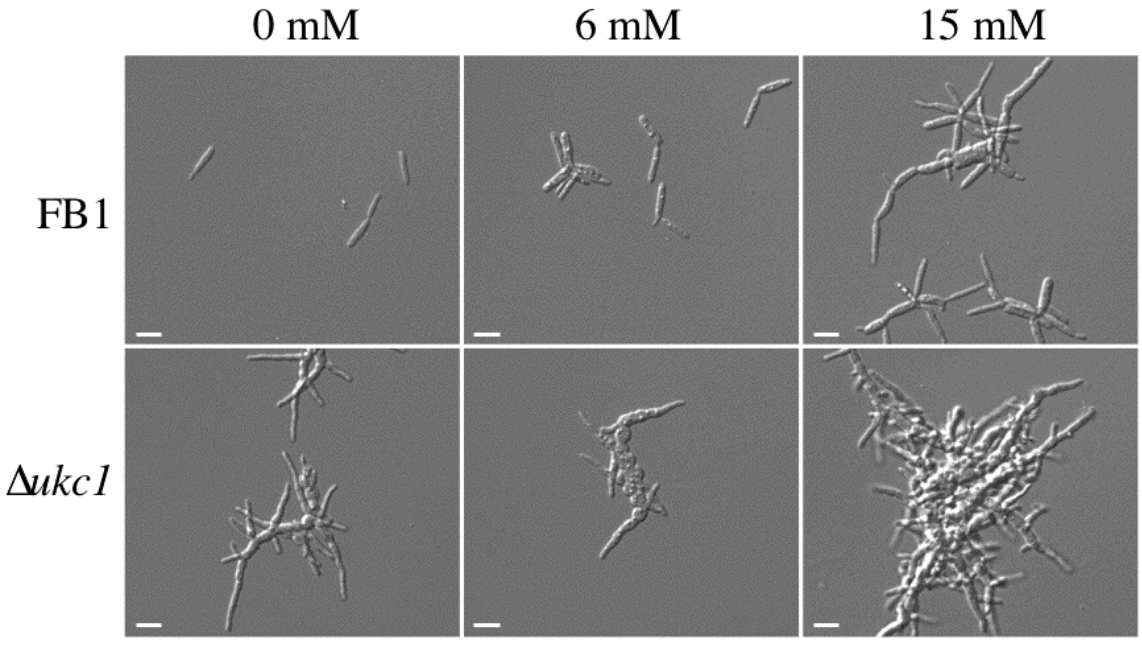

Figure 38: Influence of exogenous cAMP on the morphology of WT and Δ*ukc1* strains. The WT strain (upper panel) and the mutant strain Δ*ukc1* (lower panel) were grown overnight in CMD medium containing the indicated concentrations of cAMP. Bar, 10μm.

1.3. PKA activation cannot rescue the *mfa1* transcription defect of Δ*ukc1* cells

The observation of a link between both pathways in polar growth regulation led us to investigate whether the RAM and the cAMP pathways could regulate Prf1 activity in parallel. The addition of exogenous cAMP in the medium as for consequence an up-activation of the PKA activity resulting in Prf1 activation, leading to a strong transcription of *mfa* pheromone without pheromone stimuli. Taking into account that Δ*ukc1* strains presented a defect in *mfa1* transcription, we decided to analyse whether PKA up-activation could restore *mfa1* transcription in a Δ*ukc1* background. To this end, we carried out a Northern blot analysis of FB1 and Δ*ukc1* cells activated by external cAMP with *mfa1* as probe.

As we can see in the northern blot analysis (Fig.39), for WT FB1 cells, an addition of 6 mM cAMP highly induced *mfa1* transcription (Fig.39 lane 2), whereas an addition of 15 mM resulted in a lower *mfa1* transcription (Fig.39 lane 3). In Δ*ukc1* cells, we could observe that neither 6 mM nor 15 mM of exogenous cAMP rescued *mfa1* transcription (Fig.39 lane 5 and 6). This result showed that the defect in *mfa1* transcription of Δ*ukc1* cells could not be rescued by an activation of PKA activity, suggesting that RAM pathway regulates Prf1 independently of the cAMP pathway.

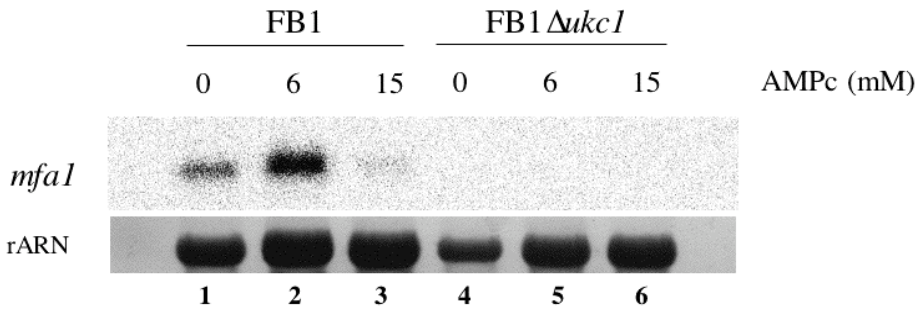

Figure 39: Northern blot analysis of pheromone gene expression in response to cAMP stimulation. Strains FB1 and FB1 Δ*ukc1* were grown overnight in CMD medium containing the indicated concentrations of cAMP. RNA was prepared and 10μg of total RNA was loaded per lane. The filter was hybridized with *mfa1* (Top). rRNA served as loading control (Bottom).

1.4. *crk1* transcription appears deregulated in Δ*ukc1* strain

In addition to regulate the transcription and the activity of Prf1, cAMP pathway is also involved in morphology regulation of *U. maydis*, in part through Crk1. In this work, we first analysed whether Crk1 regulation was affected in RAM mutant to understand whether cAMP and the RAM pathway could act in parallel on common targets.

Crk1 protein kinase was described as a regulator of cell elongation. When the transcription of *crk1* is repressed by the cAMP pathway, cells grow in a yeast like form, but when the *crk1* transcription is activated, cells switch to a filamentous form (Garrido and Pérez-Martín, 2003). To test whether *crk1* transcription could be affected by a deregulation of the RAM pathway, we performed a Northern blot analysis with *crk1* as probe (Fig.40). For the WT strain FB1, Northern blot analysis showed a low level of *crk1* transcript and this level was up-regulated in *Δukc1* strain (Fig.40) suggesting that the RAM pathway could also regulate *crk1* transcription.

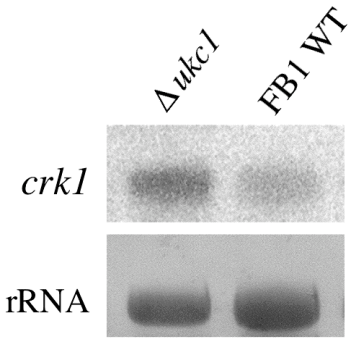

Figure 40: Up-regulation of *crk1* transcription in *Δukc1* cells. Cells were grown in CMD medium. RNA was prepared and 10μg of total RNA was loaded per lane. The filter was hybridized with *crk1* (Top). rRNA served as loading control (Bottom).

Analysing RAM mutant phenotype, we observed that cells localised at the extremity were filamentous. To test whether a deregulation of *crk1* transcription could explain the severe phenotype of RAM mutant cells, we next asked whether Crk1 up-regulation could be involved in the filamentation of RAM deleted cells. To this end, we constructed the *Δukc1 Δcrk1* double mutant, inserting *Δukc1* deletion cassette in *Δcrk1*

cells. The double mutant phenotype presented chains of round cells without filamentous cells at the extremity as we observed in *Δukc1* deletion mutant (Fig.41), suggesting that the up-regulation of *crk1* could explain a part of the severe *Δukc1* mutant phenotype.

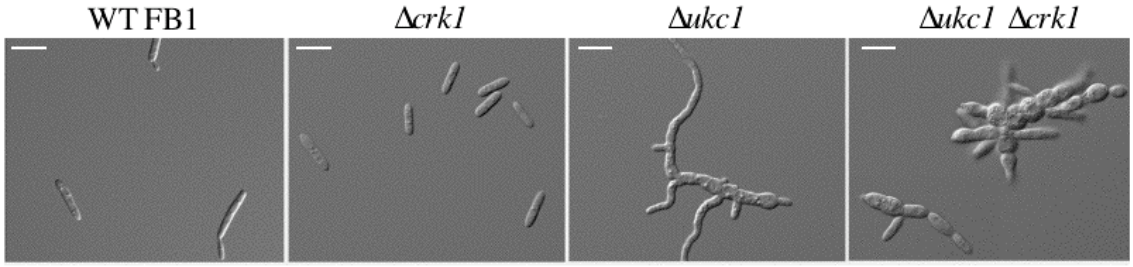

Figure 41: Repression of the filamentous defect of *Δukc1* cells by *crk1* deletion.
Cells were grown overnight in CMD medium. *Δcrk1* strain appeared affected in morphology. Cells are smaller and quite rounder than WT. The double mutant strain *Δukc1Δcrk1* presented a phenotype organised in chains as observed in *Δukc1* strain, but the morphology of the cells seems in part rescue. In this double mutant, we could not observe elongated cells as in the single mutant *Δukc1*. Bar, 10μm.

2. MAPK and RAM pathway in *U. maydis*

2.1. Pheromone MAPK and RAM pathway

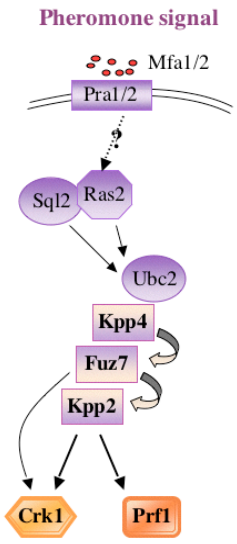

Figure 42: Pheromone MAPK pathway in *U. maydis*

The defect in pheromone response, morphology and the *crk1* up-regulation observed in Δ*ukc1* cells led us to asked whether a relationship existed between the pheromone MAPK and the RAM pathways. The up-activation of the MAPK cascade was already presented in figure 28. The constitutive form of the Fuz7 MAPKK (Fig. 42), the *fuz7DD* allele, introduced in an *ukc1*^{nar1} background, showed that cells repressing *ukc1* in YPD medium were able to form hyperpolarised cells as FB1 *fuz7DD* cells without additional phenotypes associated.

Next, we tested whether a deletion of *fuz7* allele could restore part of the Δ*ukc1* mutant phenotype. To this end, we introduced the *ukc1* deletion cassette in Δ*fuz7* cells. As we can observe in figure 43, cells deleted for *fuz7* did not present any defect, whereas Δ*ukc1* Δ*fuz7* cells presented the same phenotype as Δ*ukc1* cells. We could not observe rescue of part of the Δ*ukc1* phenotype deleting the *fuz7* allele, or activating the MAPK cascade using the *fuz7DD* allele, suggesting that both pathway act independently in *U. maydis*.

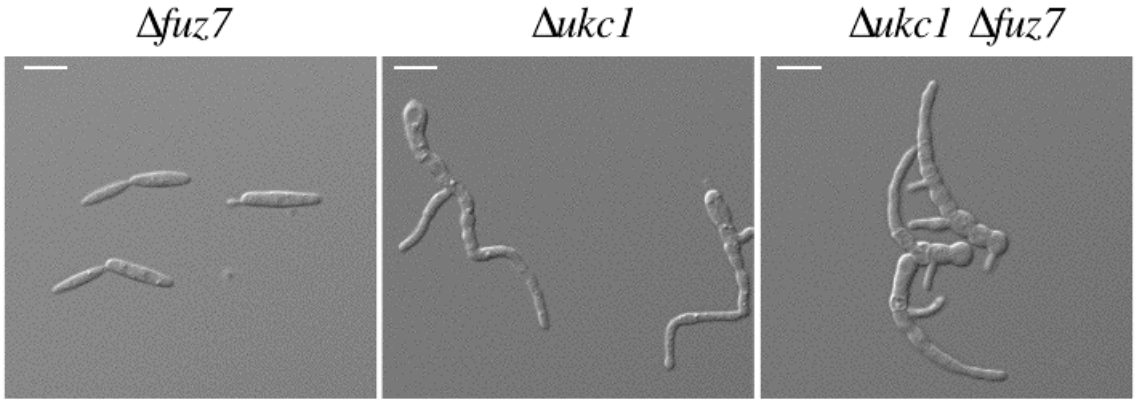

Figure 43: Influence of the *fuz7* deletion on *Δukc1* mutant phenotype.
Cells were grown overnight in CMD medium. *Δfuz7* strain presented the same phenotype as WT strain. The double mutant *Δukc1Δfuz7* and *Δukc1* strains presented a similar phenotype, with a defect in cell separation, cell morphology and cell elongation. Bar, 10*μ*m.

2.2. Crosstalk between the Cell Wall Integrity MAPK and the RAM pathways

Knowing the importance of the CWI in morphology regulation, we next analysed a possible crosstalk between the RAM and the CWI pathways, which could explain part of the aberrant morphology defect observed in RAM mutants.

2.2.1. MAPK repression can rescue part of the Δukc1 mutant phenotype.

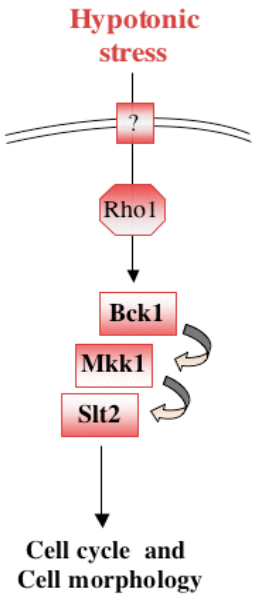

Figure 44: Cell Wall Integrity MAPK pathway in *U. maydis*.

We first decided to perform an epistasis analysis, deleting *slt2* encoding the MAPK of the cascade (Fig.44). To this end, we inserted the *slt2* deletion cassette in an *ukc1*^{nar1} background and performed phenotypic analysis of the double mutant. In figure 45, we can observe that in MM, when *ukc1* was normaly expressed, Δ*slt2 ukc1*^{nar1} cells presented a WT phenotype as cells deleted for Δ*slt2* alone. In contrast, in YPD medium, that suppressed the *ukc1* expression, Δ*slt2 ukc1*^{nar1} presented an unexpected phenotype. Cell appeared bigger than WT and did not form large aggregates of cells as Δ*ukc1*. The phenotype observed was not comparable to the cells repressing *ukc1* expression alone. Cells were not round in the central part, did not present any filamentous cells at the extremity, and were organised in chains of maximum three cells. The *ukc1* mutant phenotype appeared really attenuated by the *slt2* deletion in the Δ*slt2 ukc1*^{nar1} strain. This partial rescue of the morphological defect by *slt2* deletion suggested that the RAM pathway could act in relation with the CWI pathway to control polar growth in *U. maydis*.

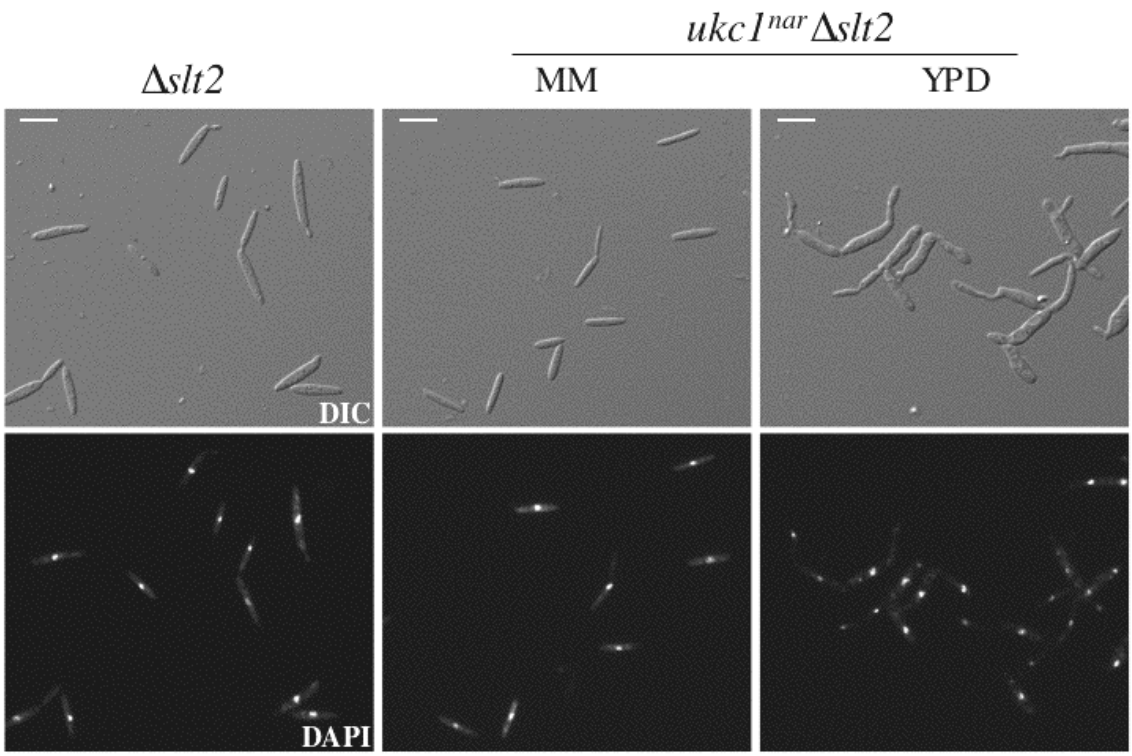

Figure 45: Rescue of the *ukc1* repression phenotype by *slt2* deletion.
Photos were captured after incubation in YPD or MM media. Δ*slt2 ukc1*^{nar1} strain grown overnight in inducible medium (MM), presented a WT phenotype as cells deleted for *slt2* alone (data not show). In YPD, the repression of *ukc1* expression induced a defect in cell separation but not comparable to the defects observed in *Δukc1* cells. Here we observed chains of two or three cells. The morphology of the cells seem affected by the *ukc1* repression, leading to an increase of cell volume, but not comparable to the *Δukc1* mutant phenotype. The central cell was not round and hyperelongation of the apical cells was not observed. Bar, 10μm.

2.2.2. Up-regulation of MAPK cascade suppresses the polar growth induced in Δukc1 mutant cells.

Observing the partial rescue of the *Δukc1* mutant phenotype by the *slt2* deletion, we next asked whether an up-regulation of the CWI MAPK cascade could also have an influence on the *Δukc1* phenotype. To this end, we used a constitutive form of the MAPK kinase Mkk1 (Fig.44), the Mkk1^{DD} protein, that mimics the active form of the MAPKK (Carbó, doctoral thesis). Mkk1^{DD} construct was introduced in an *ukc1*^{nar1} strain. The allele *mkk1*^{DD} was under the control of the P_{crg1} promoter induced in arabinose medium. As we can observed in figure 46, induction of *mkk1*^{DD} expression in

MMA medium, provoked the appearance of two or three nuclei, and an increased in cell volume comparing with the WT phenotype (MMD medium). Interestingly, *mkk1*^{DD} *ukc1*^{nar1} cells grown in YPA, repressing *ukc1* expression and inducing *mkk1*^{DD} allele at the same time, presented a different phenotype as cells repressing *ukc1* alone (YPD). The phenotype observed in YPA was organised in chains of cells extremely round and without branching or elongated cells, as normally induced by *ukc1* repression in YPD (Fig.46). This surprising phenotype suggested that an up-activation of the CWI pathway could negatively regulate polar growth, acting in relation with the RAM protein network.

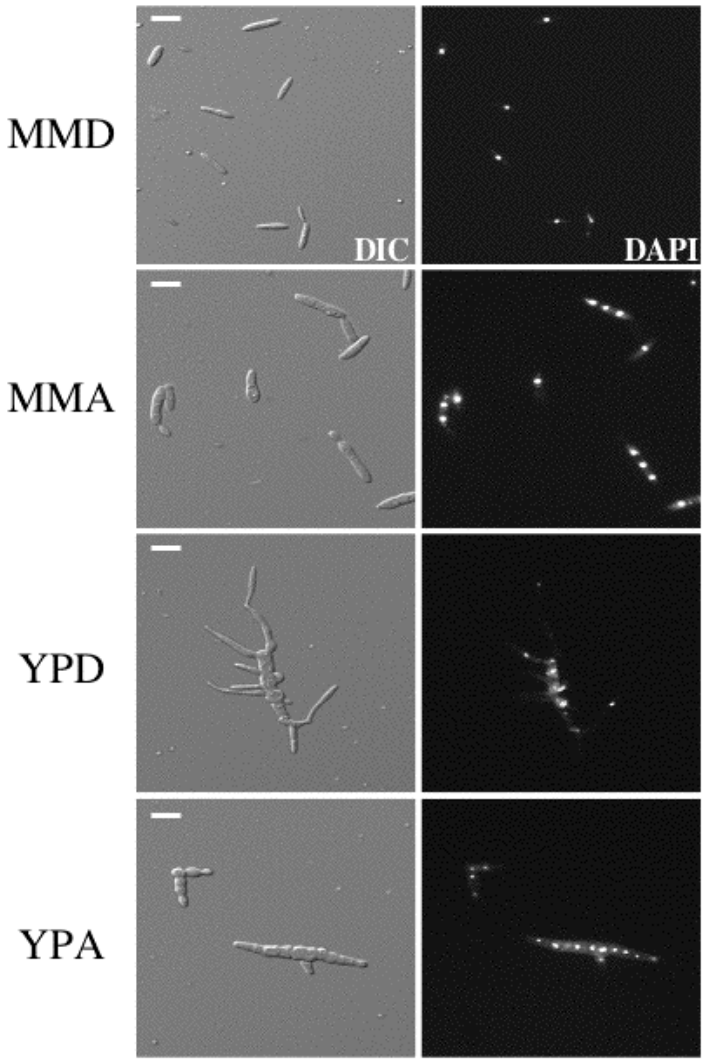

Figure 46: *Mkk1*^{DD} repressed polar growth in *ukc1*^{nar1} cells.
Photos were captured after overnight incubation in YPD, YPA, MM or MMA media. *mkk1*^{DD} *ukc1*^{nar1} cells grown overnight MMD presented a WT phenotype. In MMA, the expression of *mkk1*^{DD} provoked nucleus multiplication induced by a cell cycle acceleration in G2 phase (Carbó, doctoral thesis). In YPD medium, repression of *ukc1* induced a typical Δ*ukc1* phenotype. In YPA medium, the induction of *mkk1*^{DD} expression led to a defect in polar growth. Cells appeared round and organized in chains without production of elongated structures or branching as observed in YPD medium. Bar, 10μm.

2.2.3. Δukc1 does not perturb CWI pathway functions

The CWI is a MAPK cascade involved in the maintenance of the cell wall structure during cell growth and in the presence of external compounds that cause cell wall stress. Deletion of *slt2* in *U. maydis* provokes a growth defect in stress conditions as high temperature or addition of drugs in the medium. We already observed a possible relationship between the RAM and the CWI pathway, and in order to know whether both pathways could regulate common targets, we analysed the CWI function upon *ukc1* deletion. To this end, we constructed the double mutant Δ*slt2*Δ*ukc1* and carried out a drug and temperature sensitivity assay. To evaluate the ability of FB1, Δ*slt2*, Δ*ukc1* and Δ*slt2*Δ*ukc1* to grow in stress conditions, cells were spotted in medium containing calcofluor white (CFW), congo red (CR) and chlorpromazine (CPZ), agents known to activate the CWI in *U. maydis* (Carbó, doctoral thesis). They were also grown in CMD medium at normal growth temperature (28º) or restrictive temperature (36º). In figure 47, FB1 grew normally in all media. Δ*ukc1* cells also seemed not be affected by the high temperature as the different drugs added in the medium. In contrast, the Δ*slt2* strain presented a high sensitivity to CFW, CPZ and CR as well as to restrictive temperature (36ºC). Interestingly, it appeared that the double mutant Δ*slt2*Δ*ukc1* grew as the Δ*slt2* strain. Both strains presented the same difficulties to grow in the presence of stress agents or restrictive temperature. This result suggested that the RAM pathway did not act in cell wall respond adaptation as the CWI pathway, but that they could act as two distinct signaling cascades regulating polar growth, with a relation that remains to be discovered.

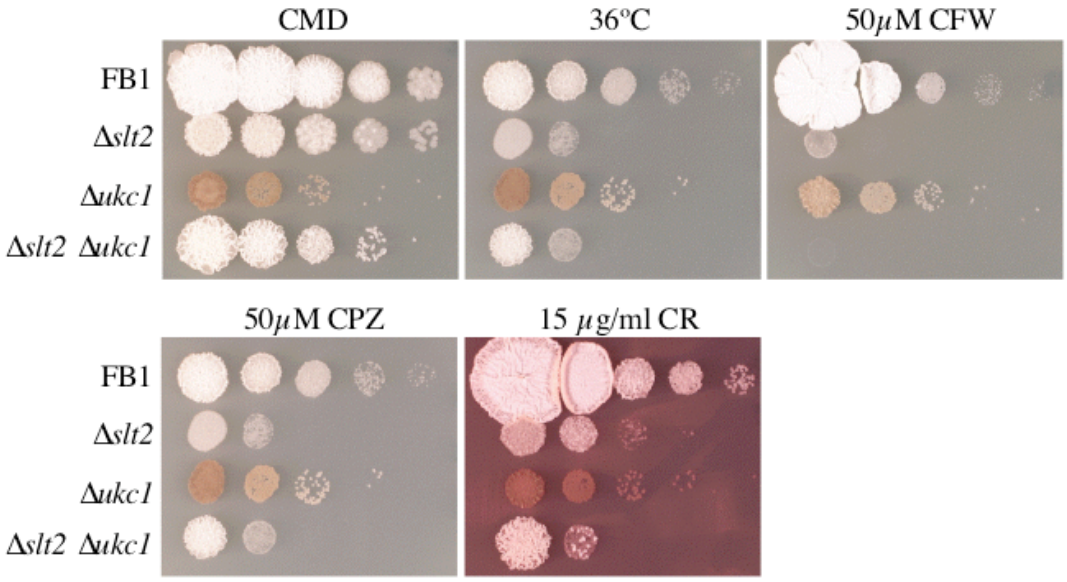

Figure 47: Sensitivity of Δ*slt2*Δ*ukc1* strain against cell wall disturbing compounds.
Cells were grown in CMD liquid medium until an OD_{600} of 1. Cells were diluted serially and 5μl were spotted on CMD plates alone or CMD plates supplemented with calcofluor white (CFW), chlorpromazine (CPZ) and congo red (CR). The plates were incubated for 2 days at 28ºC or 36ºC in the restrictive temperature assay. Here Δ*ukc1* strain is easily notable by the brown colour that present this strain grew in plates, a consequence of a high pigments formation.

Discussion

In this work, we characterised the components and the functions of the RAM pathway in *U. maydis*. We first analysed the involvement of the RAM pathway in morphogenesis and polar growth. Next we identified the possible reasons of the virulence defect observed in RAM mutants and finally, we studied the relationship between the RAM and other protein networks known in *U. maydis*.

Conservation of the RAM pathway components in *U. maydis*

All Ndr protein regulators have been identified in few organisms as *S. cerevisiae*, *C. albicans* and *C. neoformans*. In *S. cerevisiae*, these regulator proteins are Mob2, Hym1, Sog2, Kic1 and Tao3 and appear to function in the same signaling network, regulating Cbk1p activity (Bidlingmaier *et al.*, 2001; Weiss *et al.*, 2002; Nelson *et al.*, 2003). In this work we first identified the *U. maydis* homologue of Mob2. We demonstrated that it is indispensable for Ukc1 function as deletion of *mob2* gene resulted in the same phenotype that cells deleted for *ukc1*. The conservation of the SMA domain in the Ukc1 protein sequence and the Mob1/phocein sequence in the Mob2 homologue suggested that Ukc1-Mob2 could physically interact. An immunoprecipitation confirmed that both proteins interacted and could form a central Ukc1-Mob2 complex also in *U. maydis*. In addition of Mob2, we identified the homologues of four components involved in Cbk1 regulation in *S. cerevisiae*, the protein Hym1, Tao3, Sog2 and Kic1. An *in silico* analysis showed that the functional and characteristic domains were conserved between *S. cerevisiae* and *U. maydis*

homologues. To know whether they were involved in Ukc1 activity regulation, we created strains deleted for each of these genes. We could observe that each homologue gene deletion presented the same defects as cells deleted for *ukc1*, suggesting their indispensable participation in Ukc1 regulation. These data suggest a complete conservation of RAM components and organisation of the RAM pathway in *U. maydis*. Nevertheless, some difference comparing to *C. albicans* and *S. cerevisiae* appeared in the function of the RAM pathway in *U. maydis*. First, the RAM pathway components appeared essential in these organisms (Kurischko *et al.*, 2005) whereas is not the case in *U. maydis*. The second difference is related to the target of the RAM pathway. RAM is an abbreviation referring to both morphology and Ace2p localization, a transcriptional factor that specifically localizes to daughter cells in *S. cerevisiae*. To know whether the RAM pathway could have the same function regulating the equivalent of Ace2 in this fungus, we searched for an Ace2 homologue in *U. maydis*. The closest match, Um10181, is predicted to contain two C_2H_2-Zn finger domains at its C-terminal end (like Ace2). However, a reciprocal Blast search (UmAce2 *vs S. cerevisiae*) revealed that this protein is more similar to SWI5p than to Ace2p. The deletion of *ace2* in *U. maydis* confirmed that this transcriptional factor does not present the same function as Ace2p of *S. cerevisiae*. Indeed, the deletion phenotype of *ace2* did not present the specific cell separation defect observed in *S. cerevisiae*. Thus at present, no clear Ace2 homologue has been found in the *U. maydis* genome and an equivalent functioning gene has not been identified. This result suggested that we might find another name for this protein network in *U. maydis*, without reference to Ace2, and predicted different functions for this RAM pathway in *U. maydis*.

Ukc1 is localized at different cells part throughout the cell cycle

To analyse whether the RAM pathway could have different functions in *U. maydis* compared to *S. cerevisiae*, we next analysed the subcellular localisation of Ukc1 creating a fusion protein Ukc1-GFP. We observed that Ukc1-GFP protein localized at the apical growth sites until cells are ready to separate. At this stage, Ukc1-GFP protein is found at the cell separation site. Interestingly, Ukc1-GFP also localized at the cells extremity of cells forming an hyperpolarysed conjugative tube, suggesting that Ukc1 could play a function in polarized growth as it has been demonstrated for different Ndr kinases (Tamaskovic *et al.*, 2003).

Ukc1-GFP appeared to localise to both sides of the bud neck, just before cell separation. Interestingly, Cbk1p in *S. cerevisiae* localizes in the same way before cell separation (Colman-Lerner *et al.*, 2001), suggesting an additional function of this pathway in cell separation regulation, through the activation of target different of Ace2.

In addition, Ukc1-GFP is localized within the nucleus of both mother and daughter cells, throughout the cell cycle, whereas Cbk1p has been found transitory localised within the daughter nucleus in *S. cerevisiae* (Colman-Lerner *et al.*, 2001; Weiss *et al.*, 2002). These data allow us to think that Ukc1 could play an important function into the nucleus, regulating transcription, as suggested by the *crk1* and *prf1* transcription alteration observed in this work.

Cytoskeleton protein organisation and morphology appeared affected in Δ*ukc1* mutant cells

Δ*ukc1* cells presented a severe mutant phenotype, with defects in cell size, cell separation and cell elongation. In this study we addressed whether proteins involved in morphology maintenance and cell separation could be affected in RAM mutants and so explained the phenotype observed. We first asked whether septins organisation was affected in RAM deleted cells because of their involvement in cell separation and morphology. We found that localization of the four septins identified in *U. maydis* was not affected in Δ*ukc1* mutants. Septins could formed filaments and were recruited to the cell separation site and the cell ends as in WT cells. These data showed that cell separation and cell morphology defect were not due to a mislocalisation of septin proteins. Little is known about the spacial and temporal rearrangements involved in cell separation but it seems that other protein than septins, involved in cell structure and morphology maintenance, localize at the bud neck for full separation. Analysing the F-actin organisation in Δ*ukc1* mutants, we observed that actin filaments seemed functional. Myo5 accumulation at the cell tip looked normal suggesting functional F-actin cable, however we can not exclude the possibility of subtle differences in the assembly or dynamics of F-actin cables. In contrast, that F-actin patches accumulated at the cell tips more than in WT cells. It remains unclear whether this accumulation is the reason of cell separation and cell morphology defect observed in RAM mutant or a consequence. Interestingly, the same result has been obtained in *C. neoformans* where actin patches were found concentrated at cell extremity whereas in *S. cerevisiae* or *C.*

albicans, actin patches were concentrated at cell separation site and absent at the growing tip in RAM mutants. These data suggested that the RAM pathway could have a conserved function regulating actin structures localisation in fungi.

RAM pathway and polarity in *U. maydis*

Mutation of RAM components result in loss of polarized morphogenesis in *S. cerevisiae* (Rackie *et al.*, 2000; Bidlingmaier *et al.*, 2001; Weiss *et al.*, 2002; Nelson *et al.*, 2003; Kurischko *et al.*, 2005). In *C. neoforman* however, RAM mutants cause constitutive hyperpolarised cells rather than loss of polarity (Walton *et al.*, 2006). Thus, the conserved components of the RAM network may play divergent roles in regulating cell polarity in different fungi.

In *U. maydis*, we could observe a more complex phenotype as those described in other fungi, thus it was not evident to conclude about the role of the RAM pathway in polarity regulation. Indeed, we could observe two distinct phenotypes for the RAM mutants. First, the central part of cell aggregates in mutant strains, was composed of round cells with an increase in cell size, which suggested a loss of polarity. But at the inverse, apical cells appeared very elongated suggesting that RAM mutation promoted growth polarization. In addition, polarity defect were also visible through a defective bud site selection (mutant form daughter cell at both extremity) and by the formation of branching cells. By consequence, analysing Δ*ukc1* mutant phenotype, we could ask us whether the RAM pathway acted negatively or positively on polarity in *U. maydis*. In order to respond at this challenging question we first test whether a cell cycle arrest, using $wee1^{DD}$ allele, could induce the formation of hyperpolarysed cells. We could

observe that cells lacking *ukc1* were still able to hyperpolarize suggesting that the polarity machinery was active in this mutant, and arguing in favour of a negative control of polar growth by the RAM pathway in *U. maydis*. In the same way, we could observe that *fuz7*^{DD} was also able to induce formation of an hyperpolarysed conjugative tube in cells lacking *ukc1*, or that AB31 cells repressing *ukc1*, could formed an hyperpolarised infective tube. A second argument in favour of a negative control of polarity by the RAM pathway in *U. maydis*, was the up-regulation of the regulator of filamentation *crk1* observed in Δ*ukc1* cells. This increase at the transcriptional level of *crk1* suggested that the RAM pathway could negatively regulate the expression of this gene to repress polar growth in WT cells. Taken together, these data suggested that in *U. maydis,* polar growth could be negatively regulated by the RAM pathway.

Nevertheless, another question remained to be elucidated. If the RAM pathway is a negative regulator of polarity, why central cells were round in Δ*ukc1* mutants. One possible explanation could be that inactivation of Ukc1 provoked a strong deregulation of cell signaling. Knowing that Ukc1 protein could play pleiotropic function, we can easily imagine a strong molecular desorganisation and incoherence in cell signal. Cells without a coherent molecular signal could be unable to maintain a normal morphology and could present a round phenotype with defects in bud site selection and branching. This phenotype has been observed in several *U. maydis* mutants, as cells deleted for MyoV (Schuchardt *et al.*, 2005). So, one possibility to explain this round cell phenotype will be a disorganization and not a positive control of the RAM pathway in polarity.

RAM pathway appeared indispensable for virulence in *U. maydis*

Virulence programme and signaling regulation are highly studied in the phytopathogenic fungus *U. maydis*. The cAMP and the MAPK pathway have been identified regulating the central Prf1 transcriptional factor involved in the activation of the virulence programme. In this work, we suggest that the RAM pathway could also regulate the pathogenic growth in *U. maydis*, acting at different levels during the infective cycle. First we identified that Δ*ukc1* cells were defective in cell-cell fusion but also, that *prf1* transcription was abolished. These two defects appeared to be independent because a constitutive activation of *prf1* was unable to restore mating between Δ*ukc1* cells. Even though in this work we have not identified the causes of the *prf1* transcription or cell fusion defects, but the characterisation of the RAM pathway in different organisms and the result obtained in this work allow us to propose putative hypothesis that might explain the virulence defect of Δ*ukc1* cells observed.

prf1 transcription was abolished in Δ*ukc1* cells

In *S. cerevisiae*, deletion of the central Ndr kinase *cbk1*, leads to a defect in polarity and mating. Recently, Δ*mpt5* has been identified as a suppressor of the mating defect observed in a strain deleted for *cbk1* (Bourens *et al.*, 2009). Mpt5 is a member of the PUF family of RNA binding proteins. This protein recruits the Not-complex to the 3´UTR of RNA to reduce the translation of over 200 mRNAs, including the mating genes of *S. cerevisiae* (Mat genes) (Goldstrohm *et al.*, 2006, 2007; Seay *et al.*, 2006). Interestingly, Cbk1 and Mpt5 have been shown to physically interact to regulate RNA metabolism, through the binding of the Not-complex. The model proposed in *S.*

cerevisiae to explain the mating rescue in the Δ*mpt5*Δ*cbk1* strain is that Cbk1p could phosphorylate Mpt5p, to inhibit the repressive function of Mpt5p. This phosphorylation leads to the inhibition of the constitutive translation repression that would be relieved by the deletion of *mpt5* (Fig.48). It will be very interessant to study whether this attractive model proposed by Bourens *et al*. (2009), could explain in *U. maydis* the defect in *prf1* transcription observed in Δ*ukc1* cells.

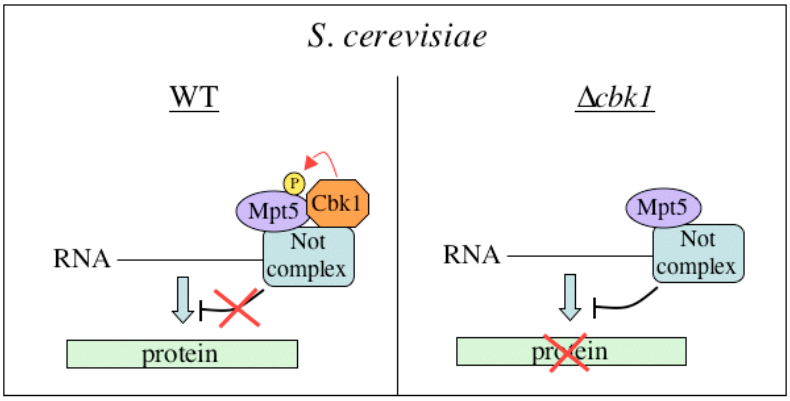

Figure 48: Model for the hypothetical function of Cbk1 in RNA metabolism control in *S. cerevisiae*, based on the hypothesis describe by Bourens *et al*., (2000).

In addition, knowing that an up-regulation of PKA activity could not rescue the defect in *prf1* transcription in Δ*ukc1* cells, we can suggested that both pathways did not regulate *prf1* at the same level. cAMP is involved in *prf1* regulation at the transcriptional and post-transcriptional level but no evidence in translational control has been shown yet. Thus, we could assume that Ukc1 could act at the translational level in *prf1* regulation, to control pheromone signal transduction and why not, other genes´expression necessary for full virulence.

The defect in *prf1* transcription could be sufficient to explain the avirulence of the RAM mutants in *U. maydis*, but our work showed that Δ*ukc1* mutant cells were also affected in cell fusion.

Δ*ukc1* strains are defective in cell-cell fusion

The central Ndr kinase of the RAM pathway is named Cbk1 for Cell wall biosynthesis kinase, and has been shown to control the expression of several genes encoding cell wall proteins in *C. albicans* (McNemar and Fonzi, 2002). In yeast, the lipid composition of a membrane has profound effects on biophysical properties that may affect membrane fusability. Yeast plasma membrane is highly enriched in ergosterol and it has been recently demonstrated that defects in ergosterol membrane composition abolish cell fusion in *S. cerevisiae* (Jin *et al.*, 2008). Interestingly, in *C. albicans* the RAM pathway adjusts ergosterol levels and RAM mutants cannot enhance expression of ergosterol biosynthesis genes in response to serum (Song *et al.*, 2008). Taken together, these data suggested that the RAM pathway could be involved in the regulation of the membrane ergosterol concentration, which will be critical for effective cell fusion. In *U. maydis*, another observation can lead to the same hypothesis. Indeed, filamentous cells of Δ*ukc1* mutant appeared wavy comparing with WT filaments that are strictly straight. This wavy phenotype could be a consequence of a membrane composition defect. So, it would be extremely interesting to see whether ergosterols could be disorganized or affected in their concentration in the membrane of RAM mutant in *U. maydis*.

The RAM pathway acts in connection with cAMP and MAPK pathway in *U. maydis*

In this work, we provided evidence that the RAM pathway is one of the signaling cascade involved in morphology and polarity regulation in *U. maydis*. MAPK pathway and cAMP pathway were already identified to regulate morphology and

filamentation and a challenging question was to know whether the joined activity of the RAM pathway could modulate the morphology and the polarity growth in *U. maydis*.

RAM and cAMP pathways seem to act in parallel in *U. maydis*

The RAM pathway has been already shown to act in parallel to the cAMP pathway in *S. cerevisiae* (Schneper *et al.*, 2004) and in *N. crassa* (Gorovits and Yarden 2003; Seiler *et al.*, 2006). In both organisms, the cAMP and the RAM pathways regulate positively polar growth. In *U. maydis*, our analysis suggested a relationship between these pathways. We observed that inhibition of the PKA activity induced a strong filamentation of Δ*ukc1* cells, as we could observe in WT cells. In contrast, the up-activation of the PKA activity inhibited filamentation in WT cells and reduced apical elongated cells in Δ*ukc1* cells. Thus, a modulation of the cAMP pathway activity could modify the Δ*ukc1* mutant phenotype, suggesting a crosstalk between both pathways. In addition, in *U. maydis* the cAMP pathway is known to regulate negatively polar growth. In this work we showed that the RAM network was also involved in negative control of polar growth suggesting that both pathways could act in parallel to regulate polarity in *U. maydis*. Interestingly, *U. maydis* is one of the few organisms in which the cAMP pathway has been shown to act negatively on polarity. In the majority of the cases, as in *S. cerevisiae*, *S. pombe* or *C. albicans*, cAMP act positively on polar growth, as the RAM pathway. It seems so that regulation of polar growth by the RAM pathway was still the same that cAMP regulation. This phenomenon could be explained by the regulation of common protein targets involved in polarity regulation. In *S. cerevisiae*, it has been shown that cAMP and RAM pathways regulate in parallel the Rho protein (Schneper *et al.*, 2004). Rho protein is involved in the repression of polar growth, and cAMP and RAM pathways negatively control Rho to induce polar growth (Fig.49). In

our case, we identified as common target the *crk1* gene, a positive regulator of filamentation. The repression of the cAMP and RAM pathways on *crk1* inhibit polar growth, and when one of these networks is affected, cells can filament (Fig.49 and 50). To resume, we could hypothesize that the positive or negative function of the RAM pathway on polarity regulation is dependent on the function played by the common target shared with the cAMP pathway. The common target influencing polarity could act negatively on polarity, as Rho protein, or positively as *crk1*.

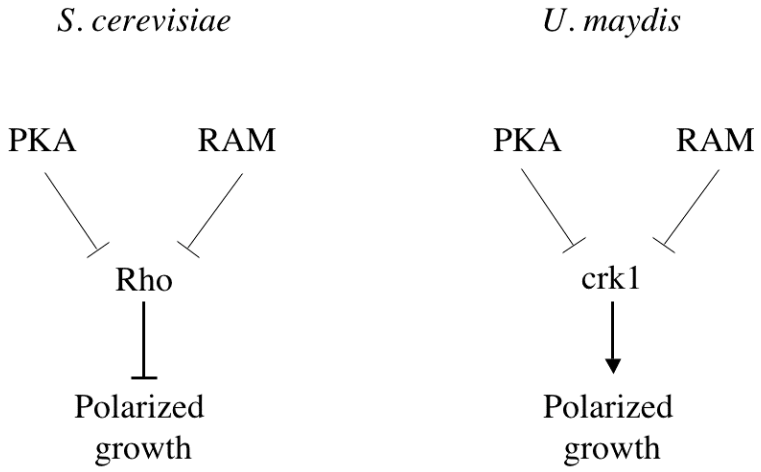

Figure 49: Model for the role of the RAM pathway in polarized growth regulation in parallel to the cAMP pathway (PKA). In *S. cerevisiae* the model is represented according to Schneper *et al.*, 2004.

RAM and pheromone MAPK pathways seem to act independently

The cAMP pathway has been shown to act in parallel to the pheromone signaling MAPK cascade in several organisms (Lengeler *et al.*, 2000) and recently it has been demonstrated in *N. crassa* that loss of the MAPK protein composing the pheromone signal cascade could restore a part of the deletion *cot-1* mutant phenotype, Cot-1 being the homologue of Ukc1 in *N. crassa* (Maerz *et al.*, 2008). In this work, observing a defect in pheromone response for *Δukc1* mutant cells, we asked whether the RAM pathway could act in relationship with the MAPK pathway also in *U. maydis*. Our

genetic analysis showed that Δ*fuz7*Δ*ukc1* presented a Δ*ukc1* phenotype because of the WT phenotype of Δ*fuz7*. In addition, an up-activation of this MAPK pathway using a *fuz7*^{DD} construct, induced filamentation with a defect in morphology in the central mutant cells. We have not identified any rescue or additive defects in comparaison to the single mutant phenotype Δ*ukc1,* Δ*fuz7* or *fuz7*^{DD} in our genetic experiments. These results suggested that both signaling cascades might act independently in morphology regulation.

RAM and Cell Wall Integrity pathways could genetically interact in *U. maydis*

The CWI pathway has been recently described in *U. maydis* (Carbó Doctoral thesis). This pathway has been shown to negatively regulate polar growth through the regulation of the cell cycle progression. Deletion of one of the CWI components is not translated onto morphological changes but an up-regulation of its activity leads to cells with more than one nucleus, separated by a septum.

Interestingly, the RAM pathway has been shown to genetically interact with the CWI pathway in *N. crassa* (Maerz *et al.*, 2008). The recent characterisation of the CWI in *U. maydis* allowed us to ask whether the CWI and the RAM pathway could have a relationship regulating polar growth in *U. maydis* too. To respond to this question, we performed epistasis analysis, which allowed us to suggest a genetic interaction between both pathways. Indeed, we observed that Δ*slt2* could partly restore the severe Δ*ukc1* phenotype and that up-activation of the MAPK cascade using Mkk1^{DD} in a Δ*ukc1* background, resulted in an unexpected phenotype, organized in long chains of short cells rounder than WT cells.

We demonstrated in this work that the genetic interaction observed was not due to a direct regulation of the RAM pathway on CWI function, since *ukc1* deletion did not

influence the Δ*slt2* drugs resistances. These data suggested that the genetic interaction between both pathways only concern polarity regulation. In this case, we can imagine that the RAM pathway could have an action upstream Slt2 protein kinase or that the RAM network act as target of the CWI pathway to regulate polarity (Fig.50).

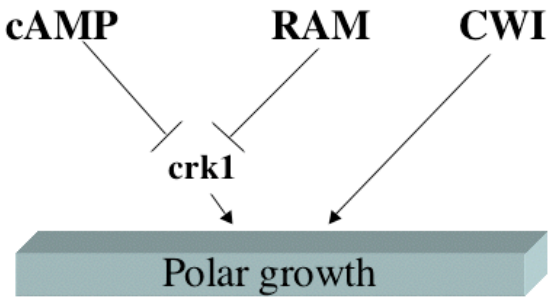

Figure 50: Model summarizing the potential connections between the cAMP, the RAM and the CWI pathway.

Conclusions

1. The components of the RAM pathway are conserved in *U. maydis* but the Ace2 homologue does not seem to be involved in cell separation regulation in *U. maydis*.

2. The complex between Ukc1 and Mob2 is conserved in *U. maydis* and its localisation is strongly regulated at each cell cycle stage.

3. The RAM pathway influences actin patches localisation in *U. maydis* but not septins protein localisation or microtubules organisation.

4. The RAM pathway is involved in the negative control of growth polarity in *U. maydis*.

5. The filamentation observed in Δ*ukc1* mutant cells could be partly explained by an up-regulation of the *crk1* kinase transcription.

6. At the pathogenic level, the RAM pathway is necessary for pheromone response through *prf1* regulation and for cell fusion.

7. The RAM pathway could play a function in parallel to the cAMP pathway and could genetically interact with the Cell Wall Integrity pathway in *U. maydis*.

Resumen en español

I. Introducción

La regulación de la morfología es un tema central de la vida eucariota. Los organismos requieren la coordinación de numerosas rutas de señalización para controlar muchos procesos celulares como la división celular, la organización del citoesqueleto, o el transporte de vesículas. Esta regulación morfológica se vuelve especialmente importante en hongos dimórficos debido a que deben desarrollar más de una estructura celular durante su ciclo de vida. Los hongos dimórficos cambian de una forma de levadura a una forma filamentosa, desarrollan hifas y esporas. Todos estos cambios morfológicos son necesarios para la viabilidad celular, la adaptación al medio y para la virulencia. En los últimos tiempos, el estudio de la regulación morfológica que ocurre en estos organismos durante estos procesos se ha convertido en un desafío interesante.

En los hongos dimórficos se conocen dos vías diferentes de señalización capaces de controlar las respuestas inducidas por los cambios ambientales, jugando así, un papel importante en la adaptación morfológica. Estas vías son, la ruta del AMPc y las cascadas MAPK (Lengeler *et al.*, 2000; Borges-Walmsley y Walmsley, 2000). Más recientemente, se ha descrito una nueva vía de señalización implicada en el control de la morfología, de la separación celular y de la regulación de la polaridad. Esta vía se conoce como la ruta RAM (Regulación de actividad Ace2p y Morfogénesis). A pesar de que esta ruta, hasta el momento, se ha descrito en pocos organismos, se ha demostrado que tiene un papel conservado en la regulación de la morfología.

Ustilago maydis, es un hongo fitopatógeno, responsable de la enfermedad conocida como el carbón del maíz (Holliday, 1974). En los últimos años se ha convertido en un modelo ideal para estudios de fitopatología a un nivel molecular debido a su fácil manejo en el laboratorio y a la existencia de un gran número de técnicas y herramientas

para su modificación genética (Bolker, 2001; Kämper, 2004). Este hongo que tiene la capacidad de adoptar diferentes estructuras celulares durante su ciclo de vida, se presenta como un modelo ideal para el estudio de los procesos moleculares que regulan los cambios morfologícos. La caracterización de la ruta RAM en *U. maydis* puede llevar a un mejor entendimiento de su función a nivel molecular así, como de su integración en un contexto de señalización celular. Este trabajo, puede contribuir también, a una mejor comprensión del proceso de regulación de la morfología en los hongos filamentosos.

El modelo *Ustilago maydis*

En *U. maydis*, la virulencia y el desarrollo sexual están conectados (Kahmann y Kämper, 2004). Este hongo dimórfico tiene una fase de vida haploide en la que crece como levadura se divide por gemación y es saprófito (Fig. 3, a). Para completar su ciclo sexual, debe pasar por una fase patógena, en la que crece como un micelio dicarionte en el interior de la planta de maíz. La transición de la fase saprófita a la patógena se inicia con el apareamiento de dos células haploides compatibles para los alelos de tipo sexual *a* y *b* (Fig. 3, b). El reconocimiento de las células compatibles tiene lugar mediante un sistema de feromona-receptor y da lugar a la formación de los tubos de conjugación que pueden fusionarse y desarrollar el filamento dicarionte denominado tubo infectivo (Fig. 4) (Mayorga y Oro, 1999; Müller *et al.*, 1999; Andrews *et al.*, 2000). El filamento dicarionte crece apicalmente sobre la superficie de la planta hasta encontrar un lugar apropiado para la penetración (Fig. 3, c) (Snetselaar y Mims, 1992, 1993), y una vez dentro, prolifera intercelularmente (Snetselaar y Mims, 1992).

La fusión entre dos células compatibles requiere la transducción de la señal inducida por las feromonas. La transición dimórfica y el mantenimiento del dicarionte (Fig. 4) son

regulados principalmente por dos vías de señalización, la ruta del AMPc y la cascada de respuesta a feromona MAPK (Hartmann *et al*., 1996; 1999). Durante el crecimiento patogénico las rutas AMPc y MAPK trabajan de un modo coordinado. La activación de la ruta AMPc permite la activación de la PKA compuesta de la subunidad reguladora Ubc1 y de la subunidad catalítica Adr1 (Dürrenberger *et al*.; 1998, Gold *et al*.; 1997). Esta activación induce en *U. maydis* el programa de virulencia y bloquea la filamentación de las células.

La otra ruta implicada en la adaptación a las señales ambientales, en *U. maydis* es la cascada de respuesta a feromona MAPK. Esta cascada está compuesta de una proteína MAPKKK (Kpp4/Ubc4) (Andrews *et al*., 2000), una MAPKK (Fuz7/Ubc5) (Banuett y Herskowitz, 1994) y una MAPK (Ubc3/Kpp2) (ruta violeta de la Fig. 5) (Mayorga y Gold, 1999; Müller *et al*., 1999.

En *U. maydis*, una acción conjunta de la cascada de respuesta a feromona MAPK y la ruta del AMPc, regulan la fusión celular y el dimorfismo (Lengeler *et al*., 2000). La integración de ambas señales depende de la activación del factor de transcripción Prf1, y de la regulación de la proteína Crk1 (Garrido y Pérez-Martín, 2003).

Prf1 reconoce los elementos de respuesta a feromona (PREs) localizados en la región reguladora de los genes inducidos en respuesta a feromona (Urban *et al*., 1996) y también su propia expresión (Fig. 6 A). A nivel post-transcripcional, la actividad de Prf1 esta regulada por fosforilación de las vías MAPK y PKA (Fig. 6 B). De este modo, el nivel de fosforilación de Prf1 ajusta su función como regulador transcripcional. La integración de ambas señales se ha propuesto también en un estudio de Crk1. Este trabajo deja en evidencia el papel principal que tiene Crk1 en la regulación de la morfogénesis, así la sobre expresión de éste, aumenta el crecimiento filamentoso mientras que la deleción de *crk1* elimina el fenotipo filamentoso inducido por un

mutante defectuoso en un componente de la ruta del AMPc (Garrido y el Perez-Martin; Garrido *et al.,* 2004).

Además de las rutas de AMPc y de feromona MAPK conocidas en *U. maydis*, recientemente en nuestro laboratorio se ha caracterizado otra cascada MAPK, la ruta de integridad celular (CWI) (N. Carbó, tesis doctoral 2009). Esta cascada está compuesta de una proteína MAPKKK (Bck1), una MAPKK (Mkk1) y una MAPK (Slt2) (ruta en rojo de la Fig. 5). N. Carbó demostró que la ruta CWI en *U. maydis* no está implicada en la regulación de la virulencia sin embargo, parece tener un papel en la regulación del ciclo celular y de la morfología.

RAM: una nueva ruta de señalización

La ruta RAM ha sido estudiada de manera intensiva durante los diez últimos años en diferentes organismos donde se ha demostrado su papel en la regulación de procesos importantes del desarrollo celular. Esta ruta ha sido descrita por primera vez en *S. cerevisiae* por Bidlingmaier y colegas (2001). Esta compuesta de seis proteínas: Cbk1p, Mob2p, Kic1p, Hym1p, Tao3p y Sog2p (Fig. 2) (Nelson *et al.*, 2003). Cbk1p es una quinasa del tipo NDR (Relacionada con Dbf2 Nuclear), miembro de la súper familia de proteínas serina/treonina quinasas AGC (Hergovich et al., 2006). Cbk1 forma un complejo con la proteína Mob2p y este complejo Cbk1p-Mob2p es regulado por las proteínas Kic1p, Hym1p, Sog2p y Tao3. Esta ruta controla la separación celular regulando la localización del factor de transcripción Ace2p. Ace2p es trasladado al núcleo de la célula hija donde regula la transcripción de los genes necesarios para la separación celular. La ruta RAM está también implicada en el control de la morfología celular y en la regulación de la polaridad pero las dianas implicadas en estos procesos no se han identificado aún.

El papel de la ruta RAM en la regulación de la morfología es evidente dado que la pérdida de función de uno de sus componentes conduce a defectos en separación celular, en selección del sitio de gemación, en crecimiento polar y en integridad celular. Las células mutantes son más redondas que las células WT y organizadas en cadenas (Bidlingmaier *et al*., 2001; Weiss *et al.*, 2002).

Conociendo la implicación de la ruta RAM en la regulación de la polaridad, esta vía de señalización se ha estudiado en diversos organismos (tabla X). De modo interesante, en algún caso como *C. neoformans* o *C. elegans*, la ruta RAM está implicada en el control negativo de la polaridad, contrariamente a la regulación positiva que fue demostrada en otros organismos. Estudios recientes han demostrado que este ruta actúa en relación con otras vía de señalización como la ruta AMPc, MAPK o calcineurina. En *A. nidulans*, *C. neoformans*, *C. elegans* o en células de Mamífero, la ruta de la calcineurina (Ca^{2+}-calmodulina-activa) juega una función importante directamente o en paralela con la ruta RAM. Pero mucho más se conoce de la relación entre la ruta RAM y otras vías de señalización en *N. crassa*, donde recientemente se ha propuesto una relación entre la ruta RAM, PKA y MAPK. En este hongo, diferentes estudios han demostrado que la inhibición de la actividad de la PKA puede suprimir el fenotipo mutante *cot-1* termo sensible (ts) (Gorovits y Yarden, 2003; Seiler et al., 2006). También, se ha demostrado una conexión entre la ruta RAM y la vía de señalización MAPK. En este caso, la pérdida de función de *mak2*, una proteína quinasa de la vía de fusión celular y fertilidad MAPK, puede rescatar el fenotipo *cot-1*(ts).

En todos estos organismos se ha observado una relación entre la ruta RAM y otros rutas bien caracterizadas. En estos casos, la ruta RAM podría jugar un papel clave controlando la morfología celular según diversas señales ambientales o según la concentración de los metabolitos Ca^{2+} o AMPc.

En *U. maydis*, Dürrenberger y colegas (1999) identificaron la proteína Ukc1, que pertenece a la familia de proteína quinasa NDR como Cot-1p de *N. crassa* o Cbk1p de *S. cerevisiae*, que son los componentes centrales de la ruta RAM. La interrupción del gen *ukc1* en un fondo haploide causó células sumamente deformadas en su morfología, organizadas en cadenas de células redondas y alargadas en la extremidad. Además, las células mutantes fueron incapaces de generar filamentos aéreos durante el acoplamiento y defectuosas en su capacidad de causar infección en plantas de maíz (Dürrenberger et al., 1999). Estos resultados sugieren un papel importante par la quinasa Ukc1 en el control de la morfología y patología en *U. maydis*.

Por lo cual, la caracterización de la ruta RAM, en nuestro modelo de estudio *U. maydis,* podría contribuir a el entendimiento de como ocurren los cambios morfológicos indispensable para la adaptación y la virulencia de muchos hongos patógenos.

II. La ruta RAM en *U. maydis*

Conservación de los componentes de la ruta RAM en *U. maydis*

Son pocos los organismos en que todos los reguladores de la proteína Ndr han sido identificados, entre ellos *S. cerevisiae*, *C. albicans* y *C. neoformans.* En este trabajo, primero identificamos en *U. maydis* el homólogo de Mob2p. La deleción del gen *mob2* causó el mismo fenotipo que los mutantes *ukc1Δ* (Fig.18), demostrando su participación en la regulación de Ukc1. La conservación del dominio SMA en la

secuencia de la proteína Ukc1 y la conservación de la secuencia Mob1/phocein en el homólogo Mob2 sugirió que Ukc1-Mob2 pudieran interacciónar físicamente (Fig.13 y 17). Mediante un ensayo de immunoprecipitation, confirmamos que ambas proteínas interaccionan físicamente in vivo, formando en *U. maydis* el complejo Ukc1-Mob2 al igual que en *S. cerevisiae* (Fig.19). Además de Mob2, identificamos los homólogos de cuatro proteínas reguladoras de Cbk1p en *S. cerevisiae*, las proteínas Hym1, Tao3, Sog2 y Kic1. Un análisis *in silico* mostró que los dominios funcionales y característicos de estas proteínas están conservados entre *S. cerevisiae* y *U. maydis* (Fig.20). Para estudiar si los homólogos de estas proteínas estaban implicados también en la regulación de la actividad de Ukc1, creamos células delecionadas para cada uno de estos genes. Cada una de las estirpes mutadas presentó el mismos fenotipo que las células delecionadas para *ukc1*, sugiriendo su implicación en la regulación de Ukc1 (Fig.21). Estos resultados sugieren una conservación completa de todos los componentes y de la organización de la ruta RAM en *U. maydis*. Sin embargo, existen differencias encuanto las funciónes de la ruta RAM entre *U. maydis* y *C. albicans* y *S. cerevisiae*. Primero, los componentes de esta ruta son esenciales en estos dos organismos (Kurischko *et al.*, 2005) mientras que no lo son en *U. maydis*. La segunda diferencia está relacionada con las dianas de la ruta RAM. Para saber si la ruta RAM podría tener el mismo papel regulando el equivalente de Ace2p en este hongo, buscamos un homólogo de Ace2 en *U. maydis*. Identificamos la proteína Um10181 como potencial homólogo pero, una búsqueda reciproca (UmAce2 contra *S. cerevisiae*) reveló que esta proteína es más similar a SWI5p que a Ace2p. La deleción de *ace2* en *U. maydis* confirmó que este factor de trascripción no juega el mismo papel que Ace2p en *S. cerevisiae*. Efectivamente, las células sin *ace2* no presentaron defectos en separación celular como se ha descrito en *S. cerevisiae* (Fig.21).

Por tanto, hasta el momento, ningún homólogo claro de Ace2 ha sido encontrado en el genoma de *U. maydis* .

Ukc1 se localiza en diferentes partes de la célula durante el ciclo celular

Para analizar si la ruta RAM tenía diferentes funciones en *U. maydis* comparado con *S. cerevisiae*, analizamos la localización subcelular de Ukc1 mediante la proteína de fusión Ukc1-GFP (Fig.16). Observamos que la proteína Ukc1-GFP se localiza de manera dinamíca a lo largo del ciclo celular. Aparece en el sitio de gemación y después en los sitios de crecimiento apical. Cuando las células madre e hija van a separarse, Ukc1-GFP desaparece de los ápices y se acumule en el sitio de división celular, en el cuello de la gema. Cabe destacar que justo antes de la separación celular, Ukc1-GFP aparece a ambos lados del cuello. De modo interesante, Cbk1p en *S. cerevisiae* se localiza de igual manera antes de la separación celular (Colman-Lerner *et al.*, 2001), sugiriendo una función adicional para esta ruta en la regulación de la separación celular, por la activación de una diana diferente de Ace2.

Cabe mencionar que, además de su localización en el apex celular durante el creciemiento vegetativo, Ukc1-GFP también se localiza en el ápice del tubo conjugativo, indicando que Ukc1 podría jugar un papel en el crecimiento polarizado como ya ha sido demostrado para diferentes Ndr quinasas (Tamaskovic *et al.*, 2003). Además, Ukc1-GFP se localiza durante todo el ciclo celular en el núcleo tanto de la madre como de la célula hija, mientras que Cbk1p se localiza transitoriamente dentro del núcleo de la célula hija en *S. cerevisiae* (Colman-Lerner *et al.*, 2001; Weiss *et al.*, 2002). Estos datos nos permiten pensar que además de jugar un papel en la separación celular y en el crecimiento polar, Ukc1 podría también estar involucrada en la

regulación de la transcripción, debido al efecto en transcripción de los genes *crk1* y de *prf1* observado en las células delecionadas para *ukc1*.

La organización del citoesqueleto y la morfología están afectados en células *ukc1Δ*

Las células *ukc1Δ* presentan un fenotipo severo, con defectos en el tamaño, en la separación y en la elongación celular. En este estudio nos preguntamos si las proteínas implicadas en el mantenimiento de la morfología y de la separación celular podrían estar afectadas en las células mutantes de la ruta RAM. Primero, analizamos la organización de las septinas, proteínas involucradas en separación celular y morfología. Usando septinas fusionadas al gen de la GFP, encontramos que la localización de las cuatro septinas identificadas en *U. maydis* no estaban afectadas en las células Δ*ukc1* (Fig.25). Analizando la organización de la F-actina en las células *ukc1*Δ, observamos que los filamentos de actina parecieron funcionales (Fig.23). La acumulación de Myo5 en la punta de la célula sugiere que los cables de F-actina funcionaba normalmente, sin embargo no podemos excluir la posibilidad de sutiles diferencias en el ensamblaje o dinámica de los cables de F-actina. Por el contrario los "*patches*" de F-actina se encontraron acumulados en las puntas de las células mutantes más que en células silvestres (Fig.22). Aún queda por confirmar si esta alta acumulación de actina es la razón o la consecuencia del defecto en separación celular o de morfología observado en los mutantes de la ruta RAM. Curiosamente, el mismo resultado ha sido obtenido en *C. neoformans* donde los "*patches"* de F-actina se concentran en la extremidad celular mientras que en *S. cerevisiae* o *C. albicans*, los "patches" F-actina se concentran en el sitio de separación celular en los mutantes de la ruta RAM. Estos datos sugirieron que la

ruta RAM pudiera tener una función conservada en la regulación de la localización de los "*patches*" de F-actina en hongos.

La ruta RAM y la polaridad en *U. maydis*

La mutación de algún componente de la ruta RAM causa pérdida de polaridad en *S. cerevisiae* (Rackie *et al.*, 2000; Bidlingmaier *et al.*, 2001; Weiss *et al.*, 2002; Nelson *et al.*, 2003; Kurischko *et al.*, 2005). En *C. neoformans* sin embargo, los mutantes de la ruta RAM resultan en células hiperpolarizadas (Walton *et al.*, 2006). Así, esta ruta de señalización puede jugar diferentes papeles en la regulación de la polaridad en distintos hongos. En *U. maydis*, se observa un fenotipo más complejo que el descrito en otros hongos, lo que dificulta concluir sobre las funciones de esta ruta en polaridad. Efectivamente, se observan dos fenotipos distintos en los mutantes RAM. Primero, la parte central de los mutantes, está compuesta de células redondas de mayor volumen que las silvestres, lo que sugiere una pérdida de polaridad. Por el contrario, las células apicales crecen muy alargadas sugiriendo un control negativo del crecimiento polar por parte de Ukc1. Además, existe un defecto en la selección del sitio de gemación, el mutante gema por ambas extremidades, y por la parte central, dando lugar a ramificaciones (Fig.14). En consecuencia, analizando este fenotipo, nos preguntamos si la ruta RAM actúa negativamente o positivamente sobre la polaridad en *U. maydis*. Para responder a esta pregunta analizamos que sucedía con el crecimiento polar en un mutante *ukc1Δ* en distintas condiciones en las cuales *U. maydis* induce un crecimiento hiperpolarizado. Primero estudiamos si el crecimiento polar inducido por una parada del ciclo celular mediante la sobre-expresión de *wee1* (regulador negativo de la transición G2/M), se veía afectado en un mutante *ukc1Δ*. Las células *ukc1Δ* fueron capaces de hiperpolarizar, indicando que la maquinaria de polaridad seguía activa en este mutante

(Fig.26). De la misma manera, pudimos observar que *fuz7*^{DD} (variedad activa de la MAPKK de respuesta a feromona) también era capaz de inducir la formación de un tubo de conjugación hiperpolarizado en ausencia de Ukc1 (Fig.28). Un segundo argumento a favor de un control negativo de la polaridad por la ruta RAM en *U. maydis*, es el aumento de la transcripción del regulador de filamentación *crk1* observada en la célula Δ*ukc1* (Fig.40). Este aumento del nivel de transcripción de *crk1* sugiere que la ruta RAM puede regular la expresión de este gen negativamente para reprimir el crecimiento polar.

Todos estos resultados sugieren que en *U. maydis*, el crecimiento polar podría estar regulado negativamente por la ruta RAM. Sin embargo, si esta ruta es un regulador negativo de polaridad, ¿por qué las células centrales son redondas?. Una posible explicación podría ser que la inactivación de Ukc1 provoca una desregulación fuerte de la señalización. Las células sin una señal coherente podrían ser incapaces de mantener una morfología normal y podrían presentar un fenotipo redondo con defectos en la selección de sitio de gemación. Este fenotipo ha sido observado en varios mutantes de *U. maydis*, como en células mutantes de MyoV (Schuchardt *et al.*, 2005). Por tanto, una posible explicación de este fenotipo de células redondas sería una desorganización general de las rutas de señalización celular y no un control positivo de la ruta RAM sobre la polaridad.

La ruta RAM es indispensable para la virulencia en *U. maydis*

El programa de virulencia y la regulación de la vía de señalización están muy estudiados en el hongo fitopatógeno *U. maydis*. Las rutas del AMPc y MAPK han sido identificadas como reguladores de Prf1, un factor de transcripción implicado en la activación del programa de virulencia. Con este trabajo, sugerimos que la ruta RAM

también podría regular el crecimiento patogénico en *U. maydis*, actuando a diferentes niveles durante el ciclo infectivo. Primero, identificamos que las células Δ*ukc1* son defectuosas en fusión cellular (Fig.30), pero también, que la transcripción de *prf1* está suprimida (Fig.33). Estos dos defectos parecen ser independientes porque una activación constitutiva de *prf1* fue incapaz de restaurar la fusión celular entre células Δ*ukc1*.

La ruta RAM actúa en conexión con la ruta AMPc y MAPK en *U. maydis*

Con este trabajo, proporcionamos pruebas de que la ruta RAM es una cascada de señalización implicada en la regulación de la morfología y la polaridad en *U. maydis*. Las rutas MAPK y AMPc han sido identificadas como reguladores la morfología y la filamentación, por lo que nos preguntamos si la ruta RAM podría modular la morfología y el crecimiento polar en *U. maydis* en conexión con estas otras rutas descritas.

Las rutas RAM y AMPc parecen actuar en paralelo en *U. maydis*

Ya se ha demostrado que la vía RAM actúa en paralelo de la ruta AMPc en *S. cerevisiae* (Schneper *et al.*, 2004) y en *N. crassa* (Gorovits y 2003 Yarden; Seiler *et al.*, 2006). En *U. maydis*, nuestro análisis sugirió una relación entre estas dos rutas. Observamos que la inhibición de la actividad PKA indujo una fuerte filamentación de las células Δ*ukc1*, al igual que observamos en las células silvestres (Fig.37). Al contrario, la sobre-activación de la actividad de la PKA inhibió la filamentación de las células silvestres y redujo el alargamiento apical de las células Δ*ukc1* (Fig.38). Así, una modulación de la actividad de la ruta AMPc podría modificar el fenotipo de las células Δ*ukc1*, sugiriendo una

interferencia entre ambas vía de señalización. Además, se sabe que en *U. maydis* el AMPc regula negativamente el crecimiento polar. Con este trabajo mostramos que la ruta RAM también puede estar implicada en el control negativo del crecimiento polar lo que sugiere que ambos rutas podrían actuar en paralelo para regular la polaridad en *U. maydis*.

Las rutas RAM y MAPK activada por feromona parecen actuar por separado

Recientemente ha sido demostrado en *N. crassa* que la pérdida de la proteína MAPK que compone la cascada de señalización de feromona podría restaurar en parte el fenotipo del mutante *cot-1*, Cot-1 es el homólogo de Ukc1 en *N. crassa* (Maerz *et al.*, 2008). Entonces nos preguntamos si en *U. maydis* la ruta RAM también, podría actuar en relación con la ruta MAPK de feromona. Nuestro análisis genético mostró que tanto la activación constitutiva o la deleción de *fuz7* en células Δ*ukc1*, presentaron un fenotipo aditivo (Fig.28 y 43), sugiriendo que ambas rutas actúan de manera separada en la regulación de la polaridad.

La ruta RAM y la ruta de integridad celular podrían interaccionar genéticamente en *U. maydis*

Además de las rutas AMPc y de la feromona, se ha mostrado que la ruta RAM podría interaccionar genéticamente con la ruta CWI en *N. crassa* (Maerz *et al.*, 2008). La reciente caracterización de la ruta CWI en *U. maydis* nos permitió preguntarnos si la ruta RAM y CWI están relacionadas en cuanto a la regulación del crecimiento polar. Para responder a esta pregunta, realizamos un análisis de epistasia, que nos permitiera verificar la existencia de una interacción genética entre ambas ruta. Efectivamente,

observamos que las células Δ*slt2* podían en parte restaurar el severo fenotipo de las células Δ*ukc1* (Fig.45) y que una sobre activación de esta cascada MAPK, usando $Mkk1^{DD}$ en un fondo Δ*ukc1*, resultó en un fenotipo aberrante caracterizado por cadenas largas de células cortas y más redondas que las células WT (Fig.46). La observación de un fenotipo aberrante y no aditivo o no compensatorio en estos mutantes, sugirió una interacción genética entre las rutas RAM y CWI en *U. maydis*.

Por tanto, sugerimos también en este trabajo que la ruta RAM no influye en el papel de la regulación de la integridad celular de la ruta CWI. Efectivamente, observamos que la mutación Δ*ukc1* no restauró el defecto de resistencias a las drogas del mutante Δ*slt2* (Fig.47), lo que supone que la ruta RAM no juega un papel en la regulación de la integridad celular o que si fuera así, la interacciona entre ambas rutas ocurre a un nivel superior a la proteína Slt2 (Fig. 50).

Appendix

Appendix 1

Name oligo	*sequences*
cbx1	TCT GGG TTT CGC GCG AGA TCT CAC AGA GCA
cbx2	AAT TGC ACA GAT CAA GAA GGA CAT GGC CGT
smut3	ATT CAC GTT TTG TAG CAC ACG ACT C AC ATC
smut4	CACCACCCAATCGACGCGGAAGGCAACCCA
pnar1	GGT GAA TAG TGA GAA CAG TCT CGA TCA CTC
tag1	CCA AAT GTT TGA ACG ATC TGC AGC
gfp1	ACGCTGAACTTGTGGCCGTTTACGTCG
crg1	GAGATCACGACACCGCGAGGTTTGCGGTGA
ukc1-1	CGA CTG CTG AGG AAG GAC GAT ATG CGC CCA
ukc1-2	CGG GGT ACC AGT AGA AGG TGC TGC TGT GCT
ukc1-3	CGA GGC CAT CTA GGC CAC CAA AGA GGA ACA AAG
ukc1-4	CGG GGT ACC TTG TAA AAG TTT TCC AGC TTC
ukc1-5	GGT CTT CGA GCT CGG CTG CAC GCT TGA TAC
ukc1-6	GCA GGC CTG AGT GGC CGC GCG CGC ACT TCA ATC
ukc1-7	ATT CGC ATC AGC TCG ACG AAT CCG TTT ACT
ukc1-8	CCA GGC GGC GCT GCA ACA TCC GTT GTC GAG
ukc1-11	GGC GGA TCC TGG CCG AGT GCG TGC TTG CTC TCG
ukc1-12	GGC CAA TTG GAG GAC AGT CTC GTT GCT CTG GTA
ukc1-13	GAA GGA CCA GCT GGC ACA TGT GCG CGC
ukc1-14	CCATGCCATGGGGAGGACAGTCTCGTTGCTCTC
ukc1-17	CGGAAGCTTTCTCGCCTCCAACCACGGTCCGGT
mob2-1	AGC TGT GAC ACC GGG CGA GGT GGA GGA
mob2-2	CGG GGT ACC GGC ATG GGC AGA GGT AGA CAA
mob2-3	GTC GGC CAT CTA GGC CCG TAG ATT CAA CTT GCG
mob2-5	CGGGGTACCGAGTGGTACATTTTTACGAGT
mob2-6	GCG GCC TGA GTG GCC CTG AAT GCA TCG GTC AGA
mob2-7	ATG CAG GAT TGA AGC TGG GCA AGT ACT
mob2-8	TTC GTA CAG CGG CAA GAA GGA GGA CTA
mob2-15	CGCGCGGATCCATGTCGTTCTTCAACTCCATC
tao3-01	CGT GCC ACG GTG TAC CTG GAG CTG TGA CGC TGT AGC
tao3-3	GCA GGC CAT CTA GGC CAC GTC CCG CAA CCA ATA

tao3-6	GAC GGC CTG AGT GGC CGA GAC GCT ACT CGT GAC
tao3-7	GGT ACG TGT GGA AAG AAC TGT AGC GCT TGG
tao3-8	AGC AGC AAT CGG AAT CCC TCT TCT CTT CAA
tao3-9	AAA GGG TAT TTC GGA TAG GTC GAG CTC GTG
hym1-1	CTG AAA CAC GAA TTC CAA ATG GGG AAT CCT
hym1-2	CGG GGT ACC GAG AAT TAC GGA ATC GTG AAT
hym1-3	GCA GGC CAT CTA GGC CAA GAG AAT GAG TGA GAA
hym1-6	CAG GGC CTG AGT GGC CCC TCA TCC CGA CTG TGC
hym1-7	GCC GAA GTC GCC GAG ATC GCA GCT ACT CTT
hym1-8	GAG GCG CTC GCG TTT CGC GAT CAG GAT GCA
sog2-1	CGA AAT GAT GTA CTG CTT GAC AGA TGC TCG TCG
sog2-2	GCG GTT TAA ACG TGT CCA CTT GTC TGC TGT GAA GGC
sog2-3	CGC GGC CAT CTA GGC CGA AGG TGG ACA GAT GAT CGG T
sog2-4	GAC GGC CTG AGT GGC CGG TAA GGA GAG AAG GGG TGA C
sog2-5	CGC AGT TTA AAC AAC ACA TCC TAC TCA GTG GAC GTG GTG
sog2-6	ATA TGC GAC GGT TCG ACA TGG CTC CTC GAT TCA
nakch2	GTTTGGCGGATTCTTTGCGAGCGGATTC
nak1-3	CGGGATCCTCAACATCAAGGATTTCGGCGACA
nak1-6	GTGTTTGCTGGGCCGTACGAGAGGCAAT
nak1-7	TGT GAC GCC TAG GAG ACG AGG TGC GGG TGG AGG CGA GGG
nak1-10	GCA GGC CAT CTA GGC CTG AAG CTG TAG GGC TCG ATG
nak1-11	CAG GGC CTG AGT GGC CTT GAC GCT CTT TGG ATT
ace2-6	CTT GGC ACC ACT GAT ATG CAG TAA ACA CCA
ace2-7	CGA GGC CAT CTA GGC CGC CTT CAG CGA GCT AGG C
ace2-9	CAG TGT CTG ACC AGA AGG TTG TCG TGG CGG
ace2-10	CGA GGC CTG AGT GGC CTT AGG CCG CCA CTC GTC A
ace2-11	GAA AGG TAT ACC TTG GCA CCA CTG
ace2-12	TCT ATC CAG TTG AAT ATG ACT CTT CGA AAG

References

Alfa, C., Fantes, P., Hyams, J., McLead, M. and Warbrick, E. (1993). Experiments with Fission Yeast: A laboratory course manual. Cold Spring Harbor Laboratory Press, New York.

Amberg, D.C. (1998). Three-dimensional imaging of the yeast actin cytoskeleton through the budding cell cycle. Mol. Biol. Cell, 9:3259-3262.

Andrews, D.L., Egan, J.D., Mayorga, M.E. and Gold, S.E. (2000). The *Ustilago maydis ubc4* and *ubc5* genes encode members of a MAP kinase cascade required for filamentous growth. Mol. Plant Microbe Interact., 13:781-786.

Ausubel, L.J., Krieger, J.I. and Hafler, D.A. (1997). Changes in cytokine secretion induced by altered peptide ligands of myelin basic protein peptide 85-99. J. Immunol., 159:2502-2512.

Banuett, F. (1992). *Ustilago maydis*, the delightful blight. Trends Genet., 8:174-180.

Banuett, F. and Herskowitz, I. (1989). Different a alleles of *Ustilago maydis* are necessary for maintenance of filamentous growth but not for meiosis. Proc. Natl. Acad. Sci. U S A, 86:5878-5882.

Banuett, F. and Herskowitz, I. (1994). Identification of *fuz7*, a *Ustilago maydis* MEK/MAPKK homolog required for a-locus-dependent and independent steps in the fungal life cycle. Genes Dev., 8:1367-1378.

Banuett, F. and Herskowitz, I. (1996). Discrete developmental stages during teliospore formation in the corn smut fungus, *Ustilago maydis*. Development, 122:2965-2976.

Banuett, F. and Herskowitz, I. (2002). Bud morphogenesis and the actin and microtubule cytoskeletons during budding in the corn smut fungus, *Ustilago maydis*. Fungal Genet. Biol., 37:149-170.

Barrett, K.J., Gold, S.E. and Kronstad, J.W. (1993). Identification and complementation of a mutation to constitutive filamentous growth in *Ustilago maydis*. Mol. Plant Microbe Interact., 6:274-283.

Bidlingmaier, S., Weiss, E.L., Seidel, C., Drubin, D.G. and Snyder, M. (2001). The Cbk1p pathway is important for polarized cell growth and cell separation in *Saccharomyces cerevisiae*. Mol. Cell. Biol., 21:2449-2462.

Borges-Walmsley, M.W., AR. (2000). cAMP signalling in pathogenic fungi: control of dimorphic switching and pathogenicity. Trends Microbiology, 8:133-141.

Bottin, A., Kamper, J. and Kahmann, R. (1996). Isolation of a carbon source-regulated gene from *Ustilago maydis*. Mol. Gen. Genet., 253:342-352.

Bourens, M., Panozzo, C., Nowacka, A., Imbeaud, S., Mucchielli, M.H. and Herbert, C.J. (2009). Mutations in the *Saccharomyces cerevisiae* Kinase Cbk1p, lead to a fertility defect that can be suppressed by the absence of Brr1p or Mpt5p (Puf5p), proteins involved in RNA metabolism. Genetics, Jun 2009.

Brachmann, A., Weinzierl, G., Kamper, J. and Kahmann, R. (2001). Identification of genes in the bW/bE regulatory cascade in *Ustilago maydis*. Mol. Microbiol., 42:1047-1063.

Brefort, T., Muller, P. and Kahmann, R. (2005). The high-mobility-group domain transcription factor Rop1 is a direct regulator of *prf1* in *Ustilago maydis*. Eukaryot. Cell, 4:379-391.

Bretscher, A. (2003). Polarized growth and organelle segregation in yeast: the tracks, motors, and receptors. J. Cell Biol., 160:811-816.

Butty, A.C., Pryciak, P.M., Huang, L.S., Herskowitz, I. and Peter, M. (1998). The role of Far1p in linking the heterotrimeric G protein to polarity establishment proteins during yeast mating. Science, 282:1511-1516.

Carbó, N. (2009). Caracterización de la ruta de integridad celular en el hongo fitopatogeno *Ustilago maydis*. Doctoral thesis. Universidad Autónoma de Madrid.

Carbó, N. and Pérez-Martín, J. (2008). Spa2 is required for morphogenesis but it is dispensable for pathogenicity in the phytopathogenic fungus *Ustilago maydis*. Fungal. Genet. Biol., 45:1315-1327.

Castillo-Lluva, S., Alvarez-Tabares, I., Weber, I., Steinberg, G. and Perez-Martin, J. (2007). Sustained cell polarity and virulence in the phytopathogenic fungus *Ustilago maydis* depends on an essential cyclin-dependent kinase from the Cdk5/Pho85 family. J. Cell Sci., 120:1584-1595.

Chen, R.E. and Thorner, J. (2007). Function and regulation in MAPK signaling pathways: lessons learned from the yeast *Saccharomyces cerevisiae*. Biochim. Biophys. Acta., 1773:1311-1340.

Colman-Lerner, A., Chin, T.E. and Brent, R. (2001). Yeast Cbk1 and Mob2 activate daughter-specific genetic programs to induce asymmetric cell fates. Cell, 107:739-750.

Cong, J., Geng, W., He, B., Liu, J., Charlton, J. and Adler, P.N. (2001). The *furry* gene of *Drosophila* is important for maintaining the integrity of cellular extensions during morphogenesis. Development, 128:2793-2802.

Cruz, A.K., Terenzi, H.F. and Jorge, J.A. (1988). Cyclic AMP-dependent, constitutive thermotolerance in the adenylate cyclase-deficient *cr-1* (crisp) mutant of *Neurospora crassa*. Curr. Genet., 13:451-454.

Devroe, E., Erdjument-Bromage, H., Tempst, P. and Silver, P.A. (2004). Human Mob proteins regulate the NDR1 and NDR2 serine-threonine kinases. J. Biol. Chem., 279:24444-24451.

Dohrmann, P.R., Butler, G., Tamai, K., Dorland, S., Greene, J.R., Thiele, D.J. and Stillman, D.J. (1992). Parallel pathways of gene regulation: homologous regulators SWI5 and ACE2 differentially control transcription of HO and chitinase. Genes Dev., 6:93-104.

Du, L.L. and Novick, P. (2002). Pag1p, a novel protein associated with protein kinase Cbk1p, is required for cell morphogenesis and proliferation in *Saccharomyces cerevisiae*. Mol. Biol. Cell, 13:503-514.

Durrenberger, F. and Kronstad, J. (1999). The *ukc1* gene encodes a protein kinase involved in morphogenesis, pathogenicity and pigment formation in *Ustilago maydis*. Mol. Gen. Genet., 261:281-289.

Durrenberger, F., Wong, K. and Kronstad, J.W. (1998). Identification of a cAMP-dependent protein kinase catalytic subunit required for virulence and morphogenesis in *Ustilago maydis*. Proc. Natl. Acad. Sci. U S A, 95:5684-5689.

Emoto, K., He, Y., Ye, B., Grueber, W.B., Adler, P.N., Jan, L.Y. and Jan, Y.N. (2004). Control of dendritic branching and tiling by the Tricornered-kinase/Furry signaling pathway in *Drosophila* sensory neurons. Cell, 119:245-256.

Errede, B. and Levin, D.E. (1993). A conserved kinase cascade for MAP kinase activation in yeast. Curr. Opin. Cell Biol., 5:254-260.

Galagan, J.E. *et al.*, (2003). The genome sequence of the filamentous fungus *Neurospora crassa*. Nature, 422:859-868.

Gallegos, M.E. and Bargmann, C.I. (2004). Mechanosensory neurite termination and tiling depend on SAX-2 and the SAX-1 kinase. Neuron, 44:239-249.

Garrido, E. and Perez-Martin, J. (2003). The *crk1* gene encodes an Ime2-related protein that is required for morphogenesis in the plant pathogen *Ustilago maydis*. Mol. Microbiol., 47:729-743.

Garrido, E., Voss, U., Muller, P., Castillo-Lluva, S., Kahmann, R. and Perez-Martin, J. (2004). The induction of sexual development and virulence in the smut fungus *Ustilago maydis* depends on Crk1, a novel MAPK protein. Genes Dev., 18:3117-3130.

Gartner, A., Nasmyth, K. and Ammerer, G. (1992). Signal transduction in *Saccharomyces cerevisiae* requires tyrosine and threonine phosphorylation of FUS3 and KSS1. Genes Dev., 6:1280-1292.

Gillissen, B., Bergemann, J., Sandmann, C., Schroeer, B., Bolker, M. and Kahmann, R. (1992). A two-component regulatory system for self/non-self recognition in *Ustilago maydis*. Cell, 68:647-657.

Gold, S., Duncan, G., Barrett, K. and Kronstad, J. (1994). cAMP regulates morphogenesis in the fungal pathogen *Ustilago maydis*. Genes Dev., 8:2805-2816.

Gold, S.E., Brogdon, S.M., Mayorga, M.E. and Kronstad, J.W. (1997). The *Ustilago maydis* regulatory subunit of a cAMP-dependent protein kinase is required for gall formation in maize. Plant Cell, 9:1585-1594.

Goldstrohm, A.C., Hook, B.A., Seay, D.J. and Wickens, M. (2006). PUF proteins bind Pop2p to regulate messenger RNAs. Nat. Struct. Mol. Biol., 13:533-539.

Gorovits, R. and Yarden, O. (2003). Environmental suppression of *Neurospora crassa cot-1* hyperbranching: a link between COT1 kinase and stress sensing. Eukaryot. Cell, 2:699-707.

Hartmann, H.A., Kahmann, R. and Bolker, M. (1996). The pheromone response factor coordinates filamentous growth and pathogenicity in *Ustilago maydis*. Embo J., 15:1632-1641.

Hartmann, H.A., Kruger, J., Lottspeich, F. and Kahmann, R. (1999). Environmental signals controlling sexual development of the corn Smut fungus *Ustilago maydis* through the transcriptional regulator Prf1. Plant Cell, 11:1293-1306.

He, Y., Fang, X., Emoto, K., Jan, Y.N. and Adler, P.N. (2005). The tricornered Ser/Thr protein kinase is regulated by phosphorylation and interacts with furry during *Drosophila* wing hair development. Mol. Biol. Cell, 16:689-700.

Hergovich, A., Lamla, S., Nigg, E.A. and Hemmings, B.A. (2007). Centrosome-associated NDR kinase regulates centrosome duplication. Mol. Cell, 25:625-634.

Hergovich, A., Stegert, M.R., Schmitz, D. and Hemmings, B.A. (2006). NDR kinases regulate essential cell processes from yeast to humans. Nat. Rev. Mol. Cell Biol., 7:253-264.

Hoffman C. and Winston F. (1987). A ten minutes DNA preparation from yeast efficiently release autonomous plasmids for transformation of *Escherichia coli*. Gene, 57:267-272.

Holliday R. (1974). *Ustilago maydis*. In Handbook of genetics. USA: Plenium Press, New York, 1:575-595.

Jansen, J.M., Barry, M.F., Yoo, C.K. and Weiss, E.L. (2006). Phosphoregulation of Cbk1 is critical for RAM network control of transcription and morphogenesis. J. Cell Biol., 175:755-766.

Jin, H., McCaffery, J.M. and Grote, E. (2008). Ergosterol promotes pheromone signaling and plasma membrane fusion in mating yeast. J. Cell Biol., 180:813-826.

Johns, S.A., Leeder, A.C., Safaie, M. and Turner, G. (2006). Depletion of *Aspergillus nidulans cotA* causes a severe polarity defect which is not suppressed by the nuclear migration mutation *nudA2*. Mol. Genet. Genomics, 275:593-604.

Jorgensen, P., Nelson, B., Robinson, M.D., Chen, Y., Andrews, B., Tyers, M. and Boone, C. (2002). High-resolution genetic mapping with ordered arrays of *Saccharomyces cerevisiae* deletion mutants. Genetics, 162:1091-1099.

Kaffarnik, F., Muller, P., Leibundgut, M., Kahmann, R. and Feldbrugge, M. (2003). PKA and MAPK phosphorylation of Prf1 allows promoter discrimination in *Ustilago maydis*. Embo J., 22:5817-5826.

Kahmann, R., Basse, C. and Feldbrugge, M. (1999). Fungal-plant signalling in the *Ustilago maydis*-maize pathosystem. Curr. Opin. Microbiol., 2:647-650.

Kahmann, R. and Kamper, J. (2004). *Ustilago maydis*: How its biology relates to pathogenic development. New Phytol., 164:31-42.

Kaiser C., M.S., and Mitchell A. (1994). Methods in Yeast Genetics. Cold Spring Harbor Laboratory Press, New York.

Kaksonen, M., Sun, Y. and Drubin, D.G. (2003). A pathway for association of receptors, adaptors, and actin during endocytic internalization. Cell, 115:475-487.

Kämper, J., *et al.*, (2006). Insights from the genome of the biotrophic fungal plant pathogen *Ustilago maydis*. Nature, 444:97-101.

Karos, M. and Fischer, R. (1996). *hymA* (hypha-like metulae), a new developmental mutant of *Aspergillus nidulans*. Microbiology, 142:3211-3218.

Kilmartin, J.V. and Adams, A.E. (1984). Structural rearrangements of tubulin and actin during the cell cycle of the yeast *Saccharomyces*. J. Cell Biol., 98:922-933.

Klosterman, S.J., Martinez-Espinoza, A.D., Andrews, D.L., Seay, J.R. and Gold, S.E. (2008). Ubc2, an ortholog of the yeast Ste50p adaptor, possesses a basidiomycete-specific carboxy terminal extension essential for pathogenicity independent of pheromone response. Mol. Plant Microbe Interact., 21:110-121.

Klosterman, S.J., Perlin, M.H., Garcia-Pedrajas, M., Covert, S.F. and Gold, S.E. (2007). Genetics of morphogenesis and pathogenic development of *Ustilago maydis*. Adv. Genet., 57:1-47.

Kronstad, J., De Maria, A.D., Funnell, D., Laidlaw, R.D., Lee, N., de Sa, M.M. and Ramesh, M. (1998). Signaling via cAMP in fungi: interconnections with mitogen-activated protein kinase pathways. Arch. Microbiol., 170:395-404.

Kruger, J., Loubradou, G., Regenfelder, E., Hartmann, A. and Kahmann, R. (1998). Crosstalk between cAMP and pheromone signalling pathways in *Ustilago maydis*. Mol. Gen. Genet., 260:193-198.

Kurischko, C., Weiss, G., Ottey, M. and Luca, F.C. (2005). A role for the *Saccharomyces cerevisiae* regulation of Ace2 and polarized morphogenesis signaling network in cell integrity. Genetics, 171:443-455.

Laemmli, U.K. (1970). Cleavage of structural proteins during the assembly of the head of bacteriophage T4. Nature, 227:680-685.

Lamson, R.E., Winters, M.J. and Pryciak, P.M. (2002). Cdc42 regulation of kinase activity and signaling by the yeast p21-activated kinase Ste20. Mol. Cell Biol., 22:2939-2951.

Lee, N., D'Souza, C.A. and Kronstad, J.W. (2003). Of smuts, blasts, mildews, and blights: cAMP signaling in phytopathogenic fungi. Annu. Rev. Phytopathol., 41:399-427.

Lee, N. and Kronstad, J.W. (2002). *ras2* controls morphogenesis, pheromone response, and pathogenicity in the fungal pathogen *Ustilago maydis*. Eukaryot. Cell, 1:954-966.

Lengeler, K.B., Davidson, R.C., D'Souza, C., Harashima, T., Shen, W.C., Wang, P., Pan, X., Waugh, M. and Heitman, J. (2000). Signal transduction cascades

regulating fungal development and virulence. Microbiol. Mol. Biol. Rev., 64:746-785.

Longtine, M.S. and Bi, E. (2003). Regulation of septin organization and function in yeast. Trends Cell Biol., 13:403-409.

Maerz, S., Ziv, C., Vogt, N., Helmstaedt, K., Cohen, N., Gorovits, R., Yarden, O. and Seiler, S. (2008). The nuclear Dbf2-related kinase COT1 and the mitogen-activated protein kinases MAK1 and MAK2 genetically interact to regulate filamentous growth, hyphal fusion and sexual development in *Neurospora crassa*. Genetics, 179:1313-1325.

Mayorga, M.E. and Gold, S.E. (1998). Characterization and molecular genetic complementation of mutants affecting dimorphism in the fungus *Ustilago maydis*. Fungal Genet. Biol., 24:364-376.

Mayorga, M.E. and Gold, S.E. (1999). A MAP kinase encoded by the *ubc3* gene of *Ustilago maydis* is required for filamentous growth and full virulence. Mol. Microbiol., 34:485-497.

Mayorga, M.E. and Gold, S.E. (2001). The *ubc2* gene of *Ustilago maydis* encodes a putative novel adaptor protein required for filamentous growth, pheromone response and virulence. Mol. Microbiol., 41:1365-1379.

McNemar, M.D. and Fonzi, W.A. (2002). Conserved serine/threonine kinase encoded by CBK1 regulates expression of several hypha-associated transcripts and genes encoding cell wall proteins in *Candida albicans*. J. Bacteriol., 184:2058-2061.

Mendoza-Mendoza, A., Eskova, A., Weise, C., Czajkowski, R. and Kahmann, R. (2009). Hap2 regulates the pheromone response transcription factor *prf1* in *Ustilago maydis*. Mol. Microbiol., Mar 2009.

Millward, T.A., Heizmann, C.W., Schafer, B.W. and Hemmings, B.A. (1998). Calcium regulation of Ndr protein kinase mediated by S100 calcium-binding proteins. Embo J., 17:5913-5922.

Mulhern, S.M., Logue, M.E. and Butler, G. (2006). *Candida albicans* transcription factor Ace2 regulates metabolism and is required for filamentation in hypoxic conditions. Eukaryot. Cell, 5:2001-2013.

Müller, P., Aichinger, C., Feldbrugge, M. and Kahmann, R. (1999). The MAP kinase *kpp2* regulates mating and pathogenic development in *Ustilago maydis*. Mol. Microbiol., 34:1007-1017.

Müller, P., Katzenberger, J.D., Loubradou, G. and Kahmann, R. (2003. A). Guanyl nucleotide exchange factor Sql2 and Ras2 regulate filamentous growth in *Ustilago maydis*. Eukaryot. Cell, 2:609-617.

Müller, P., Leibbrandt, A., Teunissen, H., Cubasch, S., Aichinger, C. and Kahmann, R. (2004). The Gbeta-subunit-encoding gene *bpp1* controls cyclic-AMP signaling in *Ustilago maydis*. Eukaryot. Cell, 3:806-814.

Müller, P., Weinzierl, G., Brachmann, A., Feldbrugge, M. and Kahmann, R. (2003. B). Mating and pathogenic development of the Smut fungus *Ustilago maydis* are regulated by one mitogen-activated protein kinase cascade. Eukaryot. Cell, 2:1187-1199.

Nadal, M., Garcia-Pedrajas, M.D. and Gold, S.E. (2008). Dimorphism in fungal plant pathogens. FEMS Microbiol. Lett., 284:127-134.

Nelson, B., Kurischko, C., Horecka, J., Mody, M., Nair, P., Pratt, L., Zougman, A., McBroom, L.D., Hughes, T.R., Boone, C. and Luca, F.C. (2003). RAM: a conserved signaling network that regulates Ace2p transcriptional activity and polarized morphogenesis. Mol. Biol. Cell, 14:3782-3803.

Perez-Martin, J., Castillo-Lluva, S., Sgarlata, C., Flor-Parra, I., Mielnichuk, N., Torreblanca, J. and Carbo, N. (2006). Pathocycles: *Ustilago maydis* as a model to study the relationships between cell cycle and virulence in pathogenic fungi. Mol. Genet. Genomics, 276:211-229.

Racki, W.J., Becam, A.M., Nasr, F. and Herbert, C.J. (2000). Cbk1p, a protein similar to the human myotonic dystrophy kinase, is essential for normal morphogenesis in *Saccharomyces cerevisiae*. Embo J., 19:4524-4532.

Robinson, M.J. and Cobb, M.H. (1997). Mitogen-activated protein kinase pathways. Curr. Opin. Cell Biol., 9:180-186.

Sambrook, J. and Gething, M.J. (1989). Protein structure. Chaperones, paperones. Nature, 342:224-225.

Schmitt, M.E., Brown, T.A. and Trumpower, B.L. (1990). A rapid and simple method for preparation of RNA from *Sacchomyces cerevisiae*. Nucleic. Acid. Res., 18:3091-3092.

Schneper, L., Krauss, A., Miyamoto, R., Fang, S. and Broach, J.R. (2004). The Ras/protein kinase A pathway acts in parallel with the Mob2/Cbk1 pathway to effect cell cycle progression and proper bud site selection. Eukaryot. Cell, 3:108-120.

Schuchardt, I., Assmann, D., Thines, E., Schuberth, C. and Steinberg, G. (2005). Myosin-V, Kinesin-1, and Kinesin-3 cooperate in hyphal growth of the fungus *Ustilago maydis*. Mol. Biol. Cell, 16:5191-5201.

Schulz, B., Banuett, F., Dahl, M., Schlesinger, R., Schafer, B.W., Martin, T., Herskowitz, F. and Kahmann, R. (1990). The b alleles of *U. maydis*, whose combinations program pathogenic development, code for polypeptides containing a homoeodomain-related motif. Cell, 60:295-306.

Seay, D., Hook, B., Evans, K. and Wickens, M. (2006). A three-hybrid screen identifies mRNAs controlled by a regulatory protein. Rna, 12:1594-1600.

Seiler, S., Vogt, N., Ziv, C., Gorovits, R. and Yarden, O. (2006). The STE20/germinal center kinase POD6 interacts with the NDR kinase COT1 and is involved in polar tip extension in *Neurospora crassa*. Mol. Biol. Cell, 17:4080-4092.

Sgarlata, C. and Perez-Martin, J. (2005). Inhibitory phosphorylation of a mitotic cyclin-dependent kinase regulates the morphogenesis, cell size and virulence of the smut fungus *Ustilago maydis*. J. Cell Sci., 118:3607-3622.

Shi, J., Chen, W., Liu, Q., Chen, S., Hu, H., Turner, G. and Lu, L. (2008). Depletion of the MobB and CotA complex in *Aspergillus nidulans* causes defects in polarity maintenance that can be suppressed by the environment stress. Fungal Genet. Biol., 45:1570-1581.

Snetselaar, K.M. and Mims, C.W. (1992). Sporidial fusion and infection of maize seedlings by the smut fungus *Ustilago maydis*. Mycologia, 84:193-203.

Snetselaar, K.M. and Mims, C.W. (1993). Infection of maize stigmas by *Ustilago maydis*: Light and electron microscopy. Phytopathology, 83:843-850.

Snetselaar, K.M. and Mims, C.W. (1994). Light and electron microscopy of *Ustilago maydis* hyphae in maize. Mycol. Res., 98:347-355.

Song, Y., Cheon, S.A., Lee, K.E., Lee, S.Y., Lee, B.K., Oh, D.B., Kang, H.A. and Kim, J.Y. (2008). Role of the RAM network in cell polarity and hyphal morphogenesis in *Candida albicans*. Mol. Biol. Cell, 19:5456-5477.

Spellig, T., Bottin, A. and Kahmann, R. (1996). Green fluorescent protein (GFP) as a new vital marker in the phytopathogenic fungus *Ustilago maydis*. Mol. Gen. Genet., 252:503-509.

Steinberg, G., Wedlich-Soldner, R., Brill, M. and Schulz, I. (2001). Microtubules in the fungal pathogen *Ustilago maydis* are highly dynamic and determine cell polarity. J. Cell Sci., 114:609-622.

Stork, O., Zhdanov, A., Kudersky, A., Yoshikawa, T., Obata, K. and Pape, H.C. (2004). Neuronal functions of the novel serine/threonine kinase Ndr2. J. Biol. Chem., 279:45773-45781.

Sullivan, D.S., Biggins, S. and Rose, M.D. (1998). The yeast centrin, cdc31p, and the interacting protein kinase, Kic1p, are required for cell integrity. J. Cell Biol., 143:751-765.

Tamaskovic, R., Bichsel, S.J. and Hemmings, B.A. (2003). NDR family of AGC kinases essential regulators of the cell cycle and morphogenesis. FEBS Lett., 546:73-80.

Taylor, S.S., Buechler, J.A. and Yonemoto, W. (1990). cAMP-dependent protein kinase: framework for a diverse family of regulatory enzymes. Annu. Rev. Biochem., 59:971-1005.

Urban, M., Kahmann, R. and Bolker, M. (1996). Identification of the pheromone response element in *Ustilago maydis*. Mol. Gen. Genet., 251:31-37.

Voth, W.P., Olsen, A.E., Sbia, M., Freedman, K.H. and Stillman, D.J. (2005). ACE2, CBK1, and BUD4 in budding and cell separation. Eukaryot. Cell, 4:1018-1028.

Walton, F.J., Heitman, J. and Idnurm, A. (2006). Conserved elements of the RAM signaling pathway establish cell polarity in the basidiomycete *Cryptococcus neoformans* in a divergent fashion from other fungi. Mol. Biol. Cell, 17:3768-3780.

Weiss, E.L., Kurischko, C., Zhang, C., Shokat, K., Drubin, D.G. and Luca, F.C. (2002). The *Saccharomyces cerevisiae* Mob2p-Cbk1p kinase complex promotes polarized growth and acts with the mitotic exit network to facilitate daughter cell-specific localization of Ace2p transcription factor. J. Cell Biol., 158:885-900.

Yang, H.C. and Pon, L.A. (2002). Actin cable dynamics in budding yeast. Proc. Natl. Acad. Sci. U S A, 99:751-756.

Yarden, O., Plamann, M., Ebbole, D.J. and Yanofsky, C. (1992). *cot-1*, a gene required for hyphal elongation in *Neurospora crassa*, encodes a protein kinase. Embo J., 11:2159-2166.

Zallen, J.A., Peckol, E.L., Tobin, D.M. and Bargmann, C.I. (2000). Neuronal cell shape and neurite initiation are regulated by the Ndr kinase SAX-1, a member of the Orb6/COT-1/warts serine/threonine kinase family. Mol. Biol. Cell, 11:3177-3190.